UNIVERSITY OF ALBERTA

Numerical Modeling of Cuttings Transport with Foam in Inclined Wells

By

Osunde Macdonald Okunsebor ©

A thesis
submitted to the Faculty of Graduate Studies and Research
in partial fulfillment of the requirements for the degree of

Master of Science

in

Petroleum Engineering

Department of Civil and Environmental Engineering

Edmonton, Alberta
Fall, 2006

Library and
Archives Canada

Published Heritage
Branch

395 Wellington Street
Ottawa ON K1A 0N4
Canada

Bibliothèque et
Archives Canada

Direction du
Patrimoine de l'édition

395, rue Wellington
Ottawa ON K1A 0N4
Canada

Your file Votre référence
ISBN: 978-0-494-22338-3
Our file Notre référence
ISBN: 978-0-494-22338-3

NOTICE:
The author has granted a non-exclusive license allowing Library and Archives Canada to reproduce, publish, archive, preserve, conserve, communicate to the public by telecommunication or on the Internet, loan, distribute and sell theses worldwide, for commercial or non-commercial purposes, in microform, paper, electronic and/or any other formats.

The author retains copyright ownership and moral rights in this thesis. Neither the thesis nor substantial extracts from it may be printed or otherwise reproduced without the author's permission.

AVIS:
L'auteur a accordé une licence non exclusive permettant à la Bibliothèque et Archives Canada de reproduire, publier, archiver, sauvegarder, conserver, transmettre au public par télécommunication ou par l'Internet, prêter, distribuer et vendre des thèses partout dans le monde, à des fins commerciales ou autres, sur support microforme, papier, électronique et/ou autres formats.

L'auteur conserve la propriété du droit d'auteur et des droits moraux qui protège cette thèse. Ni la thèse ni des extraits substantiels de celle-ci ne doivent être imprimés ou autrement reproduits sans son autorisation.

In compliance with the Canadian Privacy Act some supporting forms may have been removed from this thesis.

While these forms may be included in the document page count, their removal does not represent any loss of content from the thesis.

Conformément à la loi canadienne sur la protection de la vie privée, quelques formulaires secondaires ont été enlevés de cette thèse.

Bien que ces formulaires aient inclus dans la pagination, il n'y aura aucun contenu manquant.

Canada

ABSTRACT

In this study, a 1-D transient state mechanistic model of cuttings transport with foam in inclined wells has been developed. The model was solved numerically to predict the optimum foam flow rate (liquid and gas rate) and rheological properties that would maximize cuttings transport efficiency in inclined well.

The model predictions of total pressure drops were compared to the results from full scale low pressure ambient temperature flow loop experiments conducted by Tulsa University Drilling Research program. The model predictions of total pressure drop were 4 to 21 % lower than the experimental result.

A detailed sensitivity analysis of the effect of gas and liquid flowing rates, drilling rate, foam rheological properties, borehole geometry, wellbore inclination, back pressure and the rate of gas and liquid influx from the reservoir on the cuttings transport efficiency in inclined wells was presented.

ACKNOWLEDGEMENT

I wish to express my sincere gratitude to Dr. Ergun Kuru, for his support and supervision throughout my M.Sc. thesis research.

I would like to express my sincere appreciation to Dr. Peter Toma for his advice and support.

My gratitude also goes to all the graduate students of the department of Petroleum Engineering who in one way or the other made my study a success.

Sincere gratitude is extended to the natural Sciences and Engineering Research Council (NSERC) of Canada for the financial support to this research work.

DEDICATION

To

My Lovely wife Oluwatoyin Okunsebor

My Sweet son Osunde Okunsebor (Jr.)

My Late parents Mr. and Mrs. Okunsebor

and

To the Almighty God.

TABLE OF CONTENTS

1 Introduction

1.1 Overview--1

1.2 Statement of Problems-- ----------4

1.3 Objectives of Research--- ----------6

1.4 Scope of Research--- ----------6

2 Literature Review

2.1 Mechanisms of Cuttings Transport --8

2.1.1 Mechanisms of Cuttings Transport in Vertical Wells----------------------8

2.1.2 Mechanisms of Cuttings Transport in Horizontal Wells-------------------9

2.1.3 Mechanisms of Cuttings Transport in Inclined Wells---------------------10

2.2 Flow Pattern in Inclined Wells---11

2.3 Forces Acting on a Single Solid Particle in an Inclined Well-------------------12

2.3.1 Dynamic Forces Acting on a Cutting in Inclined Wells---------------------13

2.3.2 Drag Coefficient Models---14

2.3.3 Static Forces Acting on a Cutting in Inclined Wells-------------------------23

2.3.4 Force Analysis for the Rolling and Lifting Mechanism---------------------24

2.3.4.1 Force Analysis for Rolling Mechanism-----------------------------------25

2.3.4.2 Force Analysis for Lifting Mechanism-----------------------------------26

2.4 Critical Conditions for Cuttings Transport in Wells-----------------------------28

2.5 Experimental Models of Cutting Transport in Inclined wells-------------------30

2.6 Empirical and Mechanistic Models of Cuttings Transport in Inclined Wells--31

2.7 Physical Properties of Foam---34

2.7.1 Foam--35

2.7.1.1 Classification of Foams--35

2.7.1.2 Foam Density---37

2.7.1.3 Foam Rheology--37

2.7.1.4 Foam Viscosity---41

2.7.1.5 Foam Stability---42

2.8 Cuttings Transport with Foam---43

3. Development of Mechanistic Model of Cuttings Transport with Foam in Inclined Wells

3.1 Model Development--45

3.1.1 Geometry of Cutting Transport Model--46

3.1.2 Forces Acting on Cuttings within the Control Volume------------------------48

3.1.3 Forces Due to Deposition and Entrainment of Cuttings----------------------61

3.1.3.1 Depositional and Entrainment Velocity-------------------------------------63

3.1.4 Conservation of Mass and Momentum Equations----------------------------65

3.1.5 Boundary Conditions--68

3.1.6 Initial Conditions---68

3.1.7 Method of Solution---68

3.1.8 Foam-Cutting Flow in Drilling Annulus--------------------------------------69

3.1.9 Foam Flow across the Bit Nozzle--69

3.1.10 Foam Flow in Drill Pipes---70

4. Method of Numerical Solution of the Foam -Cuttings Flow Models

4.1 Discretization of the Physical Model--71

4.2 Discretization of Momentum Equations---72

4.2.1 Discretization of the Momentum Equations of the Solid Component-------72
4.2.2 Discretization of the Momentum Equations of the Fluid (foam) Component---74
4.2.3 Discretization of the Momentum Equations of the Cuttings Bed-------------76
4.3 Formulation of Velocity –Correction Equations-----------------------------------78
4.4 Discretization of the Mass Balance Equations--------------------------------------81
4.4.1 Discretization of the continuity equation for the solid component in the upper layer---81
4.4.2 Discretization of the continuity equation for the foam component in the upper layer---81
4.4.3 Discretization of the continuity equation for the cuttings bed---------------82
4.5 Formulation of Pressure-Correction Equation---------------------------------------82
4.6 Numerical Method for Transient Foam-Solids Flow Model----------------------85

5. Results and Discussions

5.1 Verification of Model Predictions---88
5.2 Sensitivity Analyses of the Factors Affecting Cuttings Transport---------------89
5.2.1 Effect of Gas Injection Rate on Bottomhole Pressure and Cuttings Concentration---89
5.2.2 Effect of Liquid Injection Rate on Bottomhole Pressure and Cuttings Concentration---90
5.2.3 Effect of Drilling Rate on Bottomhole Pressure and Cuttings Concentrations---92
5.2.4 Effect of Inclination on Bottomhole Pressure and Cuttings Concentration---93

5.25 Effect of Back Pressure on Bottomhole Pressure and Cuttings Concentration----------95

5.2.6 Effect of Water Influx on Bottomhole Pressure and Cuttings Concentration----------96

5.2.7 Effect of Gas Influx on Bottomhole Pressure and Cuttings Concentrations----------97

5.2.8 Transient Bottomhole Pressure and Cuttings Concentration----------99

6 Conclusions and Recommendations

6.1 Conclusions----------103

6.2 Recommendations----------104

Reference----------105

Appendix A: Derivation of Continuity Equations for the Two Layered Model-----119

Appendix B: Derivation of Momentum Equations for the Two Layered Model----125

Appendix C: Deposition and Re-suspension During Cuttings Transport in inclined wells----------133

Appendix D: Well Geometry----------137

LIST OF TABLES

Table 5.1: Input Data used for Model Verification Study--------------------------------88

Table 5.2: Comparison of Model Predictions with Experimental Results-------------88

Table 5.3: Base Data Used for Simulation of Foam Drilling in Inclined Wells-------90

LIST OF FIGURES

Figure 2.1: Forces acting on a cutting in vertical well ----------------------------------9

Figure 2.2: Forces acting on a cutting in horizontal well---------------------------------10

Figure 2.3: Sliding and Saltation mechanism in inclined wells--------------------------11

Figure 2.4 Forces on cutting in an inclined well--13

Figure 3.1 Schematic view of two-Layer model for cuttings transport with foam in inclined wells ---46

Figure 3.2 Two-layer model of cuttings transport with foam in inclined wells--------48

Figure 3.3: Forces acting on layers within control volume-------------------------------49

Figure 3.4: Pressure force acting on the suspended solids--------------------------------50

Figure 3.5: Friction between moving bed and wellbore-----------------------------------60

Figure 4.1: Staggered grid system---71

Figure 5.1 Average cuttings concentration variation gas and liquid injection rate----91

Figure 5.2 Bottomhole pressure variation with gas and liquid injection rate----------92

Figure 5.3 Average cuttings concentration variation drilling rate-----------------------92

Figure 5.4 Bottomhole pressure variation with drilling rate-----------------------------93

Figure 5.5 Average cuttings concentration variation with inclination------------------94

Figure 5.6 Bottomhole pressure variation with inclination-------------------------------94

Figure 5.7 Gas injection rate variation with well inclination-----------------------------95

Figure 5.8 Cuttings concentration profile variation with inclination--------------------95

Figure 5.9 Average cuttings concentration variation with back pressure---------------96

Figure 5.10 Bottomhole pressure variation with back pressure--------------------------96

Figure 5.11 Cuttings concentration profile variation with water influx from reservoir---97

Figure 5.12 Pressure profile variation with water influx from reservoir---------------97

Figure 5.13 Cuttings concentration variation with gas influx from the reservoir-----98

Figure 5.14 Pressure profile variation with gas influx from reservoir-----------------99

Figure 5.15 Transient bottomhole pressure---100

Figure 5.16 Transient average cuttings concentration at different drilling rate------100

Figure 5.17 Transient bottomhole pressure at different inclination--------------------101

Figure 5.18 Transient average cuttings concentration at different inclination--------101

Figure 5.19 Cuttings concentration profile along wellbore----------------------------102

Figure D-1: Geometry for the case in which the pipe is completely above the cuttings bed---137

Figure D-2: Geometry for the case in which the pipe is partially covered by the cutting bed---139

Figure D-3: Geometry for the case which the pipe is completely covered by the cutting bed---141

NOMENCLATURE

A	Cross-sectional area, ft^2
A_s	Characteristic area of cuttings, ft^2
C	Volumetric concentration, dimensionless
C_D	Drag coefficient, dimensionless
C_L	Lift coefficient, dimensionless
C_{fl}	Foam concentration in lower layer, dimensionless
C_{s1}or C_b	Solid concentration in lower layer, dimensionless
CBHP	Circulating bottom hole pressure (psia)
d	Diameter, ft
D	Diameter of pipe, ft
D_H	Hydraulic diameter, ft
D_o	Diameter of outer pipe, ft
D_i	Hydraulic diameter, ft
f	Friction factor, dimensionless
F	Force, Ibft/sec^2
F_{Ds}	Drag force on suspended solids, Ibft/sec^2
F_{Df}	Drag force on foam, Ibft/sec^2
F_{Gs}	Gravity force on suspended solids, Ibft/sec^2
F_{Gf}	Gravity force on foam, Ibft/sec^2
F_{prs}	Pressure force on suspended solids, Ibft/sec^2
F_{prf}	Pressure force on foam, Ibft/sec^2

$F_{s\text{-}w}$	Shear force due to contact of suspended solids with wellbore, Ibft/sec^2
$F_{f\text{-}w}$	Shear force due to contact of foam with wellbore, Ibft/sec^2
$F_{B\text{-}w}$	Shear force due to contact of cuttings bed with wellbore, Ibft/sec^2
$F_{B\text{-}2}$	Shear force due to contact of cuttings bed with the upper layer, Ibft/sec^2
$F_{ent\text{-}Bs}$	Force due to entrainment of solids from upper to lower layer, Ibft/sec^2
$F_{ent\text{-}Bf}$	Force due to entrainment of foam from upper to lower layer, Ibft/sec^2
$F_{ent\text{-}S}$	Force due to entrainment of solids from lower to upper layer, Ibft/sec^2
$F_{ent\text{-}f}$	Force due to entrainment of foam from lower to upper layer, Ibft/sec^2
$F_{Dep\text{-}s}$	Force due to deposition of solids from upper to lower layer, Ibft/sec^2
$F_{Dep\text{-}f}$	Force due to deposition of foam from upper to lower layer, Ibft/sec^2
$F_{Dep\text{-}Bs}$	Force due to deposition of solids from upper to lower layer, Ibft/sec^2
$F_{Dep\text{-}Bf}$	Force due to entrainment of foam from upper to lower layer, Ibft/sec^2
g	Acceleration of gravity, ft/sec^2
g_c	Newton's law conversion factor, ft-lbm/lbf-sec^2
K	Consistency index, Ibf-sec^n/ft^2
L	Distance from center of pipe to center of hole, ft
$\dot{m}$	Mass flow rate, Ibm/sec
N	Total number of particles in the control volume
n	Flow behaviour index, dimensionless
$N_{Re}(n,\bar{k})$	Modified Reynolds number for laminar flow in annulus, dimensionless
$\tilde{N}_{Re}$	Modified Reynolds number, dimensionless
P	Pressure in wellbore, psia

P_b	Back pressure, psia
P_{bh}	Bottomhole pressure, psia
PI	Specific productivity index, ft^2/(psi.sec)
ΔP	Pressure drop, psia
ΔP_d	Parasitic pressure loss, psia
ΔP_b	Pressure drop across the bit, psia
q	Flow rate, ft^3/sec
Q	Flow rate, ft^3/sec
r	Radius, ft
Re	Reynolds number, dimensionless
ROP	Rate of Penetration, ft/hr
s	Mass source term, Ibm/(sec$\cdot$ft^3)
s_f	Source term of foam, Ibm/(sec$\cdot$ft^3)
s_g	Source term of gas influx, Ibm/(sec$\cdot$ft^3)
s_o	Source term of oil influx, Ibm/(sec$\cdot$ft^3)
s_w	Source term of water influx, Ibm/(sec$\cdot$ft^3)
S	Wetted perimeter, ft
$S_{f\text{-}w}$	Total wetted perimeter of foam with pipe and well of wellbore, ft
$S_{s\text{-}w}$	Total wetted perimeter of suspended solids with pipe and well of wellbore, ft
$S_{B\text{-}w}$	Total wetted perimeter of bed with pipe and well of wellbore, ft
S_i	Length of interface between Layers, ft
ΔS	Length of control volume, ft
t	Time, sec.

u	Velocity, ft/s
u_c	Critical deposition velocity, ft/sec
$\langle u_s \rangle$	Volume-average velocity, ft/s
$\tilde{u}_s$	Mass average velocity, ft/s
V	Volume, ft^3
v_D	Depositional velocity, ft/sec.
v_E	Entrainment velocity, ft/sec.
v_t	Terminal settling velocity of solids, ft/sec
X	Coefficient used in critical velocity correlation, dimensionless
y	Distance between the bottom of outer and inner pipes, ft
Z	Gas deviation factor
β_v	Coefficient accounting for drag force, lbm/(sec·ft^3)
Φ_c	Optimum gas liquid ratio, dimensionless
θ	Well inclination from the vertical, degree
$Ø$	Cutting angle of repose, degree
$\in$	Eccentricity, dimensionless
γ	Shear rate, 1/s
μ	Viscosity of foam, cp
μ_a	Apparent viscosity, cp
μ_e	Effective viscosity, cp
μ_p	Plastic viscosity, cp
Γ	Foam quality, dimensionless

ρ	Density, lbm/ft^3
$\bar{\rho}$	Bulk density, lbm/ft^3
τ_y	Yield strength, psia
τ	Shear stress, psia
τ_w	Shear stress at the wall, psia
ψ	Particle sphericity

Subscripts

1, B	bed/lower layer
2	upper layer
an	wellbore annulus
b	condition at the choke
B-i	interface between bed and upper layer
bh	bottomhole
dp	drill pipe
f	foam
f-w	foam-wellbore interface
g	gas
h	hole
i	interface between the upper and lower layer
I	number of computational cell
In	injection
l	liquid phase

nozz	bit nozzle
N	last control cell
p	particle
re	reservoir
s	solids
sc	surface condition.
t	total
w	wellbore

CHAPTER 1

INTRODUCTION

1.1 Overview

Underbalanced drilling (UBD) refers to a drilling operation where the circulating bottomhole pressure is less than the formation pressure.

Underbalanced drilling operation is generally designed to ensure underbalanced drilling condition is achieved throughout the entire drilling and completion operation (Wang et al., 1997). To achieve underbalanced drilling condition at all times, the selection of the drilling fluid is of great importance. Based on the type of drilling fluid used, UBD operations can be classified under four different categories (McLennan et al. (1997)): Air/gas drilling in which low density air or gas like nitrogen is used as the drilling fluid; Gasified liquid drilling in which a gas-liquid two phase drilling fluid is used for the drilling operation; Foam drilling which involves using stable foam with high viscosity for good cutting lifting ability and low variable density to maintain an underbalanced condition at all times; Flow drilling which involves using liquid with density below the formation's hydrostatic pressure gradient.

Field applications have proven that UBD techniques has many advantages including minimized formation damage, increased drilling rate, improved formation evaluation while drilling, minimized lost circulation, reduced occurrence of differential pipe and logging tools sticking, enhanced detection of all producing zones, and enhanced earlier production from reservoir.

With underbalanced drilling, the invasion of the formation by fine particles in the drilling fluid is minimized or completely eliminated reducing formation damage to a minimum. This benefit accounts for the use of underbalanced drilling in horizontal well drilling (Bennion et al., 1998). Culen et al. (2003) conducted a field test to compare conventional overbalanced drilling with UBD in horizontal well in Saih Rawl in Oman, and observed an increase in the ultimate oil recovery as a result of using UBD.

Underbalanced drilling facilitates faster drilling. Negrao et al. (1999), Rojas et al. (2002) and Jaramillo (2003) presented several case histories, where significant increase in drilling rate was observed by using UBD as compared to the conventional drilling performance.

Reservoir evaluation is made possible while using underbalanced drilling technique. This is possible because the reservoir is producing hydrocarbon while drilling underbalanced. For conventional drilling, reservoir evaluation while drilling is difficult as the formation has been severally damaged due to invasion of drilling fluid. Lage et al. (1996), and Hannegan and Divine (2002) reported failure of drill stem test in wells that was conventionally drilled.

Producing zones which would have been missed using conventional drilling could be easily detected with UBD. This is mainly due to the fact that when drilling underbalanced, formation fluids flow into the wellbore and are carried to the surface by the circulating fluid for observation. The presence of oil in the circulating fluid received at the surface is an indication of the presence of a hydrocarbon zone. This is usually not the case with conventional drilling where formation fluid never flows into the wellbore during the drilling process. Cade et al. (2003) gave a case study of a field in Lithuania where a hydrocarbon zone missed by conventional drilling was detected while drilling underbalanced (UBD).

UBD also have the advantage of reducing or eliminating differential pipe sticking and sticking of logging tools in open hole. Amoco (1995) showed that the probability of pipe and logging tool sticking is much higher in overbalanced drilled wells as compared to UBD wells.

There is also the advantage of early production from the hydrocarbon zone while drilling underbalanced. With the formation pressure higher than the drilling fluid pressure, reservoir fluids are forced into the wellbore from where they are transported to the surface. Since production occurs naturally in UBD, the need for simulation treatment to enhance production is reduced, hence saving time and money.

The net effect of the above listed benefits of UBD is an increase in productivity from the production zone which makes the project economically feasible.

This research will focus on foam drilling. Foam is an agglomeration of gas bubbles separated from each other by thin liquid films Bickerman (1973). Foam can also be defined as a dispersion of gas bubbles in a liquid, in which at least one dimension falls within the colloidal size range. The gas is usually stabilized by surfactant. Foam can be obtained by in-situ generation at the point of injection or can be preformed by passing the various fluid components through a porous medium. Preformed foam is preferred to in-situ generated foam as a circulating fluid because of its ability to withstand more contamination.

Foam as a drilling fluid is commonly used for underbalanced drilling because of its low variable density which makes adjustment of foam density possible in order to keep control of the circulating bottomhole pressure and its high effective viscosity which gives a superior cuttings lifting and transport ability. The variable density of foam is attributed to the presence of gaseous component in foam whose volume changes as it flows from the surface, down the hole and back to the surface due to change in pressure and temperature.

The change in the volume of the gaseous component with pressure causes the quality of foam to change. Foam quality is defined as the ratio of the volume of gas in the foam to the total volume of foam at a given pressure. Okpobiri and Ikoku (1986) recommended keeping the foam quality between 50-60 % at the bottom and below 96% at the surface for effective cuttings transport. Above 96% foam quality, they concluded that foam becomes unstable and break into mist.

In a field case study from Western Venezuela, Rojas et al. (2002) reported that drilled solids as heavy as 15g were lifted successfully by using foam as a drilling fluid. Based on laboratory investigation, Anderson (1984) reported that from laboratory that foam has a lifting ability about 2 to 10 times that of water. Apart from having a good lifting ability and the ability to maintain an underbalanced drilling condition, foam is also used to remove formation fluids that enter the borehole while drilling and also serve as an insulating medium if loss circulation is a problem.

The prediction of the performance of foam is difficult due to the compressible nature of foam which makes foam flow mechanism quite complex. This is attributed to the fact that unlike conventional drilling fluids only very little is known about the hydraulic and rheological properties of foam. This problem associated with foam flow makes determination of the optimum gas/liquid injection rates for effective cuttings transport while achieving maximum drilling rate a problem. Other questions exist on how to combine the various different controllable variables in order to achieve efficient cuttings transport while maintaining maximum drilling rate.

In this research, a transient mechanistic model is presented for the prediction of foam drilling performance in inclined wells. The new model considers foam rheological properties, drag coefficient of cuttings in foam, formation fluid influx, drillpipe eccentricity, inclination effect and drilling rate and thereby provides an effective numerical solution to simulate the hydraulics of foam drilling in inclined wells which in the past have been a major problem.

1.2 STATEMENT OF PROBLEM

Cuttings transport is one of the most important factors affecting drilling cost, time and quality of oil and gas wells. Inadequate hole cleaning can result in costly drilling problems such as stuck pipe, excessive bit wear, reduced drilling rate, lost circulation, and high torque and drag.

Hole cleaning is affected by many parameters, such as well geometry (diameter, inclination, eccentricity), cuttings characteristics (size, porosity of bed), drilling fluid properties (rheology, density, drag coefficient), and drilling operational parameter (drilling rate, drilling fluid circulation rate). Optimization of drilling hydraulics design requires a good understanding of the mechanics of cuttings transport.

Advantages of drilling with foam (i.e., high drilling rate, improved bit life, minimized formation damage and environmental impact, improved formation evaluation, reduced lost circulation, etc.) can be restrained by poor hole cleaning. The interaction between foam and the drill cuttings must be investigated to make the efficient use of all the benefits of using foam as a drilling fluid. Better understanding of how drilling operational parameters affect cuttings transport with foam will lead to a more widespread use of foam as a drilling fluid.

Several hydraulic design models for drilling vertical wells with foam were proposed by Krug and Mitchell (1972), Okpobiri and Ikoku (1986), Harris et al. (1991), Guo et al. (1995), Liu and Medley (1996), Valko and Economides (1997), and Owayed (1997). These models were developed by assuming steady-state flow conditions, therefore, they can not be used to analyse the transient nature of solids transport with foam. In addition, assuming a homogeneous flow, these models did not consider the slip velocity between cuttings and the foam. In homogeneous flow, particles are considered uniformly dispersed in the foam and slip velocity of solids was neglected in the calculation of pressure drops in the vertical well. Other aspects such as the friction between the drilled solids and borehole wall and water or /gas influx from reservoir were not properly addressed in most of the existing models.

Very few research studies have been reported on solids transport with foam in horizontal wells (Thondavadi and Lemlich, 1985; Herzhaft et al., 2000; Martins et al., 2001; Ozbayoglu et al., 2003). Thondavadi and Lemlich (1985), Herzhaft et al. (2000), and Martins et al. (2001) conducted experimental studies. Ozbayoglu et al. (2003) presented a 1D three-layer mechanistic model for foam cuttings flow. Ozbayoglu et al.'s model also assumes steady state flow conditions and, therefore, it can not be used for analysing the transient behavior of foam-cuttings flow in horizontal wells. The effect of reservoir fluid influx was not taken into account in the Ozbayoglu et al's model either.

Capo (2003) conducted an experimental study of cuttings transport with foam in inclined wells. Capo reported that foam cuttings transport exhibits a critical behavior within the range of 55 to 65 degrees where in-situ cuttings concentration reaches the highest values.

Recently, an unsteady-state model of cuttings transport with foam has been presented by Li (2005). Li's model includes the effect of slip velocity between the cuttings and foam. It also considers the effect of formation fluid influx into the wellbore. However, Li's results are limited to vertical and horizontal wells and do not apply for the transport of cuttings at intermediate inclination angles.

For cost-effective and trouble free drilling of inclined borehole sections using foam, a more comprehensive approach of modeling cuttings transport with foam in inclined wells is needed. The current research project is, therefore, proposed to analyse the transient non-homogenous flow of cuttings transport with foam through inclined wells.

1.3 OBJECTIVES OF RESEARCH

This research will focus on the numerical modeling of foam drilling hydraulics and cuttings transport in inclined wells. The main objectives of this research include:

(1) Develop 1-D transient mechanistic models of cuttings transport with foam in inclined wells,

(2) Provide numerical solutions of the mechanistic models of foam-cuttings transport in inclined wells,

(3) Develop a numerical wellbore simulator that could be used for hydraulic optimization of foam drilling operation in inclined wells (i.e., effective transport of cuttings while keeping the bottom hole pressure at minimum).

1.4 SCOPE OF RESEARCH

The major tasks accomplished throughout this research can be summarized as follows:

(1) A 1-D transient model of solids-foam flow in inclined wells has been developed. This task requires the formulation of governing equations for the fully suspended solids-foam flow and the associated boundary conditions within the inclined drilling circulating system. This task also requires for the selection of closure equations to complete the governing equations of solids and foam phases. The closure equations

include the correlations to calculate the foam rheology and density, foam and solids friction factors, drag coefficient for power law fluid and the hydraulic diameter of the open flow area.

(2) The proposed model has been solved numerically. The numerical solution of the model has been implemented into a wellbore simulator. A well-known numerical method for dilute two-fluid flow model in fluid mechanics is adopted, and modified to discretize the governing equations for foam-solids flow in inclined wells. Numerical wellbore simulator is then, developed by using the proposed numerical method and FORTRAN programming language.

(3) The accuracy of the model predictions has been checked by comparing model prediction of pressure losses in inclined wellbores to the experimental data available from the literature.

CHAPTER 2

LITERATURE REVIEW

The literature review focuses on mechanism of cuttings transport in vertical well, horizontal and inclined wells. It also looks into foam drilling with focus on the foam rheology, foam stability, foam flow and cuttings transport with foam.

2.1 Mechanisms of Cuttings Transport.

2.1.1 Cuttings Transport Mechanism in Vertical Wells.

When vertical wells are drilled, cuttings are generated at the bottom of the hole which needs to be transported to the surface. The movement of cuttings upward to the surface is achieved by means of drilling fluids which are pumped from the surface through the pipe to the bottom of the hole, up through the annular space and back to the surface. One of the major functions of the drilling fluid is to lift cuttings from the hole as they are formed so as to prevent cuttings accumulation. Problems associated with inefficient cuttings transport are; reduction in penetration rate, wear of bit, pipe stuck, high torque and drag and other hole problems.

For cuttings to be transported to the surface as they are formed, the fluid must possess certain energy (force) which is a function of the fluid properties and pressure applied at the surface. In vertical wells, this force is called the drag force, which is the major force pushing the cuttings out of the hole. The other force acting on the solid cuttings is the gravitational force which acts against the drag force. These external forces acting on the cuttings control their movement. Fig 2.1(A) shows an upward movement of the cuttings when the drag force is greater than the gravitational force. Fig 2.1(B) shows a downward movement of the cuttings when the drag force is lower than the gravitational force i.e. settling of cuttings due to gravity and Fig 2.1(C) represent a critical condition where the forces are balanced over the particle and its movement is determined by its previous motion.

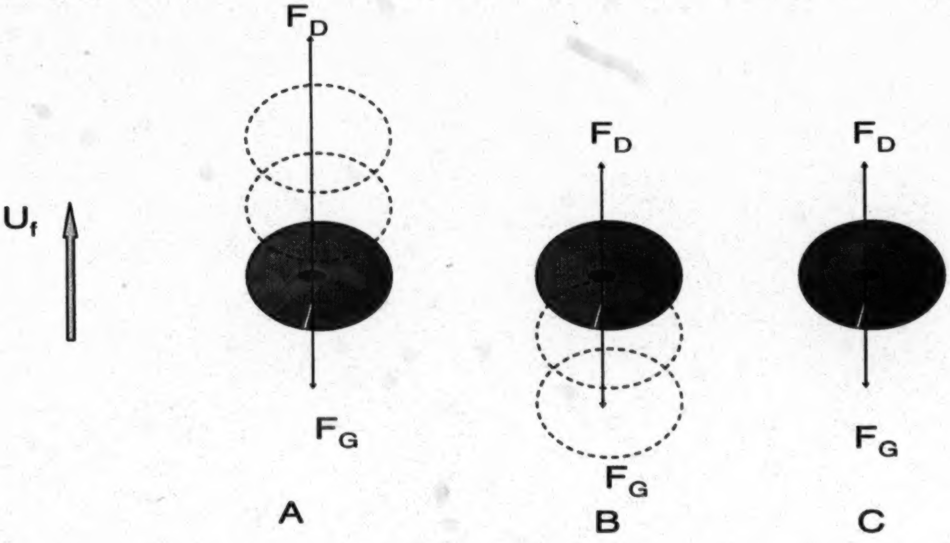

Figure 2.1: Forces acting on a cutting in a vertical well

2.1.2 Cuttings Transport Mechanism in Horizontal Wells.

For horizontal wells, cuttings are also generated when they are drilled and as a result needs to be transported to the surface. Gavignet and Sobey (1989) and Ford et al. (1990) concluded that two major mechanisms are responsible for cuttings displacement in horizontal wells: saltation and sliding are responsible for cuttings transport in horizontal wells. In saltation, the cuttings are lifted to a position from where they are being carried by the fluid to the surface and this occurs when the lift force is greater than the gravitation force on the cuttings. Fig 2.2 (A) shows a lifted cutting which is being transported by the drag force to the surface. Sliding on the other hand is the transport mechanism which results when the lift force is not effective but the drag force is sufficient to overcome the frictional force between the cuttings and the wellbore and as a result the cuttings are moved along the wellbore to the surface as shown in Fig 2.2(B). Fig 2.2(C) shows a condition in which the gravitational force is higher than the lift force and the drag force is less than the frictional force. In this case, the cuttings would accumulate to form cuttings bed.

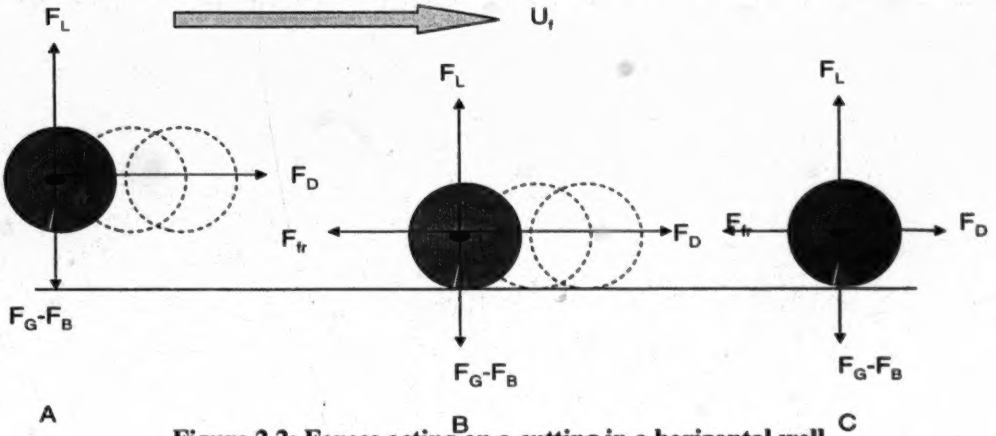

Figure 2.2: Forces acting on a cutting in a horizontal well

2.1.3 Cuttings Transport Mechanism in Inclined Wells.

Different forces acts on cuttings being transported in an inclined wellbore. The combined effect of these forces at different wellbore angles result to different mechanism which plays a major role in transporting cuttings generated at the bit to the surface. The wellbore angle has considerable effect on the hole cleaning process; this is reflected on the effect its changes have on the forces acting on the cuttings and the mechanism that dominate. An increase in the wellbore angle would:

Decrease the axial component of the gravitational force and increase the frictional force thereby increasing the effect of the drag force. There is also decrease in the axial component of the slip velocity which promotes rolling but an increase in the radial component of the slip velocity which hinders lifting process. High cuttings slippage as explained above account for the worst cutting transport at angle of inclination in the 40 to 45^0 range. This is true however, when relative low flow rate are used (Okrajni and Azar (1986)).

Produce a net decrease in lifting force due to increase in the radial component of the gravitational force.

Clark and Bickham (1994) suggested that three mechanisms are responsible for that the mechanism that dominates at any time depends on the angle of inclination. They suggested rolling mechanism at high wellbore angle, lifting mechanism at low wellbore angle while the settling mechanism (sedimentation) dominates near vertical wellbore angles. Gavignet and Sobey (1989) and Ford et al. (1990) suggested that two different mechanisms are responsible for cuttings transport in inclined wells; the sliding/rolling in which the cuttings moves along the low side wall of the annulus and saltation/suspension where the cuttings are transported in suspension. The sliding and saltation mechanisms are shown in Fig 2.3(A) and Fig 2.3(B) respectively.

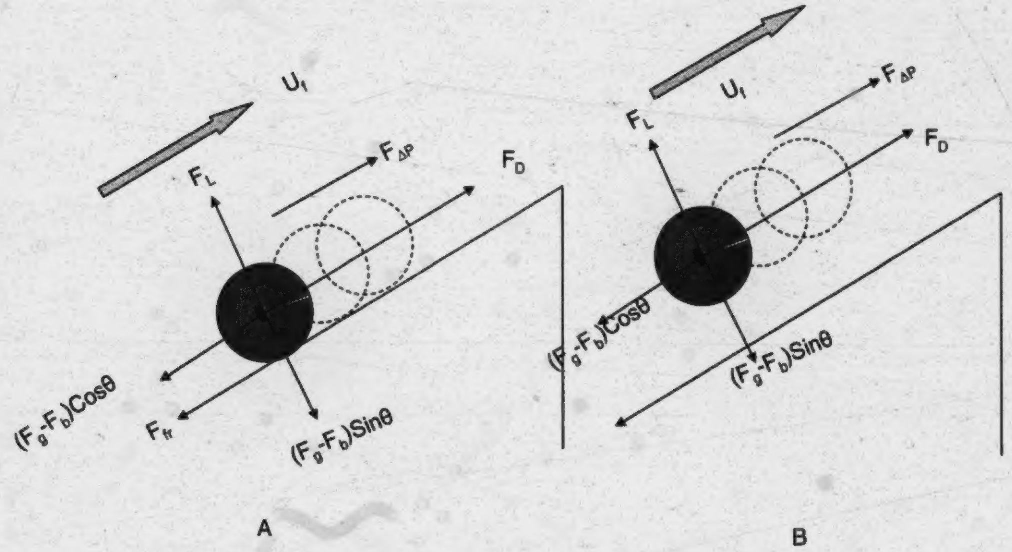

Figure 2.3: Sliding and Saltation mechanisms in inclined well

2.2 Flow Pattern in Inclined Wells.

Flow patterns were observed during cuttings transport experiments by researchers. Ford et al. (1990) from their experiment observed and identified seven types of flow patterns which includes; Homogeneous Suspension, Heterogeneous Suspension, Saltation /Suspension, Sand Clusters, Separated Moving Beds, Continuous Moving Bed, and Stationary Bed.

Luo et al. (1992) observed three type of flow patterns for cuttings transport in inclined wells depending on the hole angle and fluid properties which includes: (1) Heterogeneous suspension, this type of flow pattern results when the fluid velocity is high enough to set up a strong lift force which overcomes the gravity force causing the cuttings to be lifted and suspended in the fluid. For this flow pattern, there is usually a concentration gradient with more cuttings suspended in the lower half of the wellbore. (2) Separated Beds/Dunes, this type of flow pattern results when the fluid velocity is not high enough to create lift force to suspend all the cuttings. The result of this is the formation of cuttings bed with discontinuous interface between the solid beds and the carrying fluid. (3) Continuous Moving Bed, this flow pattern results when the velocity of the fluid is such that the lift force is weak to suspend the cuttings in the fluid but the drag force is strong enough to drag the deposit of cuttings forward and thus a layer of cuttings bed is formed on the low side of the wellbore. They also recognized Stationary Bed which usually results when fluid velocity is so low that both the drag and lift forces cannot move the cuttings forward but did not consider it as one of the flow pattern since it usually avoided during drilling operation.

Kelessidis et al. (2003) from their study of cuttings transport in inclined wells concluded that the main factors that determine flow pattern in pipes are the liquid properties, the solid loading, and the properties of the solid and liquid. They suggested five types of flow patterns namely: the fully suspended symmetric flow pattern, the asymmetric flow pattern, a moving bed flow pattern, a three layer flow pattern and finally full blockage in which the solids pile up in the pipe and blocks it.

2.3 Forces on a Single Solid Particle in an Inclined Well.

Different authors have analyzed forces on cuttings being transported in an inclined well. Luo et al. (1992) for better understanding of the cuttings transport mechanism in inclined wells, analyses the forces acting on a cutting on the low side of the wellbore. Clark and Bickham (1994) obtained the velocity needed to initiate flow of cuttings in an inclined well for both the rolling and lifting mechanism by the balance of the forces acting on the cutting resting on the low side of the wellbore for the rolling mechanism and that in suspension for the lifting mechanism. Ford et al. (1996) based their minimum transport velocity (MTV) model on the balance of forces acting on a single cutting resting on the low side of the borehole. From the force analysis carried out by these authors, two major groups of force are observed: Dynamic forces and Static forces. See fig 2.4 for forces acting on a cutting in an inclined well.

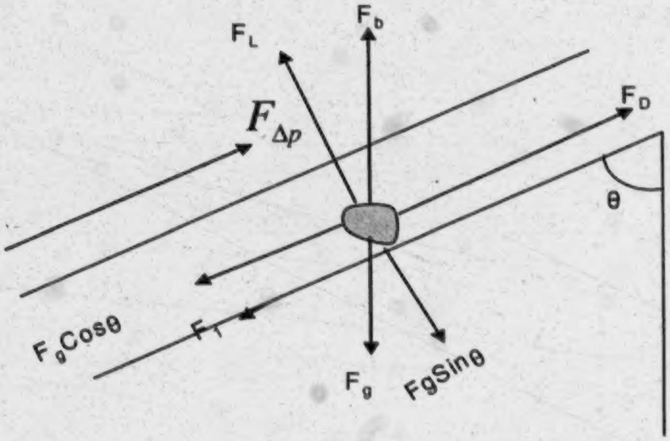

Fig 2.4 Forces acting on a cutting in an inclined well

2.3.1 Dynamic Forces Acting on a Cutting in Inclined Wells.

Dynamic forces comprise of the lift force, drag force and the pressure force. The drag and lift forces are supplied by the fluid (its properties) and are usually experienced by a particle due to relative motion between the body and the surrounding fluid. These forces actually result due to pressure and shear stress distribution on a body.

Drag Force. The determination of the drag force is quite complex when compared to the determination of the gravitational and buoyant forces. This is attributed to the variability of factors that affect it. These factors which includes; the type of fluid, the particle being transported (the particle shape, size and density), the density and viscosity of the fluid should be considered for proper determination of the drag force.

The drag force which is a resistant force induced when particles moves through a fluid has two components (Peden, 1987); the viscous component which is represented by

$$F_{Dv} = \frac{1}{2} C_{Dv} A_P \rho_f \left(u_f - u_s\right)^2 \qquad 2.1$$

Ap is the characteristic area of the particle parallel to the direction of motion. The second component is the pressure component and is represented by;

$$F_{Dp} = \frac{1}{2} C_{Dp} A_N \rho_f \left(u_f - u_s\right)^2 \qquad 2.2$$

Where A_N, is the characteristic area of the particle perpendicular to the direction of flow.

The addition of these two components gives the total drag force represented by;

$$F_D = \frac{1}{2} C_D A_S \rho_f \left(u_f - u_s\right)^2 \qquad 2.3$$

Where A_s is the characteristic area of the cutting and C_D is the drag coefficient
The above equation can also be re-written as

$$F_D = \frac{1}{8} C_D \pi d^2 \rho_f \left(u_f - u_s\right)^2 \qquad 2.4$$

2.3.2 Drag Coefficient Models.

The drag coefficient C_D is required for the calculation of the drag force on the cuttings supplied by the fluid. Numerous studies have been conducted to develop correlations for the determination of the drag coefficient in both Newtonian and non-Newtonian fluids with spherical and non spherical particles.

McCabe (1956) developed correlations for drag coefficient as a function of particle Reynolds number for Newtonian fluid around a smooth sphere for the creeping, intermediate and Newtonian flow regimes:

Stokes regime or Creeping flow

$$C_D = \frac{24}{\mathrm{Re}_p} \quad , \quad \mathrm{Re}_p \prec 0.1 \qquad 2.5$$

Intermediate flow regime

$$C_D = \frac{18.5}{\mathrm{Re}_p^{0.6}} \quad , \quad 2 \prec \mathrm{Re}_p \prec 500 . \qquad 2.6$$

Newtonian (Turbulent) flow regime

$$C_D = 0.44 \quad , \quad 500 \prec \mathrm{Re}_p \prec 200{,}000 \qquad 2.7$$

Where

$$\mathrm{Re}_p = \frac{D_p \rho_f \left(u_f - u_s\right)}{\mu} \qquad 2.8$$

Haider and Levenspiel (1989), Gausier (1995), Hartman et al. (1994), Swamee and Ojha (1991) also presented expressions for drag coefficient for Newtonian fluids.

Clift et al. (1978) recommended standard correlations for the determination of drag coefficient of spherical particles in both Newtonian and non Newtonian fluids for all flow regimes. They came up with the following expressions for the drag coefficient:

$$C_D = \frac{3}{16} + \frac{24}{\mathrm{Re}_p} \quad , \quad 0.01 \prec \mathrm{Re}_p \qquad 2.9$$

$$Log\left(\frac{C_D \,\mathrm{Re}_p}{24} - 1\right) = -0.881 + 0.82 \log \mathrm{Re}_p - 0.05 (\log \mathrm{Re}_p)^2 \quad , \quad 0.01 \prec \mathrm{Re}_p \prec 20 \qquad 2.10$$

$$Log\left(\frac{C_D \,\mathrm{Re}_p}{24} - 1\right) = -0.7133 + 0.6305 \log \mathrm{Re}_p \quad , \quad 20 \prec \mathrm{Re}_p \prec 260 \qquad 2.11$$

$$LogC_D = 1.6435 - 1.1242\log \mathrm{Re}_p + 0.1558(\log \mathrm{Re}_p)^2 \quad , \quad 260 \prec \mathrm{Re}_p \prec 1500$$

2.12

$$LogC_D = -2.4571 + 2.5558\log \mathrm{Re}_p - 0.9295(\log \mathrm{Re}_p)^2 + 0.1049(\log \mathrm{Re}_p)^3$$

2.13

$$1500 \prec \mathrm{Re}_p \prec 12000$$

$$LogC_D = -1.9181 + 0.6370\log \mathrm{Re}_p - 0.0636(\log \mathrm{Re}_p)^2 \quad , \quad 12000 \prec \mathrm{Re}_p \prec 44000$$

2.14

$$LogC_D = -4.339 + 1.5809\log \mathrm{Re}_p - 0.1546(\log \mathrm{Re}_p)^2 \quad , \quad 44000 \prec \mathrm{Re}_p \prec 10^5$$

2.15

$$C_D = 29.78 - 5.3\log \mathrm{Re}_p \quad , \quad 10^5 \prec \mathrm{Re}_p \prec 4\times10^5 \qquad 2.16$$

$$C_D = 0.1\log \mathrm{Re}_p - 0.49 \quad , \quad 4\times10^5 \prec \mathrm{Re}_p \prec 10^6 \qquad 2.17$$

$$C_D = 0.19 - \frac{8\times10^4}{\mathrm{Re}_p} \quad , \quad \mathrm{Re}_p \geq 10^6 \qquad 2.18$$

$$\mathrm{Re}_p = \frac{\rho V^{2-n} d^n}{K} \qquad 2.19$$

The fact that most drilling fluids commonly used in drilling operations show non-Newtonian flow behavior calls for the need to estimate drag coefficient in this type of fluids.

Dedegil (1987) developed an expression for drag coefficient for Bingham plastic type fluids. He expressed his result as a function of Reynolds number for the three different flow regimes. Dedegil results were based on his experimental data.

$$C_D = \frac{24}{\mathrm{Re}_B} \quad , \quad \mathrm{Re}_B \prec 8 \qquad 2.20$$

$$C_D = \frac{22}{\mathrm{Re}_B} + 0.25 \quad , \quad 8 \prec \mathrm{Re}_B \prec 150 \tag{2.21}$$

$$C_D = 0.4 \qquad , \qquad \mathrm{Re}_B \prec 150 \tag{2.22}$$

$$\mathrm{Re}_B = \frac{\rho_f (u_f - u_s) d_p}{\mu_p} \tag{2.23}$$

Where μ_p is the plastic viscosity.

Shah (1982) expressed the drag coefficient of a power law fluid as an implicit function of the particle Reynolds number. He obtained an expression of the form given in equation (2.24)

$$\sqrt{C_D^{2-n}\,\mathrm{Re}_p^2} = A + \mathrm{Re}_p^B + C \tag{2.24}$$

Where A, B, and C are unknown constants which are functions of fluid model parameter n. The above equation is valid for Reynolds number greater than 0.01 but less than 100 and value of n greater than 0.281 but less than 1.

$$\mathrm{Re}_p = \frac{\rho_f V_t^{2-n} d_p^n}{8^{n-1} K} \tag{2.25}$$

V_t is the terminal settling velocity and K is the consistency index for the power law fluid.

Fang (1992) derived a correlation for power law fluid, as follows

$$C_D = \frac{50.28}{\mathrm{Re}^{0.875}} \qquad , \qquad \mathrm{Re} \prec 100 \tag{2.26}$$

Above this value of Reynolds number, C_D approaches a constant value of one.

$$\mathrm{Re}_B = \frac{\rho_f (u_f - u_s) d_p}{\mu_a}$$

Peden and Luo (1987) established a generalized correlation for the determination of drag coefficient for both power law and Newtonian fluids from experimental data. The generalized equation is given by equation (2.27)

$$C_D = \frac{a}{\mathrm{Re}_p^e} \qquad 2.27$$

For Newtonian fluids, "a" and "e" depends on the flow regime whereas for power law fluids, these variables depend on both the flow regime and the flow behavior index. For power law fluids, they derived empirical equations for the determination of "a" and "e" for different flow regime based on their experimental data. For non-spherical particles, the drag coefficient is a function of both the particle Reynolds number and particle sphericity ψ. Particle sphericity ψ is defined as the ratio of the surface area of a spherical shape having the same volume as the particle to the actual surface area of the particle. They developed following expressions for determination of the drag coefficient depending on the flow regime.

Laminar flow

$$\begin{array}{l} a = 39.8 - 9n \\ e = 1.2 - 0.47n \end{array} \quad , \quad \mathrm{Re}_p \prec 5, n \succ 0.45 \qquad 2.28$$

Transition flow

$$\begin{array}{l} a = 42.9 - 23.9n \\ e = 1 - 0.33n \end{array} \quad , \quad 1 \prec \mathrm{Re}_p \prec 200, \qquad 2.29$$

For non spherical particles, they introduced a shape correction factor F_s so that the expression becomes

$$C_D' = F_s C_D \qquad 2.30$$

Where

$$F_s = 1.5 - 0.5\Psi \quad , \quad \mathrm{Re}_p \prec 1 \qquad 2.31$$

$$F_s = 2.6 - 1.6\Psi \quad , \quad \mathrm{Re}_p \succ 1 \qquad 2.32$$

Acharya et al., (1976) based on experimental data developed a correlation for calculating the drag coefficient for power law fluids. Their correlation for drag coefficient is represented by equation (2.33).

$$C_D = \frac{24X(n)}{\mathrm{Re}_p} + \frac{F_1}{\mathrm{Re}_p^{F_2}} \quad , \quad \mathrm{Re}_p \prec 1000, 0.5 \le n \le 1 \qquad 2.33$$

Where

$$X = 3^{1.5(1-n)}\left(\frac{2 - 22n^2 + 29n}{n(n+2)(2n+1)}\right) \qquad 2.34$$

$$F_1 = 10.5n - 3.5$$
$$F_2 = 0.32n + 0.13 \qquad 2.35$$

Grahams and Jones (1995) also derived empirical correlation for the determination of drag coefficient for power law fluids from numerical analysis. For their correlation, the drag coefficient was expressed as a direct function of Reynolds number and flow behavior index.

$$C_D = \frac{35.2(2)^{1.03n}}{\mathrm{Re}^{1.03}} + n\left(1 - \frac{20.9(2)^{1.11n}}{\mathrm{Re}^{1.11}}\right), \qquad \frac{2^{n+1}}{10} \le \mathrm{Re}_p \le 4(2)^n, 0.4 \le n \le 1 \qquad 2.36$$

Darby (1996) developed an empirical correlation for the determination of drag coefficient for power law fluids from numerical analysis. The expressions for his correlation is given by equation (2.37).

$$C_D = \left(C_1 + 4.8\left(\frac{X}{\text{Re}}\right)^{0.5}\right)^{0.2} \quad , \quad \text{Re}_p \le 100, 0.4 \le n \le 1 \tag{2.37}$$

$$C_1 = \left(\left(\frac{1.82}{n}\right)^{8} + 34\right)^{-0.125} \tag{2.38}$$

$$X = \frac{1.33 + 0.37n}{1 + 0.7n^{3.7}} \tag{2.39}$$

Ceylan et al. (1999): based on the results of Lali et al. (1989) also develop correlations for the determination of the drag coefficient for power law fluids.

$$C_D = \frac{24X^*}{\text{Re}_p} \quad , \tag{2.40}$$

$$X^* = X \qquad \text{for} \quad , \quad \text{Re}_p \prec 10^{-5} \tag{2.41}$$

$$X^* = X + \left(\frac{1-n^2}{3n+1}\right)\log(0.001\text{Re}) \qquad \text{for} \quad , \quad 10^{-0.5} \prec \text{Re}_p \prec 10^{-3} \tag{2.42}$$

$$X^* = X + \left(\frac{4n^4}{24}\right)\text{Re}^{\frac{3-n}{3}} \qquad \text{for} \quad , \quad \text{Re}_p \ge 10^{-3} \tag{2.43}$$

Where

$$X = 3^{2n-3}\left(\frac{n^2 - n + 3}{n^{3n}}\right) \tag{2.44}$$

Matijasic and Glasnovic (2001) based on experimental result also developed a correlation for the determination of the drag coefficient of the power law fluids.

$$C_D = (\frac{24}{\mathrm{Re}})(-1.26n + 2.3) + 0.653 \quad , \quad \begin{matrix} \mathrm{Re}_p \prec 1000 \\ 053 \leq n \leq 1 \end{matrix} \tag{2.45}$$

For all the cases above, the Reynolds number is obtained using the expression,

$$\mathrm{Re}_p = \frac{\rho V^{2-n} d^n}{K}$$

V is the terminal settling velocity.

Chhabra (2002) carried out a detailed comparison of different correlations developed by the above authors and found out that correlation by Acharya et al. (1976) and Matijasic and Glasnovic (2001) gave the best result followed by that of Darby (1996).

Bases on the work done by Chhabra (2002), the following expressions for the determination of the drag coefficient will be used for this study.

$$C_D = (\frac{24}{\mathrm{Re}})(-1.26n + 2.3) + 0.653 \qquad 0.01<\mathrm{Re}_p<700 \tag{2.46}$$

$$C_D = \frac{24X(n)}{\mathrm{Re}_p} + \frac{F_1}{\mathrm{Re}_p^{F_2}} \, , \qquad 700 \leq \mathrm{Re}_p < 1000 \tag{2.47}$$

Where

$$X = 3^{1.5(1-n)}\left(\frac{2 - 22n^2 + 29n}{n(n+2)(2n+1)}\right)$$

$$F_1 = 10.5n - 3.5$$
$$F_2 = 0.32n + 0.13$$

$$C_D = \frac{30.0}{\mathrm{Re}_p} + \frac{67.289}{e^{5.03}} \qquad \mathrm{Re}_p \geq 1000 \tag{2.48}$$

Equation (2.46), (2.47) and (2.48) are the Matijasic and Glasnovic (2001), Acharya et al. (1976) and Chien (1994) models respectively for the determination of drag coefficient for power law fluid.

Lift Force. The lift force arises due to asymmetric distribution of the fluid velocity and/or due to turbulent eddy in the annular flow causing the cuttings to be lifted from the low side of the inclined annulus and be suspended in the fluid from where the cuttings are transported by drag force to the surface. The lift force supplied by the fluid is obtained by using:

$$F_L = \frac{1}{2} C_L A_S \rho_f u_f \qquad 2.49$$

Lift Coefficient. A correlation for the determination of the lift coefficient was proposed by Clark and Bickham which was developed for spherical particle given as;

$$C_{LE} = 5.82 \left(\frac{\frac{d}{2u_f} \left| \frac{\mathrm{du}}{\mathrm{dr}} \right|}{\mathrm{Re}_p} \right)^{\frac{1}{2}} \qquad 2.50$$

If $C_{LE} > 0.09$

Then

$$C_L = C_{LE} \qquad 2.51$$

But if $C_{LE} < 0.09$

Then

$$C_L = 0.09 \qquad 2.51b$$

Pressure Force. This is the force which results due to pressure gradient experienced when fluid flow pass a solid particle. Clark and Bickham (1994) showed that this force can be expressed as

$$F_{\Delta P} = \frac{2\tau_w \pi d^3}{3D_{hyd.}} \qquad 2.52$$

For the model developed in this project, the pressure force over a given section would be considered as the difference between the entry and exit pressures of that section.

2.3.3 Static Forces Acting on a Cutting in Inclined Wells.

Static forces acting on a cutting are comprised of the gravity force, the plastic force and the friction force between the cuttings and wellbore due to contact. This group of forces tends to hold the cuttings down in the low side of the hole which if therefore not overcome would result to cuttings bed formation.

Gravitational force. This is a measure of the weight of the cuttings. For inclined wells, a component of this force acts in opposite direction to the lift force and the other component against the drag force as shown in fig 2.4. The net effect of gravity force is to pull the cuttings back into the hole. The force of gravity on a cutting is given by equation (2.53).

$$F_g - F_b = g(\rho_c - \rho_f)V \qquad 2.53$$

Where 'V' is the volume of the cutting represented as;

$$V = \frac{\pi d^3}{6}$$

The cutting is assumed to be spherical with a diameter "d"

Plastic force. This force results due to the yield stress of the drilling fluid. A cutting sitting on a cuttings bed is positioned in the interstice of neighboring cuttings held stationary by the bed. The fluid in the interstice beneath the cutting would be stagnant and plastic while that at the upper portion is flowing. Clark and Bickham (1994) derived an expression for this force given by:

$$F_p = \frac{\pi d^2 \tau_y}{2}\left(\phi + \left(\frac{\pi}{2} - \phi\right) Sin^2\phi - Cos\phi Sin\phi\right) \qquad 2.54$$

Where ϕ is the cutting angle of repose.

For power law fluid which is the case with foam considered as the drilling fluid in this study, the plastic force is neglected.

Friction Force. The frictional force is another force in this group and acts at the point of separation between the cuttings and the wall of the wellbore tending to oppose the forward motion of the cuttings. This force acts in opposite direction to the drag force supplied by the fluid. When the frictional force is greater than the driving force acting to pull the cuttings out of the hole, the cuttings tends to settle down at the lower part of the wellbore to form a bed. The lift force in this case is assumed to be ineffective. From fig 2.4 an expression for the frictional force is obtained as given by equation (2.55).

$$F_{fr} = \mu\left(\left(F_g - F_b\right)\sin\theta - F_L\right) \qquad 2.55$$

Where the term μ is the coefficient of friction.

2.3.4 Force Analysis for the Rolling and Lifting Mechanism

For more accurate force analysis, two conditions are considered. The first is when the drilling fluid has sufficient force (velocity above the critical transport velocity) to transport all the cuttings to the surface with no cutting bed formation (zero bed height condition). The second case is that where the drilling fluid transport velocity is below the critical depositional velocity. This condition is termed the sub-critical flow condition and under this condition, cuttings will be deposited at the bottom of the wellbore and cuttings bed will form. As the cuttings bed builds up under the sub-critical flow condition, the area above the cuttings bed open to flow reduces causing the drilling fluid velocity above the bed to increase. The bed continues to build until the foam (drilling fluid) velocity above the bed increases to a certain critical value called the critical foam velocity that prevents further formation of cuttings bed. At this point an equilibrium bed height is attained. Any additional deposition of cuttings to this bed height will cause the foam velocity in the neighborhood (area open to flow) of that region to increase above the critical foam velocity. This sets up a stronger fluid force (turbulent dispersing force) which causes the protruding cuttings to be displaced thereby re-establishing the local equilibrium bed height. In other words, the steady state height of the bed is obtained when the velocity in the upper layer, which for this model is the layer of fluid containing suspended particles, is sufficient to support all the particle that are still suspended. Increasing flow rate at this point would increase the magnitude of the dispersing force causing an increase in the average concentration of cuttings in the upper layer and hence a reduction in the bed height.

2.3.4.1 Force Analysis for Rolling Mechanism.

The rolling mechanism is pronounced at high wellbore angle where the wellbore complementary angle is less than the cutting angle of repose ϕ (Clark and Bickham, 1994). The cutting angle of repose is simply the angle of inclination the wellbore makes with the horizontal above which the cutting begins to slide down to the lower part of the wellbore. Considering a cutting at equilibrium under the influences of the above listed forces as shown in fig 2.4 the following force balance equations is obtained for the rolling mechanism.

The resultant force in the x-direction

$$F_D + F_{\Delta P} - (F_g - F_b)Cos\theta - F_{fr} = F_X$$

$$F_{fr} = \mu((F_g - F_b)\sin\theta - (F_L - F_p))$$

$$F_p = 0$$

$$F_X = F_D + F_{\Delta P} - (g((\rho_s - \rho_f))\frac{\pi d^3}{6}Cos\theta - \mu((F_g - F_b)\sin\theta - F_L) \qquad 2.56$$

The term (friction portion) in the bracket becomes zero when

$$F_L \succ (F_g - F_b)\sin\theta$$

This is because under this condition, the cutting will be in a lifted position with no contact with the wellbore and hence the friction force would be zero.

For a cutting at equilibrium,

$$F_X = 0$$

μ in equation (2.56) is the coefficient of static friction. Iyoho (1980) indicated that the coefficient of static friction is 0.6 since cuttings slide down the wellbore under no flow condition when the wellbore makes an angle of about 60^0 with the horizontal. A close approximation for the value of the static friction coefficient is the tangent of the angle the wellbore makes with the horizontal at which the cutting bed will just begin to slide under no flow condition. This is approximately equal to the tangent of the cutting angle of repose. Gavignet and Sobey (1989) showed that for a sliding bed, the sliding coefficient of friction is less than half the coefficient of static friction of cuttings studied by Iyoho. For their model they suggested a sliding friction factor of 0.2. It should be noted however that correlations have also been developed for the determination of this coefficient (Ozbayoglu 2003).

2.3.4.2 Force Analysis for Lifting Mechanism.

The lifting mechanism occurs at intermediate and low wellbore angles. In this case, the cuttings while resting on the wall of the wellbore would not move in the radial direction but in the axial direction. The cutting would move up into the region where the axial velocity of the fluid moves it downstream (i.e. if the drag force is sufficient to move it to the surface) as shown in figure (2.4).

For the lifting case, the resultant force in the Y-direction is:

$$F_L + (F_b - F_g)\sin\theta = F_Y \qquad 2.57$$

For a cutting at equilibrium,

$F_Y = 0$

The resultant force pulling a cutting that have been suspended and drag toward the surface is given by:

$$F_R = \sqrt{F_Y^2 + \left(F_D + \mathrm{F}_{\Delta p} - \left(F_g - \mathrm{F}_b\right)\mathrm{Cos}\theta\right)^2} \qquad 2.58$$

Below is a summary of the cases of cutting transport mechanisms in inclined wells.

$\begin{pmatrix} F_X > 0 \\ F_Y \le 0 \end{pmatrix}$ Rolling mechanism is observed (sliding upwards)

$\begin{pmatrix} F_X < 0 \\ F_Y < 0 \end{pmatrix}$ Cuttings would slide down the hole to form cutting beds.

$\begin{pmatrix} F_X = 0 \\ F_Y < 0 \end{pmatrix}$ Neither rolling nor lifting mechanism present (cuttings at equilibrium)

$\begin{pmatrix} F_X < 0 \\ F_Y = 0 \end{pmatrix}$ No lifting mechanism but cuttings slides downwards

$\begin{pmatrix} F_X = 0 \\ F_Y = 0 \end{pmatrix}$ Neither rolling nor lifting mechanism present (cuttings at equilibrium)

$\begin{pmatrix} F_X \le 0 \\ F_Y > 0 \end{pmatrix}$ Lifting mechanism is observed (cuttings would be suspended)

And

$\begin{pmatrix} F_X > 0 \\ F_Y > 0 \end{pmatrix}$ Cuttings would be lifted and dragged in suspension to the surface.

Considering the effect of these forces, cuttings can be effectively transported to the surface if the dynamic forces are optimized so as to overcome the static forces and still have sufficient energy to transport the cuttings to the surface without eroding the wellbore. This can be achieved by optimizing operating conditions of the drilling fluid and drilling operation as would be discuss in a later chapter.

Clark and Beckham(1994) showed that the fluid velocity needed to dislodge the cutting for either the lifting or the rolling mechanism can be determined by expressing the dynamic forces acting on the stationary cutting as a function of local fluid velocity.

2.4 Critical Conditions for Cuttings Transport in Wells.

Different conditions are being used as critical conditions for effective cutting transport in wells. The specification of critical condition during cutting transport is necessary to prevent cutting deposition which would eventually result to bed formation. The determination of these conditions is vital to the field engineers as they are useful in setting the lower pump rate limit.

Different authors have used different criteria as critical conditions in cuttings transport to prevent cuttings bed formation. Clark and Bickham (1994) and Ford et al. (1996) used the minimum transport velocity as the critical condition for effective cuttings transport. They developed their model for the prediction of this velocity based on the balance of forces acting on a cutting in the annulus for both the sliding and the saltation cases. This method for predicting critical condition is not common in slurry transport in pipes because of the uncertainty involved in the determination of the lift force in a multi-particle system. Oroskar and Turian (1980) developed a more superior model which takes into account the fluid properties, solid characteristics and pipe geometry to predict a critical depositional velocity for cuttings transport in horizontal wells. Their model was based on balancing the energy needed to suspend the particle with the effective energy dissipated by the turbulent eddies in the flow. Their expression for horizontal flow is given by:

$$\frac{V_D}{\sqrt{gd_p\left(\frac{\rho_s-\rho_f}{\rho_f}\right)}}=1.85C_s^{0.1536}\left(1-C_s\right)^{0.3564}\left(\frac{d_s}{D}\right)^{-0.378}\tilde{N}_{Rc}^{0.09}X^{0.30} \qquad 2.59$$

Where $\tilde{N}_{\mathrm{Re}}$ is the modified Reynolds number defined by

$$\tilde{N}_{\mathrm{Re}} = \frac{D\rho_f}{\mu}\sqrt{gd_p\left(\frac{\rho_s - \rho_f}{\rho_f}\right)} \tag{2.60}$$

For foam drilling, the effective viscosity is given by

$$\mu = K\left(\frac{3n+1}{4n}\right)^n\left(\frac{8u_f}{D}\right) \tag{2.61}$$

The Oroskar and Turian correlation had been modified by Campos (1997) for application in inclined wells by incorporating the inclination effect. This modification is shown in the expression modified by Campos given by equations (2.61b to 2.61c).

$$\frac{V_D}{\sqrt{gd_p\left(\frac{\rho_s-\rho_f}{\rho_f}\right)Sin\theta}} = 1.85C_s^{0.1536}(1-C_s)^{0.3564}\left(\frac{d_s}{D_2}\right)^{-0.378}\tilde{N}_{\mathrm{Re}}^{0.09}X^{0.30} \tag{2.61b}$$

$$\tilde{N}_{\mathrm{Re}} = \frac{D\rho_f}{\mu}\sqrt{gd_p\left(\frac{\rho_s - \rho_f}{\rho_f}\right)Sin\,\theta} \tag{2.61c}$$

Another factor which is sometimes used as critical condition is the critical cuttings concentration. The idea here is that above the certain cuttings concentration, cuttings would deposit and cuttings bed would be formed and vice-versa. Many authors have used different techniques in an attempt to determine this concentration. Doron et al. (1987) used the well-known diffusion equation to represent solids dispersion in fully suspended flow. Solving this equation, the average concentration of cuttings in the fully suspended flow is obtained which is taken as the critical cuttings concentration.

2.5 Experimental Studies of Cutting Transport in Inclined wells

Okrajni and Azar (1986) experimentally investigated the effect of mud rheology using water and bentonite/polymer mud on cuttings transport in directional wells. From their studies they observe three separate regions of hole inclination regarding cuttings transport; 0^0-45^0, 45^0-55^0 and 55^0-90^0 with effect of laminar flow dominating at low angle wells (0^0-45^0) and turbulent flow effect at higher angle well (55^0-90^0) while between 45^0-55^0, both turbulent and laminar flow have similar effect. They observe worst cuttings transport between 40^0-45^0 inclinations when flow rate is relatively low. Considering the effect of drilling fluid rheology, investigation showed that drilling fluid yield point affects the cuttings transport process for laminar flow especially when the inclination angle is between 0^0-45^0 but diminishes or becomes negligible between 55^0-90^0 inclinations. They showed that YP/PV ratio affects the cuttings transport process for the whole range of inclination angles. Further investigation reveals that drilling fluid rheology (yield value and YP/PV ratio) have no effect on turbulent flow and that annulus eccentricity has little effect for low angle wells and effect becomes moderate for high angle wells (55^0-90^0) under turbulent flow and significant when the flow becomes laminar.

Ford et al. (1990) presented an experimental investigation of drill cuttings transport in inclined wells using a 21' long borehole simulator to determine the effects of various drilling parameters on the circulation rate required to prevent cutting bed formation. They found out that two different mechanisms are responsible for cuttings transport in inclined wells; the sliding/ rolling mechanism in which the cuttings moves along the low side wall of the annulus and the cuttings are transported in suspension. They concluded that the minimum transport velocity corresponding to the two transport mechanisms were affected by different variables such as hole-angle, fluid viscosity, inner pipe rotation and cutting size. They also found out that there are about seven possible slurry flow patterns namely; homogeneous suspension, heterogeneous suspension, suspension/saltation or saltation/suspension, sand cluster, separated moving bed, continuous moving bed, and the stationary bed.

2.6 Empirical and Mechanistic Model of Cuttings Transport in Inclined wells

Doron et al. (1987) developed a two layer model with a heterogeneous suspension as the upper layer and a lower bed layer made of cuttings which are assumed to be uniformly compacted. This lower layer may either be moving or stationary. Neglecting slip between phases in each layer, two continuity equations for developed steady state flow were formulated for both the solid and the liquid phase. The model also consists of force balance equations for the upper dispersed layer and the lower moving bed layer. The force acting at the bottom of the well has two components: the dry friction force and the hydrodynamic resistance force due to the motion of the bed. The above four equations together with the turbulent diffusion equation which is used to obtain the mean cutting concentration in the second layer and operational conditions and physical properties of the two phases were solved to obtain the mean velocity in the upper layer, the mean velocity of the bed, the mean concentration in the second layer, the cutting bed height, and finally pressure drop.

Gavignet and Sobey (1989) developed a two layer mechanistic model for cutting transport in deviated wells. The model consisted of an upper layer of clear fluid and a lower layer of closely packed bed with cutting concentration of about 0.52. Mathematically, the model is made up of simple steady state momentum equations for both the upper and lower layers. They also presented an approach to determine hydraulic perimeter, area of each layer, frictional factor for the pure liquid and solids. . Gavignet and Sobey proposed that the sliding friction coefficient is usually less than half of the static friction coefficient. They used a sliding friction factor of 0.2 for the determination of the moving bed velocity and bed height based on Iyoho model. Iyoho suggested that with no flow, a cuttings bed would slide down the wellbore at an angle of about 60^0 which gives a static friction coefficient of about 0.6 (the tangent of 60^0).

Luo et al. (1992) developed an empirical model based on the forces acting on the cuttings to predict the critical-flow rate required to prevent the formation of cutting bed in deviated wells. Using the Buckingham PI theorem, four dimensionless groups were developed from seven dimensionless variables. The model developed was validated with experimental results obtained from an 8" wellbore simulator located at BP Research center Sunbury, and with field data from 8-1/2", 12-1/4" and 17-1/2" holes. Based on this model, a computer program and simple to use charts for planning and drilling of deviated wells were also developed. A correlation for critical flow rate determination based on two dimensionless groups which are believed to have significant effect on cutting transport process was formulated. This correlation is expressed as

$$\frac{V_c^{*2}}{d_s\left(\frac{\rho_s-\rho_f}{\rho_f}\right)Sin\theta}=a'\left(\frac{d_s V_c^{*}\rho_f}{\mu_a}\right)^{b'} \qquad 2.62$$

The empirical coefficient a' and b' were obtained from regression analysis.

Martins and Santana (1992) developed a two layered mechanistic model with an upper liquid layer containing suspended solid and a lower layer of cutting bed which can either be moving or stationary. The model consists of two continuity equations for the solid and liquid phase and two momentum equations for the upper and lower layer.

Clark and Bickham (1994) presented a mechanistic model based on the analysis of the forces acting on a single cutting in the annulus for both the rolling and the lifting case in combination with other auxiliary equations to obtain the critical fluid velocity (as a function of operational parameters, wellbore configuration and cutting characteristics) needed to initiate flow of cuttings during either the rolling or lifting transport mechanism. They concluded that three mechanisms are responsible for cutting displacement; rolling, lifting and the settling. The mechanism that dominates at any time depends on the angle of inclination.

Ford et al. (1996) also developed semi-empirical, mathematical models and a computer program based on experimental data obtained by Ford et al. (1990) and Peden et al. (1990) , that can be used to determine the minimum transport velocity for efficient hole cleaning. For the computer program, the rheological properties of the fluid were represented by the general Herschel-Bulkley model. They also investigated the removal of cutting beds when formed. The program was used to investigate the effect of hole-angle, transport mechanism and drill pipe diameter on the minimum transport velocity. It was also used to define an appropriate rheological model for fluid and to investigate the velocity profile in the annulus.

Larsen et al. (1997) developed an empirical model based on the combination of their experimental data (1990) generated in a 35'long and 5" diameter flow loop with basic theoretical principles to predict the critical fluid transport velocity needed in highly inclined wellbore and horizontal wells to prevent the formation of cutting bed and also to predict the annular cuttings concentration when the fluid velocity is below the critical transport velocity. They established empirical correlations, which express the cuttings concentration as a function of penetration rate and the equivalent slip velocity as a function of the fluid apparent viscosity. By incorporating the correction factors for the angle of inclination, cutting size and the drilling fluid weight into the equivalent slip velocity, a generalized equivalent slip velocity was obtained which was added to the cutting velocity to obtain the critical transport fluid velocity.

Kamp and Rivero (1999) developed a two layered model for cutting transport in highly inclined wells. The model consisted of mass balance equations for solid, liquid and the cutting bed and momentum equations for the heterogeneous layer and the bed. In this model, the cuttings bed height was governed by the mass flux of cuttings per unit interface that are deposited and that which is re-suspended. The former was found to be proportional to the mean cuttings concentration and the velocity of the suspension whereas the latter is a function of the interfacial shear stress. The model did not give the expected decrease in bed height with increase in the flow rate, results were not very sensitive to viscosity in contrast to experimental and field evidence. When comparing the experimental results with prediction of correlation, it was observed that although it gives similar trend, the model over predicted cuttings transport at a given liquid rate.

Ozbayoglu et al. (2003) developed a mechanistic one dimensional three layer model using the principle of mass and momentum conservation for a steady, isothermal flow condition. The three layer model consists of a clear fluid upper layer, a fluid and solid suspension as second layer and a stationary bed which is uniformly compacted as the third layer. In their model they also developed an empirical correlation for the determination of coefficient of static friction from experimental data. This model was developed for foam drilling but can be applied to other underbalanced drilling operations. With the mass and momentum balance equations, together with other auxiliary equations they determined the cuttings bed thickness, the velocity of each layer, the in-situ cuttings concentration of the suspension and the total pressure drop.

Kelessidis et al. (2003) developed both a two and a three layer model for cutting transport in inclined wells. The three layer model is an extension of the two layer model by the addition of a stationary bed layer as the third layer. For the two layer model, they consider an upper layer of fluid containing a suspended solids and a lower layer of solids which is moving. They developed two mass balance, two momentum equations and a turbulent diffusion equation i.e. five equations with five unknown which they solved considering other five auxiliary equations.

Doan et al. (2003) developed a two layered transient model with an upper layer of fluid with suspended solid and a lower layer of moving bed. Three time dependent mass equations and three time dependent momentum equations were developed for the fluid component and the solid component in suspension and the moving bed. The velocity of deposition and velocity of entrainment were used to represent the mass transfer rate between the suspension and the moving bed. The velocity of deposition was assumed to proportional to the hindered terminal settling velocity while the velocity of entrainment was a function of the interfacial velocity.

2.7 Physical Properties of Foam.

2.7.1 Foam.

Foam is an agglomeration of gas bubbles separated from each other by thin liquid films Bickerman (1973). Foam can be unstable, transient or stable depending upon the presence and nature of the components in the liquid. The gas is usually stabilized by surfactant

2.7.2 Classification of Foam

Foam can be classified using different criteria. Based on gas content, foam can be considered to be either wet or dry. Foam is considered "wet" when the gas bubbles are spherical and with large amount of liquid between the bubbles. For dry foam, the bubbles are polyhedral in shape with very small amount of liquid between the bubbles. Wet foams generally have low quality while dry foams have high quality.

Considering texture, foam can be classified into fine and coarse foam. Fine foams are those with small bubbles and coarse foams are those with large bubbles. Based on stability criterion, foam can be classified into two extreme types: Metastable (permanent foam) and unstable foam (transient foam). Foams generally are thermodynamically unstable because of their high interfacial energy. The fact that the liquid phase is denser than the gaseous phase makes the separation or drainage of the liquid phase from the foam itself spontaneous. This separation of phases or the drainage of one phase from the other phase causes instability and change in the physical properties of foam. The stability of foam however can be improved by certain physical processes such as circulation and agitation or by the addition of certain chemicals such as surfactant. These processes improve the stability of foam by reducing the interfacial energy and hence ensuring an excellent dispersion of the gaseous phase in the liquid phase.

The foam quality which is a measure of the amount of gas dispersed in the liquid phase defined as the ratio of the volume of gas to the volume of the foam is another criteria which can be used for the classification of foam. The foam quality (Γ) has value ranging from 0 to 1 depending on the amount of gas in the foam. The expression for the foam quality is given by:

$$\Gamma = \frac{V_g}{V_g + V_L} \qquad 2.63$$

Based on the criterion of foam quality, foam can be classified into: Dispersion when foam quality is less than 52%, wet foam when it is between 52% and 74%, and dry foam when it is between 74% and 96%.

The presence of gas component in foam makes it quality to change with temperature and pressure. The real gas law can be used to determine the gas volume ratio at different temperature and pressure. With the volume of gas in the foam at condition 1 known, the volume of gas in the foam at another condition of temperature and pressure can be obtained by using;

$$V_{g2} = V_{g1}\left(\frac{Z_2 P_1 T_2}{Z_1 P_2 T_1}\right) \qquad 2.64$$

The volume of foam at another condition of temperature and pressure can be obtained by using;

$$V_2 = V_1\left((1-\Gamma_1) + \frac{Z_2 P_1 T_2}{Z_1 P_2 T_1}\Gamma_1\right) \qquad 2.65$$

The gas density at the new condition can be obtained by using:

$$\rho_{g2} = \rho_{g1}\left(\frac{Z_1 P_2 T_1}{Z_2 P_1 T_2}\right) \qquad 2.66$$

The foam quality at the new condition can be calculated by combining equation (2.63) and (2.64) to obtain:

$$\Gamma_2 = \left(1 + \left(\frac{1-\Gamma_1}{\Gamma_1}\right)\left(\frac{Z_1 P_2 T_1}{Z_2 P_1 T_2}\right)\right)^{-1} \qquad 2.67$$

The Z- factor (gas deviation factor) in the equations above is obtained using a Yarborough and Hall approach (1974).

2.7.3 Foam Density.

The change in the volume of the gas phase of foam with change in temperature and pressure will cause the density of the foam to change. For foam flow, it is assumed that the liquid volume does not change with temperature and pressure i.e. the volume of the liquid phase is constant. For a particular pressure and temperature condition, foam is treated as a homogenous fluid and the density can be calculated by using:

$$\rho_f = \Gamma\rho_g + (1-\Gamma)\rho_L \qquad 2.68$$

To obtain the density of foam at different temperature and pressure, equations (2.65), (2.67) and (2.68) are combined:

$$\rho_{f2} = \frac{\rho_{f1} Z_1 P_2 T_1}{Z_1 P_2 T_1 (1-\Gamma_1) + Z_2 P_1 T_2 \Gamma_1} \qquad 2.69$$

2.7.4 Foam Rheology.

Several models have been suggested to describe the rheology of foam. These models suggest that foam can be classified into one of the following class of fluid: Power law fluid, Bingham plastic fluid or yield power law fluid.

Wise (1951), Raza and Marsden (1967), David and Marsden (1969), Wendorff and Ainley (1981), Sanghani and Ikoku (1983), Harris (1995), and Enzendorfer (1995) investigated foam rheology and found that foam behaves as a pseudo plastic fluid (power law fluid) and its rheology could be expressed by equation (2.70).

$$\tau = K(\gamma)^n \qquad 2.70$$

Mitchell (1969), Krug and Mitchell (1972), Beyer et al. (1972), Blauer et al. (1974), Calvert and Nezhati (1987) and Khan et al. (1988) investigated foam rheology and found that foam behaves as a Bingham plastic fluid and its rheology could be expressed by equation (2.71).

$$\tau = \tau_y + \mu_p \gamma \qquad 2.71$$

Wenzel et al. (1970), Cawiezel and Niles (1987), Reidenbach et al. (1986) Burley and Shakarin (1992), Bonilla et al. (2000), Sani et al. (2001) and Lourenco (2002) also investigated foam rheology and found that foam behaves as a yield pseudo plastic fluid also called the Herschel Buckley fluid and its rheology can be expressed by equation (2.72).

$$\tau = \tau_y + \mu_p \gamma^n \qquad 2.72$$

Valko and Economides (1992), Winkler et al (1994), Argillier et al (1998), Winkler et al. (1998) and Gradiner et al (1998) applied the volume equalized principles to describe the rheology of foam. The principles states that all volume equalized shear-stress and volume equalized shear-rate points obtained at different qualities and different geometries collapse into one curve in isothermal conditions.

Li (2004) based on Sanghani and Ikoku (1983) experimental results developed correlations for the determination of n and K through regression analysis. He found that two different correlations exist for two different ranges of foam quality. When the foam quality is less or equal to 0.915, exponential relationship exists between n and k and foam quality but above a quality of 0.915, a linear relationship exist. The equations developed by Li (2004) are given by equations (2.73) to (2.76).

For $\Gamma \leq 0.915$

$$K = 0.0074.e^{3.5163.\Gamma} \qquad 2.73$$

$$n = 1.2085.e^{-1.9897\Gamma} \qquad 2.74$$

For $0.98 > \Gamma > 0.915$

$$K = -2.1474\Gamma + 2.1569 \qquad 2.75$$

$$n = 2.5742\Gamma - 2.1649 \qquad 2.76$$

These correlations developed by Li (2004) will be used for the proposed model in this study.

David and Marsden (1969) carried out both theoretical and experimental studies on foam rheology considering both fluid slippage at the wall and semi-compressibility of foam and came up with the conclusion that foam exhibit a pseudo-plastic fluid behavior. They also observed that when slippage and compressibility is considered in the determination of apparent viscosity that it is independent of foam quality and that the apparent viscosity corrected for slippage still increases with tube diameter. They related the rheology of foam not only to the quality but also to the texture and stability of foam.

Wenzel et al. (1970) based on their experiment conducted by using a cone and plate viscometer and a concentric capillary viscometer concluded that foam is a yield power law fluid.

Blauer et al (1971) in their work, methods for prediction of frictional pressure losses in laminar, transitional and turbulent flow regime for foam flow in pipe flow was described. The Reynolds number and fanning friction factors used for the calculation of the pressure losses were calculated using effective foam viscosity, actual foam density, average velocity and true pipe diameter. They also found out that the Reynolds number and fanning friction factor for foam was similar to that of single phase fluid. Using experimental data, they expressed foam viscosity and yield as a function of foam quality. They also expressed the foam density as a function of foam quality neglecting the contribution of the gas phase and concluded that foam behaves like a Bingham plastic fluid.

Beyer et al. (1972) based on their experimental data developed explicit function for the determination of frictional pressure drop in vertical pipes and annuli. They observed slippage at the pipe wall and concluded that liquid volume fraction is the principal independent variable that affects foam flow behavior and that the total foam velocity is made of a slip component and a fluidity component.

Bonilla et al. (2000) conducted experiments using both aqueous and gelled foams and from their result concluded that the flow behavior of foam can be represented by yield power law model. For foam flow they also concluded that there is no slip at the wall.

Lourenco et al (2000) based on their experiments on foam stability developed correlations for the determination of flow behavior index and consistency index in terms of foam quality.

$$n = a_1^{'}\left(\frac{1-\Gamma}{\Gamma}\right)^{a_2^{'}} \qquad 2.77$$

$$K = b_1^{'}\left(\frac{1-\Gamma}{\Gamma}\right)^{b_2^{'}} \qquad 2.78$$

Martins et al (2001) obtained values for regression coefficients $a_1^{'}$, $a_2^{'}$, $b_1^{'}$ and $b_2^{'}$ which were given as 0.8242, 0.5164, 0.0813 and -1.5909.

Sanghani and Ikoku (1983) based on experiments conducted in a concentric annular viscometer to determine the rheology of foam concluded that the foam behaves like a power law fluid. They expressed the flow behavior index, n, and the fluid consistency, K, as function of foam quality and observed that effective viscosity increases with increasing shear rate. They concluded that for best drilling result, drilling operation should be carried out in laminar flow region with the foam quality at the bottomhole not less than 55%. They also recommended that the foam quality at any point in the wellbore should not exceed 96% otherwise foam would be unstable and break to form mist.

Ozbayoglu et al (2002) investigated foam rheology and observed that foam can be treated as either power law fluid or Bingham plastic fluid depending on the foam quality. When the foam quality is between 70-80% foam is treated as a power law fluid, but as a Bingham plastic fluid when the foam quality is above 90%. They suggested that texture and bubble size should be included in a rheological model for foam in order to develop a general model.

2.7.5 Foam Viscosity

Mitchell (1969) based on his work on foam rheology concluded that foam behaves like a Bingham plastic fluid with no slippage observed at the wall. He also found out that foam viscosity depends on both foam quality and shear rate and developed empirical correlations to determine foam viscosity for two ranges of foam quality:

When foam qualities is between 0 to 54%

$$\mu_f = \mu_L(1.0 + 3.6\Gamma) \tag{2.79}$$

When foam qualities is between 54% to 97%

$$\mu_f = \frac{\mu_L}{\left(1.0 - \Gamma^{0.49}\right)} \tag{2.80}$$

Mitchell (1971) based on Einstein's and Hatschek's theories and his experimental results divided foam rheology into four regions using foam quality. Foam with quality between 0 to 54% falls into the first region called the dispersed bubble region. In this region foam is Newtonian. Foam with quality between 54 to 74% falls into the second region called the zone of bubble interference. The third region is for foam quality between 74 to 97%, in this region the foam undergoes full bubble deformation. The fourth region is for foam with quality above 97%, this region is characterized by slug and mist flow.

Others who developed correlations for the determination of foam viscosity are Einstein (1906) and Hatschek (1910). Einstein (1906) developed viscosity correlation for uniformly dispersed region with foam quality less than 52% based on energy balance given as:

$$\mu_f = \mu_L(1.0 + 2.5\Gamma) \tag{2.81}$$

Hatschek (1910) also developed correlations for the determination of foam viscosity for two ranges of foam quality. The first correlation was for foam quality between 0 and 74%. This correlation was based on Stoke's law for a slowly falling ball.

$$\mu_f = \mu_L(1.0 + 4.5\Gamma) \tag{2.82}$$

When foam quality is between 74% and 96%, the correlation developed was based on conservation of energy during interference, deformation, and passage of packed bubbles within a flow boundary.

$$\mu_f = \frac{\mu_L}{\left(1.0 - \Gamma^{\frac{1}{3}}\right)} \qquad 2.83$$

Equations (2.80) and (2.83) can be applied only at very high shear rate where the foam viscosity becomes almost independent of shear rate.

2.7.6 Foam Stability

Foam being a two-phase system has a considerable amount of interfacial energy which accounts for the significant amount of surface free energy. Instability of foam may result from the separation of phases in foam or due to the merging of smaller bubbles to form large bubbles. The fact that the liquid phase is denser than the gaseous phase makes the separation or drainage of the liquid phase from the foam itself spontaneous. This separation of phases or the drainage of one phase from the other phase causes instability and change in the physical properties of foam. The decomposition of foam decreases the surface free energy. Ross (1969) observe that there are two spontaneous processes that control the decomposition of foam, the diffusion of gas through the liquid film resulting to the formation of larger bubbles and the rupturing of liquid film. Friberg and Satio from their experimental result on foam stability using different surfactant association structures and their combination observed that liquid crystal affects stability. Buscall et al from their work observed that stable foam are formed by the addition of sodium chloride and potassium thiocyanate. This stability was attributed to charge-stabilized foam film formed from the surfactants with the film made of anions drawn from the solution.

2.8 Cuttings Transport with Foam

Using the modified Buckingham-Reiner equation and rheological model of Mitchell (1969) to analyses foam flow in pipe and annulus, Krug and Mitchell (1972) developed charts for the determination of minimum volume of liquid and gas, and the injection-pressure required for foam drilling operation.

Okpobiri and Ikoku (1986) using an iterative approach developed a procedure for the determination of the minimum foam velocity and required wellhead injection pressure for effective cuttings transport. Semi-empirical correlations for the determination of frictional losses due to solid in the foam-cuttings mixture and a model for the determination of pressure drop across the bit due to foam flow which takes into consideration the compressibility of the foam were developed. In their study, foam-cuttings flow was assumed homogeneous and suggested that for effective cutting transport, the fluid velocity at the bottom should be at least 10% higher than the terminal velocity at the same depth.

Guo et al. (1995) developed an analytic model that can be used to calculate bottomhole pressure when drilling with foam in deviated wells. Their model was similar to that of Okpobiri and Ikoku's (1986) model except for the fact that solid friction factor of the cuttings was not taken into account. For this reason, the bottomhole pressure obtained by their approach was lower than that predicted by the Okpobiri and Ikoku's (1986) approach.

Assuming the compressibility of gaseous phase as one, Buslov et al. (1996) used an iterative computational procedure to calculate pressure losses associated with foam flow. In their study, Mitchell's (1969) viscosity model was used to determine the viscosity of foam.

Owayed (1997) developed a model similar to that of Okpobiri and Ikoku (1969), but unlike the latter he accounted for reservoir influx (water) in his model.

Capo (2003) conducted experiments on cuttings transport with foam for intermediate inclined angled wells using the LPAT-TUDRP flow loop at the University of Tulsa. He focused his studies on the effect of inclination angle, foam viscosity, foam velocity and rate of penetration on the cuttings transport process. He also went further to develop a simulator that computes pressure, flow velocity and foam quality along the wellbore under typical wellbore flow conditions. The result from experiment indicated that lower foam quality had lower cuttings accumulation and that the worst cuttings transport for inclined wells occur at around 55-65 degree inclination.

Ozbayoglu et al. (2003) developed a mechanistic one dimensional steady state three layer model for cuttings transport with foam for horizontal and highly inclined wells. An empirical correlation for the determination of static friction coefficient was established from experimental data. Their model was developed for foam drilling but can be applied to other underbalanced drilling operations. They assumed slippage exist between the solid cuttings and the foam in the suspension.

Li (2004) developed a one-dimension transient model which was solved numerically using a method presented by Crowe (1998) a modified form of the numerical method developed by Patankar (1980) to solve two phase flow. He assumed an initial fully suspended flow but cuttings would be deposited when the concentration of cuttings in the annulus goes above a critical value. He used an iterative computation procedure to calculate the pressure losses across the drill pipe and the annulus and developed a model for the calculation of pressure drop across the bit. With this model he was to predict the combination of gas-liquid injection rates and backpressure that would give good cleaning and maximum rate of penetration while keeping the bottomhole pressure minimum.

CHAPTER 3

DEVELOPMENT OF MECHANISTIC MODEL OF CUTTINGS TRANSPORT WITH FOAM IN INCLINED WELLS

A one-dimensional, transient mathematical model is developed to study cuttings transport with foam in inclined wells. A detailed description of the model development is presented in this chapter.

3.1 Model Development

In this study a two layer model is developed to investigate cuttings transport with foam in inclined well. A schematic view of two-layer model for foam-solid flow in inclined well is shown in Fig 3.1. The upper layer is made of foam with suspended cuttings having a low solid concentration and the lower layer a bed of solid cuttings which is either stationary or moving. The cuttings bed layer is considered to be uniformly compacted with cuttings concentration of 0.52. The pores are considered to be completely filled with foam. The two layer model in studying cuttings transport in inclined wells has been adopted by different researchers. Ford et al. (1990), Luo et al. (1992), Clark and Bickham (1994) and Kamp and Rivero (1999) carried out their studies considering a two layer model in which the lower layer is a stationary bed. Gavignet and Sobey (1989), Martin and Santana (1992), Kelessidis et al. (2003), and Doan et al. (2003) carried out their studies of cuttings transport in inclined well using a two layered model in which the lower layer is a moving bed.

The following assumptions are made for the development of the foam drilling model in inclined wells:

(1) Foam is considered as a homogeneous non-Newtonian fluid whose rheology can be represented by power law model.

(2) The cuttings are assumed to be spherical with uniform sizes, shape and velocity at any cross-sectional area of the well.

(3) Inflowing reservoir fluids commingle with the drilling foam completely.

(4) Inflowing reservoir fluids accelerate to the mean stream velocity instantaneously

(5) There is slippage between the foam and the solid cuttings

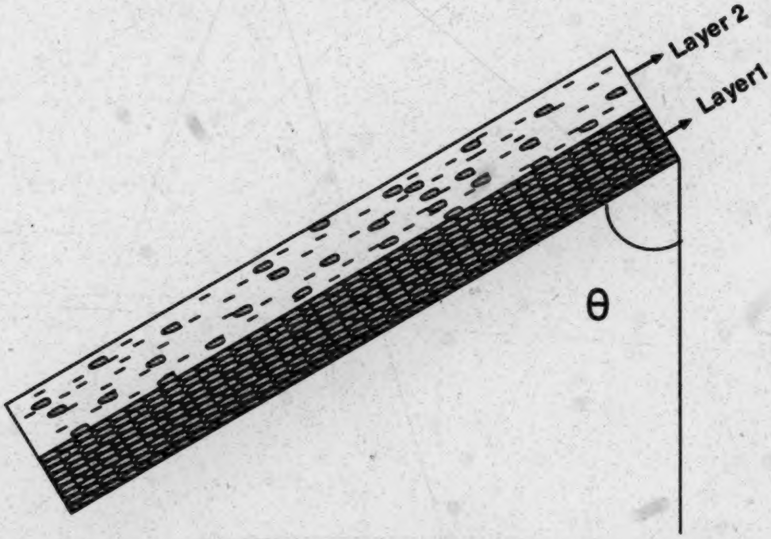

Fig 3.1 Schematic view of two-Layer model for cuttings transport with foam in inclined wells

3.1.1 Geometry of Cutting Transport Model

The two layer model is composed of an upper heterogeneous layer which is made of cuttings (the disperse phase) suspended in foam (the continuous phase). Below this layer is the cuttings bed layer which is made of particles that are cubically packed with a particle concentration of 0.52. The upper layer has a cross sectional area denoted by A_2 and two wetted perimeters; the first one is along with the drill pipe (arc GHF) and the second one is along with the wellbore (arc CFD). The sum of these two wetted perimeters gives the total wetted perimeter for the upper layer (S_{s-w} or S_{f-w}). Similarly, the lower cuttings bed layer has a cross sectional area of A_1 and two wetted perimeters; the first one is along with the drill pipe (arc GIF) and the second one is along with the wellbore (arc CED), which sums up to give the total wetted perimeter for the lower layer represented as S_{B-w}. The wetted perimeter between the upper and the lower layers is represented by S_i (length CG plus length FD). See figure 3.2 for details.

In the derivation of the wetted perimeters and cross sectional areas, three different pipe positions in relation to the cuttings bed are considered. The inner radius of the pipe is taken as r_i while the outer radius of the pipe is taken as r_o.

The hydraulic diameter is given by:

$$D_h = \frac{4A}{S} \qquad 3.1$$

Where A is the total area of the annulus open to flow and S is the total wetted perimeter.

$$A = \pi(r_o^2 - r_i^2) \qquad 3.2$$

r_i is the radius of the hole and r_o is the outer radius of the pipe.

$$S = 2\pi(r_o - r_i) \qquad 3.3$$

$$D_h = 2(r_o - r_i) \qquad 3.4$$

Determination of S_i, $S_{S\text{-}w}$, $S_{B\text{-}w}$. The values of the wetted perimeters will depend on the eccentricity of the pipe. The eccentricity is simply a measure of the distance between the center of the pipe and the centre of the hole. Eccentricity $\in$ is defined as

$$\in = \frac{L}{r_o - r_i} \qquad 3.5$$

L is the distance from the center of the pipe to the center of the hole. Eccentricity is positive when the pipe is positioned toward the bottom of the hole, and negative positioned toward the top the hole. The distance between the bottoms of the pipe and the borehole wall shown as "y" in figure 3.2 is obtained using;

$$y = (r_o - r_i)(1 - \in) \qquad 3.6$$

For determination of geometry, three cases are usually considered.

1.The pipe is above the cutting bed.

2.The pipe is partially covered by the cutting bed.

3.The pipe is completely covered by the cutting bed.

A detailed analysis of each case and derived expressions for the different geometry are shown in appendix D.

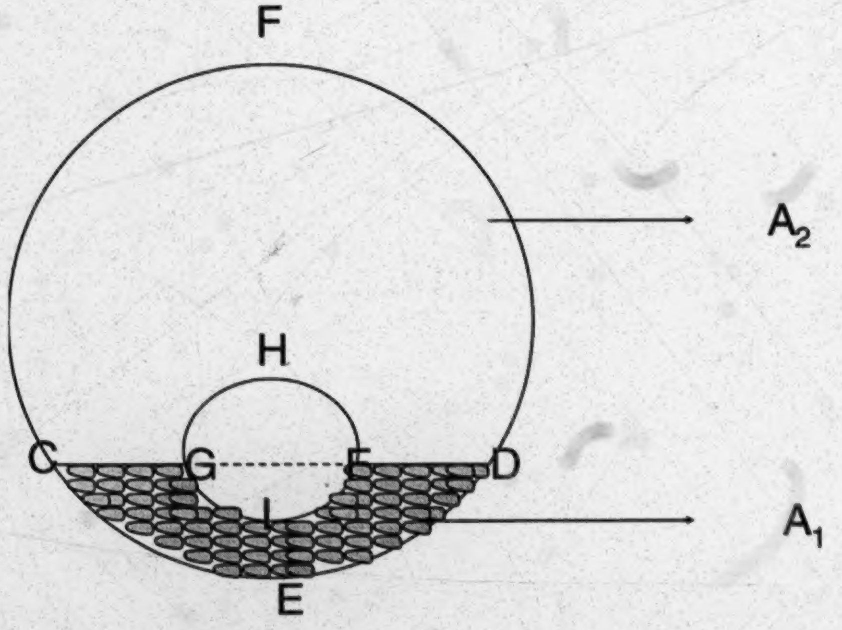

Fig 3.2 Two-Layer model for cuttings transport with foam in inclined wells

3.1.2 Forces Acting on Cuttings within the Control Volume

Certain forces act within the control volume which are responsible for the change in momentum within each layer and determine the direction in which each layer would move. Below is the description of these forces:

1. The pressure force is due to pressure differential at the entrance and exit of the control volume. The pressure forces considered in this model are those due to the suspended solids, fluid in the suspension and the one due to the cuttings bed if it is moving.
2. The drag force is due to the viscous and pressure drag of the fluid on the cuttings. The drag forces considered in this model include the one due to solids in the suspension and that due to the fluid itself.

3. The gravity force is due to the weight of the cuttings within the suspension, that due to the fluid itself and that due to the cuttings bed.

4. Shear forces are due to contact of the suspension with the wall of the pipe, borehole, and also due to interfacial contact between the suspension and the cuttings bed.

5. The frictional force at the surface of separation between the cuttings bed and the wall of the wellbore which acts to resist the forward movement of the bed in the direction of movement of the upper layer.

6. Another group of forces considered here are those associated with the deposition of solid cuttings and fluid from the upper layer into the cutting bed region and the re-suspension of solid cuttings and fluid from the moving bed layer into the suspension in the upper layer. The deposition and re-suspension processes are governed by certain factors which will be discussed.

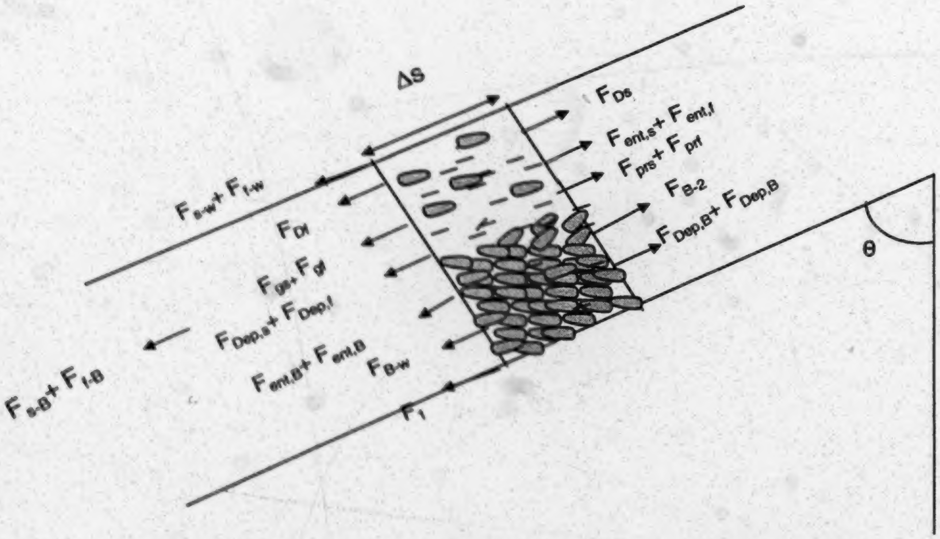

Figure 3.3 Forces acting on layers within control volume

For fully suspended flow with no cuttings bed, however, some of the forces listed above are not considered. The forces not considered for fully suspended flow include;

- The forces associated with deposition and re-suspension

- The frictional force between the bed and the wellbore.
- The interfacial frictional force between the cutting bed and the upper suspension layer since there is no wetted interfacial perimeter.

Pressure Force. The determination of the pressure force on a single particle is quite complex. Because of this, the pressure over the whole body of the system instead of single particle will be considered. The volume of the suspended solids in the control volume is,

$$V_s = C_s A_2 \Delta s \qquad 3.7$$

The above volume can be assumed to be that of a cylinder with height Δs and cross-sectional area $C_s A_2$. The pressure across the cylinder in the direction of flow can be expressed as follow;

$$F_{prs} = C_s A_2 (P_1 - P_2) = -C_s A_2 \Delta P \qquad 3.8$$

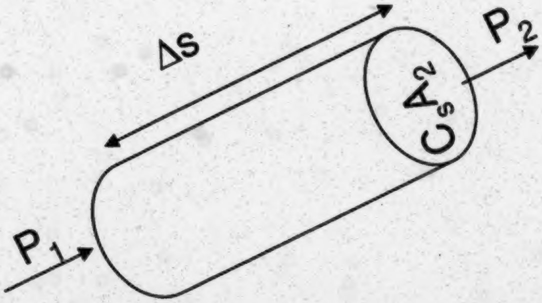

Figure 3.4: Pressure force acting on the suspended solids

Similarly for the foam in the suspension and for the cuttings bed, the pressure across the cylinder in the direction of flow is given by equations (3.9) and (3.10) respectively.

$$F_{prf} = C_f A_2 (P_1 - P_2) = -C_f A_2 \Delta P \qquad 3.9$$

$$F_{prB} = A_1(P_1 - P_2) = -A_1\Delta P \qquad 3.10$$

Gravity Force. The gravity force acting on the all particles in the system is calculated by using;

$$F_{gs} = -C_s A_2 \rho_s g \Delta s Cos\theta \qquad 3.11$$

The gravity force acting on foam in suspension within the control volume is calculated by using;

$$F_{gf} = -C_f A_2 \rho_f g \Delta s Cos\theta \qquad 3.12$$

The gravity force acting on the cuttings bed within the control volume is calculated by using;

$$F_{gB} = -A_1 \rho_1 g \Delta s Cos\theta \qquad 3.13$$

Shear Forces. This set of forces play significant roles in the cuttings transport process in inclined wells. These forces result from interaction (collision and contact) between objects (solids in suspension, fluid in the suspension, and the moving bed) with the wall of the wellbore and also due to interaction between layers. The stresses that exist during cuttings transport in inclined wells are;

- The shear stress which result from collision and contact of the cuttings in the suspension with the wall of the pipe and borehole.
- The shear stress due to contact of the fluid in the suspension with the wall of the pipe and wellbore.
- The interfacial shear stress that result from interfacial contact between the suspension layer and the bed layer.
- Finally, the shear stress due to contact of the bed with the wall of the pipe and wellbore.

However, it should be noted that depending on the layer under consideration, these shear stresses can either act as driving forces or resistant forces. From figure 3.3, it can be seen that all the stresses acting in upper layer are resistant forces whereas for the lower layer, all stresses except the interfacial shear stress act as resistant forces to the cuttings bed (the bed is assumed to be moving in the direction of the upper layer). In other words, since the velocity of the upper layer is higher than that of the lower layer, the interfacial shear stress accelerates the sliding bed and tends to slow down the upper layer. The net effect of the shear forces is a reduction in momentum since all the shear forces in the system act as resistant forces except the interfacial shear stress associated with the cuttings bed which acts in the direction of the drive force.

Doan et al (2003) assumed the hydrodynamic shear stresses in the upper suspension region and interfacial stresses to be a function of the fluid hydrodynamics only. For this study, the stresses would be expressed as a function of both the liquid and solid properties. The shear force which results from contact between the wall of the hole and the solid in the suspension is obtained by using equation (3.14).

$$F_{(s-w)} = -\tau_{s-w}.S_{s-w}.\Delta s \tag*{3.14}$$

For fully suspended flow,

$$F_{(s-w)} = -2\dot{m}_s f_s \frac{\Delta s}{D_H} u_s \tag*{3.15}$$

The shear force which results from the contact of fluid in suspension with the wall of the hole and the pipe is determined by using equation (3.16)

$$F_{(f-w)} = -\tau_{f-w} S_{f-w} \Delta s \tag*{3.16}$$

For fully suspended flow,

$$F_{(f-w)} = -2\dot{m}_f f_f \frac{\Delta s}{DH} u_f \tag*{3.17}$$

The shear force between the moving bed and the wellbore is obtained by using:

$$F_{(B-w)} = -\tau_{B-w} S_{B-w} \Delta s \qquad 3.18$$

For fully suspended flow, the above force (3.18) is zero.

Where

$$\tau_{s-w} = \frac{1}{2} C_s f_s \rho_s u_s^2 \qquad 3.19$$

$$\tau_{f-w} = \frac{1}{2} C_f f_f \rho_f u_f^2 \qquad 3.20$$

and

$$\tau_{B-w} = \frac{1}{2} f_1 \rho_1 u_1^2 \qquad 3.21$$

ρ_f, u_f, ρ_s, u_s and ρ_1, u_1 are the density and velocity of the liquid, solid and the cuttings bed respectively.

Therefore,

$$F_{(s-w)} = -\frac{1}{2} C_s f_s \rho_s u_s^2 . S_{s-w} \Delta s = -\frac{1}{2} \dot{m}_s f_s \frac{s_{s-w}}{A_2} \Delta s . u_s \qquad 3.22$$

$$F_{(f-w)} = -\frac{1}{2} C_f f_f \rho_f u_f^2 . S_{f-w} \Delta s = -\frac{1}{2} \dot{m}_f f_f \frac{s_{f-w}}{A_2} \Delta s . u_f \qquad 3.23$$

and

$$F_{(B-w)} = -\frac{1}{2} f_1 \rho_1 u_1^2 S_{B-w} \Delta s = -\frac{1}{2} \dot{m}_1 f_1 \frac{s_{B-w}}{A_2} \Delta s u_1 \qquad 3.24$$

The shear force due to contact between the suspended solids and the cuttings bed is obtained by using equation 3.25

$$F_{(s-B)} = -\tau_{s-i} S_i \Delta s \qquad 3.25$$

The shear force due to contact between the fluid in suspension and the cuttings bed is obtained by using equation 3.26

$$F_{(f-B)} = -\tau_{f-i} S_i \Delta s \qquad 3.26$$

The shear force between the upper layer and the moving bed is obtained by using equation 3.27.

$$F_{(B-i)} = \tau_{B-i} S_i \Delta s \qquad 3.27$$

Where

$$\tau_{B-i} = \tau_{s-i} + \tau_{f-i} \qquad 3.28$$

$$\tau_{s-i} = \frac{1}{2} C_s f_s \rho_s (u_s - u_1)^2 \qquad 3.29$$

$$\tau_{f-i} = \frac{1}{2} C_f f_f \rho_f (u_f - u_1)^2 \qquad 3.30$$

Therefore,

$$F_{(s-B)} = -\frac{1}{2} C_s f_s \rho_s (u_s - u_1)^2 S_i \Delta s \qquad 3.31$$

$$F_{(f-B)} = -\frac{1}{2} C_f f_f \rho_f (u_f - u_1)^2 S_i \Delta s \qquad 3.32$$

and

$$F_{(B-i)} = F_{(s-B)} + F_{(f-B)} \qquad 3.33$$

Friction Factors: The terms f_s, f_f, and f_l in equations (3.19), (3.20) and (3.21) are the solid, foam and cuttings bed frictional factor respectively. Different empirical correlations have been developed for the determination of the solid friction factor (Konno and Satio (1969), Cape and Nakamura (1973), Yang (1978), Tulay and Ozbelge (1984)). In this research, the correlation developed by Cape and Nakamura (1973) (Eqn. 3.34) which gave the highest solid frictional pressure drop was used.

$$f_s = \frac{0.206}{u_s^{1.22}} \qquad 3.34$$

The friction factor for the flow of power law fluid through pipes and the annulus depends on the flow regime. For turbulent flow of power law fluid through pipes and annulus, the Dodge and Metzner expression for fanning friction coefficient (Skelland, 1967) is used.

$$\sqrt{\frac{1}{f_f}} = \frac{4.0}{n^{0.75}} \log\left(\mathrm{Re}_f \, . f_f^{\,1-n/2}\right) - \frac{0.395}{n^{1.2}} \qquad 3.35$$

Where Re_f is the generalized Reynolds number for power law fluid modified for foam calculated using equation (3.36).

$$\mathrm{Re}_f = \frac{8^{1-n} \rho_f u_f^{2-n} d^n}{K_f \left(\frac{(3n+1)}{4n}\right)^n} \qquad 3.36$$

Martin et al. (1992) also suggested the use of equation (3.37)

$$f_f = 0.0454 + 0.645 \mathrm{Re}_{gn}^{-0.7} \qquad 3.37$$

For laminar flow of power law fluids in pipe, the fanning friction factor is obtained using;

$$f_f = \frac{16}{(\mathrm{Re}_f)} \qquad 3.38$$

Fredericksson and Bird (1958) have shown that the friction factor for the laminar flow of power law fluids in annuli could be written as follows:

$$f_f = \frac{16}{N_{\mathrm{Re}}\left(n, \bar{\kappa}\right)} \qquad 3.39$$

In which the modified Reynolds number $N_{\mathrm{Re}}\left(n, \bar{\kappa}\right)$ is defined as:

$$N_{\mathrm{Re}}\left(n, \bar{\kappa}\right) = \frac{(2R_2)^n u^{2-n} \rho / K}{2^{n-3}\left(1-\bar{\kappa}^2\right)^{n+1} / \left(1+\bar{\kappa}\right)} \Omega_p^n \qquad 3.40$$

Where

$$\bar{\kappa} = R_1 / R_2 \qquad 3.41$$

$$\Omega_p = \frac{n\Psi\left(1-\bar{\kappa}\right)^{(2n+1)/n}}{2n+1} \qquad 3.42$$

Values of Ψ was tabulated as a function of n and $\bar{\kappa}$ in Table-III of Fredericksson and Bird (1958). For convenience, values given by Fredericksson and Bird were curve fitted and could be represented by the following two parametric equations:

When $0.3 < \bar{\kappa} \le 1.0$

$$\Psi(s, \bar{\kappa}) = (0.0011s^2 - 0.0217s + 0.4972)\bar{\kappa} - 0.0009s^2 + 0.0178s + 0.5023 \tag{3.43}$$

When $\bar{\kappa} \le 0.3$

$$\Psi(s, \bar{\kappa}) = (-0.0715s^2 + 1.0241s + 0.4402)\bar{\kappa}^2 + (0.0361s^2 - 0.5412s + 0.2972)\bar{\kappa} - 0.0052s^2 + 0.0851s + 0.5237 \tag{3.44}$$

Where $s = 1/n$

Note that the values of the function $\Psi(s, \bar{\kappa})$ can be calculated by using equations (3.43) and (3.44) within less than 3% error margin of Frederickson and Bird solution.

For the turbulent flow of power law fluid in the annulus, the Reynolds number used for the calculation of the friction factor is the same as that used for turbulent flow of power law fluid through pipes.

The friction factor for the moving cuttings bed is calculated by using equations 3.45 to 3.47

$$f_1 = \frac{16}{(\mathrm{Re}_B)} \tag{3.45}$$

$$\mathrm{Re}_B = \frac{\rho_B u_B^{2-n} d_1^n}{8^{n-1} K'_B} \tag{3.46}$$

$$K'_B = K'_f \left(1 + 2.5C_{s1} + 10.05C_{s1}^2 + 0.00273e^{16.6C_{s1}}\right) \tag{3.47}$$

Drag Force. The total drag force in the control volume is obtained by summing up the drag forces acting on individual particle in the suspension. The drag force over a particle is given by:

$$F_{Dsk} = \frac{1}{2}\rho_f C_D A_{sk}\left(u_f - u_{sk}\right)^2 \qquad 3.48$$

It is assumed that all the solid cuttings move at the same velocity, and the particles have uniform size and shape. The total drag force on all the particles is given by

$$F_{Ds} = \frac{1}{2}\rho_f C_D \sum_k \left(A_{sk}\left(u_f - u_{sk}\right)^2\right) \qquad 3.49$$

Where,

$$A_{sk} = \pi d_{sk}^2 / 4$$

$$F_{Ds} = \frac{N_s}{2}\rho_f C_D A_s\left(u_f - u_s\right)^2 \qquad 3.50$$

N_s = Volume occupied by all suspended solid particles in layer 2/Volume of a solid.

$$= \frac{6C_s V_s}{\pi d^3}$$

The force on the foam fluid due to particle drag is:

$$F_{Df} = -\frac{N_s}{2}\rho_f C_D A_s\left(u_f - u_s\right)^2 \qquad 3.51$$

Frictional Force (F_l) between Bed and Wellbore. Frictional force results due to contact between the cuttings bed and the wall of the wellbore. For stationary bed, the static frictional force which acts on the bed, balances the driving forces acting on the bed. Increasing the driving force on the bed would increase the dry frictional force until it reaches a certain maximum value. At this point, increasing the driving force any further would cause the bed to slide. This maximum frictional force acting at the point of sliding is given by:

$$F_1 = \mu R \tag{3.52}$$

Where μ is the dry friction coefficient and R is the sum of normal forces exerted by the solid particles on the wall of the pipe. "R" for a moving bed consists of two components as shown in figure 3.5.

1. The first component (R_1) is that due to the submerged weight of the solid particle. R_1 is calculated using equation (3.53)

$$R_1 = \rho_1 A_1 g \Delta s \tag{3.53}$$

2. The second component is that due to transmission of stress from the interface through the cuttings in the bed. This component represented by R_2 is also known as the Bagnold stresses. Bagnold (1954,1957), showed that when fluid flows over a moving bed, a normal stress exists at the interface which is associated with the shear stress exerted by the fluid on the bed. This Bagnold stress can be calculated using equation (3.54).

$$R_2 = \frac{\tau_i S_i}{\tan \phi} \Delta s \tag{3.54}$$

Combining equations (3.52), (3.53) and (3.54) gives;

$$F_1 = \mu (\rho_1 A_1 g Sin \ \theta + \frac{\tau_i S_i}{\tan \phi}) \Delta s \tag{3.55}$$

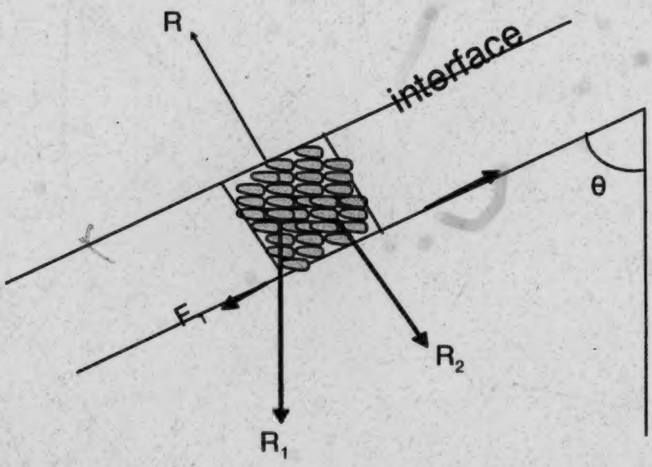

Figure 3.5: Friction between moving bed and wellbore

Where ϕ is angle of internal friction with value of $\tan\phi$ ranging from 0.35 to 0.75 depending on the type of flow and the particle characteristics; μ is the dry coefficient of friction of the cuttings bed. Iyoho (1980) indicated that the coefficient of static friction is about 0.6 since cuttings slide down the wellbore under no flow condition when the wellbore makes an angle of about 60^{0} with the horizontal. A close approximation for the value of the coefficient of static friction is the tangent of the angle the wellbore makes with the horizontal at which the cuttings bed will just begin to slide under no flow condition. This is approximately equal to the tangent of the cutting angle of repose. Gavignet and Sobey (1989) showed that for a sliding bed, the sliding coefficient of friction is less than half the coefficient of static friction of the cutting studied by Iyoho. For their model they suggested a sliding friction factor of 0.2. Ozbayoglu (2003) also presented empirical correlation based on his experimental results for the determination of this coefficient expressed as a function of A_{bed}/A_w given by:

$$\mu = 0.617\left(\frac{A_{bed}}{A_w}\right)^{0.252} \qquad 3.56$$

For stationary beds, equation (3.55) cannot be used to directly calculate the static dry friction force as this applies to a bed at the verge of motion. The static dry frictional force for a stationary bed is calculated from the momentum equation for the bed. The friction force calculated should be less than maximum dry friction obtained using equation (3.55) (Wilson, 1970). A stationary bed would be at the verge of moving if the calculated frictional force from the momentum equation (3.83) is equal to that obtained from equation (3.55).

3.1.3 Forces Due to Deposition and Entrainment of Cuttings.

As cuttings are being transported to the surface either in suspension or as a moving bed, there is usually transfer of materials from one layer to the other due to deposition and re-suspension. Mass and momentum associated with these transfers need to be incorporated into the continuity and momentum equations in order to represent a complete dynamics of the cuttings transport process. As cuttings and foam fluid are being deposited from the upper to the lower layer, so is there re-suspension of cuttings and foam fluid from the lower layer to the upper layer.

Re-suspension is the process by which in the presence of shear flow, an initially settled layer of negatively buoyant particles is dragged into the suspension upper layer and is convected away (Leighton and Acrivos, 1985). Gadala–Maria (1979) was the first to show re-suspension can occur at small values of Reynolds number for which inertia effects are insignificant and flow is laminar. From his study using coal suspension, he observed that the viscosity of the suspension decreased when sheared at a low shear rate and left overnight. But with increasing shear rate he observed an increase in the viscosity of the suspension. The reason for this decrease in the viscosity was attributed to deposition of the coal particles from the suspe nsion while the increase was attributed to the re-suspension of the already settled coal particles. Leighton and Acrivos (1986) also investigated the re-suspension process and explain it in terms of shear-induced diffusion process, in which the diffusivity resulted from inter-particle interaction within a suspension as it is sheared.

Forces are associated with deposition and re-suspension processes. The determination of these forces has been treated by several investigators in the literature. Doan et al.

(2003) calculated the deposition velocity using the method proposed by Doron et al. (1987). They have assumed that the depositional and entrainment rates determine the volumetric transfer rate across the interfacial boundary aligned in the direction perpendicular to bulk flow. The depositional rate was expressed as a function of hindered terminal velocity of a single particle. The force balance on a single particle was used to determine an expression needed for the determination of the hindered terminal velocity in inclined wells. They did not consider the inclination effect in the determination of the forces associated with these processes which, however, was included in the model described in this study.

Kamp et al. (1999) showed that the cuttings bed height was governed by the mass flux of cuttings per unit interface that are deposited and that re-suspended. The former was found to be proportional to the mean cuttings concentration and the cutting settling velocity whereas the latter is a function of the friction velocity (interfacial velocity), the cuttings bed concentration and the particle velocity.

In this study, the following expressions for the forces and masses associated with the deposition and re-suspension of fluids and cuttings from one layer to the other during cuttings transport in inclined wells are obtained. A detailed derivation of these is given in appendix C.

Mass associated with solid transfer for upper layer.

$$M_{ent,s} - M_{Dep,s} = \rho_s S_i \Delta s \Delta t \left(v_E C_{s1} - v_D C_S \right) \qquad 3.57$$

Mass associated with transfer of fluid for upper layer

$$M_{ent,f} - M_{Dep,f} = \rho_f C_{f1} S_i \Delta s \Delta t \left(v_E - \frac{C_s}{C_{s1}} v_D \right) \qquad 3.58$$

Mass change associated with the cuttings bed due to re-suspension from lower layer.

$$M_{ent,B} = v_E S_i \Delta s \Delta t \rho_1 \tag{3.59}$$

Mass change associated with the cuttings bed due to deposition from upper layer.

$$M_{Dep,B} = C_s v_D S_i \Delta s \Delta t \left(\rho_s + \frac{C_{f1}}{C_{s1}} \rho_f \right) \tag{3.60}$$

Force change associated with the solid component in the upper zone due to deposition and re-suspension:

$$F_{ent,s} - F_{Dep,s} = \rho_s \Delta s S_i \left(C_{s1} v_D u_1 - C_s v_D u_{s2} \right) Cos\theta \tag{3.61}$$

Force change associated with the fluid component in the upper zone due to deposition and re-suspension:

$$F_{ent,f} - F_{Dep,f} = \rho_f C_{f1} \Delta s S_i \left(v_E u_1 - \frac{C_s}{C_{s1}} v_D u_{s2} \right) Cos\theta \tag{3.62}$$

Force change associated with the cuttings bed due deposition and re-suspension:

$$F_{Dep,B} - F_{ent,B} = \left(\Delta s S_i C_s v_D \left(\rho_s u_{s2} + \rho_f \frac{C_{f1}}{C_{s1}} u_{f2} \right) - v_E u_1 \Delta s S_i \rho_1 \right) Cos\theta \tag{3.63}$$

3.1.3.1 Deposition and Entrainment Velocity.

Doron et al. (1987) suggested the use of the following equations for the determination of depositional rate. The equation takes into consideration the concentration effects on the hindered terminal velocity.

$$v_D = v_p (1 - C_s)^m \tag{3.64}$$

v_p is the terminal settling velocity obtained by using:

$$v_p = \sqrt{\frac{4d_p g}{3C_D}\left(\frac{\rho_s - \rho_f}{\rho_f}\right)} \qquad 3.65$$

$$m = 4.45\mathrm{Re}_p^{-0.1} \qquad \mathrm{RE_p} < 500 \qquad 3.66$$

$$m = 2.39 \qquad \mathrm{RE_p} \geq 500 \qquad 3.67$$

$\mathrm{RE_p}$ is the Reynolds number based on, v_D, the hindered terminal deposition velocity.

$$\mathrm{Re}_p = \frac{\rho_f v_D d_P}{\mu_f}$$

Where μ_f is the apparent viscosity of foam.

Doron et al (1987) expressed the entrainment rate as a function of the interfacial shear velocity. They calculated the interfacial shear velocity using equation (3.68).

$$u_{12} = \sqrt{\frac{\tau_{12}}{\rho_f}} = \sqrt{\frac{\frac{1}{2} f_i \rho_f (u_2 - u_1)^2}{\rho_f}} = (u_2 - u_1)\sqrt{\frac{f_i}{2}} \qquad 3.68$$

Doan et al (2003) assumed a linear relationship between the entrainment velocity and the difference between the interfacial velocity (u_{12}) and a critical threshold velocity (u_{12}^*), given by equation (3.69). The slope m'' they obtained from simulation study.

$$v_E = m''(u_{12} - u_{12}^*) \qquad u_{12} > u_{12}^* \qquad 3.69$$

$$v_E = 0 \qquad u_{12} \leq u_{12}^* \qquad 3.70$$

When the interfacial shear velocity is below a certain critical level as shown by equation (3.70) there would be no re-entrainment of deposited cuttings into the flowing suspension layer. In their model there was no expression for the determination of critical threshold velocity.

Kamp et al (1999) suggested using equation 3.72 for calculation of the critical threshold velocity.

$$\mathrm{Re}_p' = \left(\frac{\rho_s - \rho_f}{\rho_f} g d_p \right)^{\frac{1}{2}} \frac{d_p \rho_f}{\mu_f} \qquad 3.71$$

$$Z = \frac{\mathrm{Re}_p' \, u_{12}}{v_p} \qquad 3.72$$

When Z=Z$_c$ which has a value of 5, interfacial velocity becomes is the critical threshold velocity.

In this study, the entrainment velocity is determined by using the mass continuity equation for the cuttings bed (Eqn. 3.75).

3.1.4 Conservation of Mass and Momentum Equations.

With the mass and force balances for foam and solids in the upper layer and that of the cuttings bed layer in a control volume, the continuity and momentum equations for the solids in the suspension, foam in the suspension and the cuttings bed are derived. Altogether six equations are obtained.

Detailed derivations are given in appendix A and B. Equations (3.73), (3.74), and (3.75) are the continuity equations for the solids in the suspension, foam in the suspension and the cuttings bed respectively.

$$\frac{\partial(\rho_s C_s)}{\partial t} + \frac{\partial(\rho_s u_s C_s)}{\partial s} = -\rho_s v_D C_s \frac{S_i}{A_2} + \rho_s v_E C_b \frac{S_i}{A_2} \qquad 3.73$$

$$\frac{\partial(\rho_f C_f)}{\partial t} + \frac{\partial(\rho_f u_f C_f)}{\partial s} = -\frac{C_{f1}}{C_b} \rho_f C_s v_D \frac{S_i}{A_2} + \rho_f v_E C_{f1} \frac{S_i}{A_2} + s_f \qquad 3.74$$

$$\frac{\partial \rho_1}{\partial t} + \frac{\partial(\rho_1 u_1)}{\partial s} = \left(\rho_s + \frac{C_{f1}}{C_b} \rho_f \right) C_s v_D \frac{S_i}{A_1} - \rho_1 v_E \frac{S_i}{A_1} \qquad 3.75$$

v_D and v_E are the deposition and entrainment velocities respectively of materials deposited and re-suspended from one layer to the other.

It should be noted, however, that for fully suspended flow there is no cutting bed, hence there would be no momentum equation for it.

The foam flow rate in the upper layer is affected by fluid influx from the reservoir due to the underbalanced drilling condition. The mass influx rate of water, oil and gas from the reservoir per unit volume of the wellbore are given by equations 3.76 to 3.78

$$s_w = \frac{\rho_w PI_w (P_{re} - P)}{A_2} \qquad 3.76$$

$$s_o = \frac{\rho_o PI_o (P_{re} - P)}{A_2} \qquad 3.77$$

$$s_g = \frac{\rho_g PI_g (P_{re} - P)}{A_2} \qquad 3.78$$

Where PI is the specific productivity index, which is the volumetric inflow rate of fluid from the reservoir into the wellbore per unit pressure drop between the reservoir and the wellbore per unit length. The total mass influx from the formation into the wellbore is given by equation (3.79).

$$s_f = s_w + s_o + s_g \qquad 3.79$$

$$s_f = \frac{\rho_o q_{re,o} + \rho_w q_{re,w} + \rho_g q_{re,g}}{A_2 \Delta s} \qquad 3.80$$

The momentum equations for the suspended solid, the foam in the suspension and the cuttings bed for the inclined wells are given by equations (3.81), (3.82) and (3.83) respectively. Detailed derivations of these equations are given in appendix B.

$$\begin{aligned}
&\frac{\partial\left(C_s\rho_s u_s^2\right)}{\partial s}+\frac{\partial\left(C_s\rho_s u_s\right)}{\partial t}=\\
&-C_s\frac{\partial p}{\partial s}-C_s\rho_s g Cos\theta-\frac{1}{2}C_s f_s\rho_s u_s^2\frac{S_2}{A_2}-\frac{1}{2}C_s f_s\rho_s\left(u_s-u_1\right)^2\frac{S_i}{A_2}+\\
&\frac{3C_s}{4d_s}\rho_f C_D\left(u_f-u_s\right)^2+u_1 v_E C_b\rho_s\frac{S_i}{A_2}Cos\theta-u_s v_D C_s\rho_s\frac{S_i}{A_2}Cos\theta.
\end{aligned}\tag{3.81}$$

$$\begin{aligned}
&\frac{\partial\left(C_f\rho_f u_f^2\right)}{\partial s}+\frac{\partial\left(C_f\rho_f u_f\right)}{\partial t}=\\
&-C_f\frac{\partial p}{\partial s}-C_f\rho_f g Cos\theta-\frac{1}{2}C_f f_f\rho_f u_f^2\frac{S_{f-w}}{A_2}-\frac{1}{2}C_f f_f\rho_f\left(u_f-u_1\right)^2\frac{S_i}{A_2}\\
&-\frac{3C_s}{4d_s}\rho_f C_D\left(u_f-u_s\right)^2+u_1 v_E C_{f1}\rho_f\frac{S_i}{A_2}Cos\theta-u_f v_D\frac{C_{f1}}{C_b}C_s\rho_f\frac{S_i}{A_2}Cos\theta
\end{aligned}\tag{3.82}$$

$$\begin{aligned}
&\frac{\partial\left(\rho_1 u_1^2\right)}{\partial s}+\frac{\partial\left(\rho_1 u_1\right)}{\partial t}=\\
&-\frac{\partial p}{\partial s}-\rho_1 g Cos\theta+\frac{1}{2}c_f f_f\rho_f\left(u_f-u_1\right)^2\frac{S_i}{A_1}+\frac{1}{2}c_s f_s\rho_s\left(u_s-u_1\right)^2\frac{S_i}{A_1}-\\
&\frac{1}{2}\ f_1\rho_1 u_1^2\frac{S_{B-w}}{A_1}+\left(u_s v_D C_s\rho_s\frac{S_i}{A_1}+u_f v_D\frac{C_{f1}}{C_b}C_s\rho_f\frac{S_i}{A_1}-u_1 v_E\rho_1\frac{S_i}{A_1}\right)Cos\theta-\frac{F_1}{A_1\Delta s}
\end{aligned}\tag{3.83}$$

F_1 is the frictional force that exist between the cutting bed and wellbore.

Equations (3.81) and (3.82) can be added together to eliminate the drag force between solid cuttings and the foam in the upper layer.

$$\begin{aligned}
&\frac{\partial\left(C_s\rho_s u_s^2+C_f\rho_f u_f^2\right)}{\partial s}+\frac{\partial\left(C_s\rho_s u_s+C_f\rho_f u_f\right)}{\partial t}=\\
&-\frac{\partial p}{\partial s}-\left(C_s\rho_s+C_f\rho_f\right)g Cos\theta-\frac{1}{2}c_f f_f\rho_f u_f^2\frac{S_{f-w}}{A_2}-\frac{1}{2}c_s f_s\rho_s u_s^2\frac{S_{s-w}}{A_2}-\frac{1}{2}c_f f_f\rho_f\left(u_f-u_1\right)^2\frac{S_i}{A_2}\\
&-\frac{1}{2}c_s f_s\rho_s\left(u_s-u_1\right)^2\frac{S_i}{A_2}+u_1 v_E\frac{S_i}{A_2}Cos\theta\left(C_b\rho_s+C_{f1}\rho_f\right)-\left(u_s\rho_s+\frac{C_{f1}}{C_b}u_f\rho_f\right)v_D C_s\frac{S_i}{A_2}Cos\theta
\end{aligned}$$

3.84

Under steady state flow condition, neglecting the acceleration term and material exchange terms (between layers) in equation (3.84) would yield

$$\frac{\partial p}{\partial s}=-\left(C_s\rho_s+C_f\rho_f\right)gCos\theta-\frac{1}{2}c_f f_f\rho_f u_f^2\frac{S_2}{A_2}-\frac{1}{2}c_s f_s\rho_s u_s^2\frac{S_2}{A_2}- \\ \frac{1}{2}c_f f_f\rho_f\left(u_f-u_1\right)^2\frac{S_i}{A_2}-\frac{1}{2}c_s f_s\rho_s\left(u_s-u_1\right)^2\frac{S_i}{A_2} \qquad 3.85$$

As seen from above equation (3.85), the steady state pressure drop for the model in the upper layer consist of the two parts; the hydrostatic pressure drop due to suspension and the frictional pressure drop due to the suspension and that due to relative motion between the upper and the lower layer if a bed is formed.

3.1.5 Boundary Conditions

The gas and liquid injection rates must be specified. Drilling rate should also be specified so that the mass flow rate of the cuttings in the annulus can be calculated. Finally, back pressure is specified at the exit of the pipe.

3.1.6 Initial Conditions

Stable foam flow condition is assumed to be achieved before the drilling begins. The pressure and velocity distribution, and properties of foam are calculated and set as the initial condition of the flow model.

3.1.7 Method of Solution

In this research, the Crowe's method (Crowe, 1998) for two phase steady state flow which is a modification of the numerical solution scheme called SIMPLE developed by Patankar for single phase flow was employed with some modification to facilitate the convergence of the numerical solution. This technique was also used by Li (2004) in the development of his model for cuttings transport with foam in horizontal wells.

3.1.8 Foam-Cutting Flow in Drilling Annulus

The numerical solutions of equations (3.73) to (3.75) and (3.81) to (3.83) which describe cuttings transport with foam in the annulus of an inclined well are needed in order to determine the flowing bottom hole pressure and the cuttings concentration along the well. For foam-cuttings transport under steady state flow condition, the total pressure drop across the annulus can be calculated by using the equation (3.86)

$$\Delta P_{an} = \Delta s \sum_i \left(C_s \rho_s + C_f \rho_f\right) g Cos\theta + \Delta s \sum_i \left(\begin{array}{l} \frac{1}{2} C_f f_f \rho_f u_f^2 \frac{S_2}{A_2} + \frac{1}{2} C_s f_s \rho_s u_s^2 \frac{S_2}{A_2} + \\ \frac{1}{2} C_f f_f \rho_f \left(u_f - u_1\right)^2 \frac{S_i}{A_2} \\ + \frac{1}{2} C_s f_s \rho_s \left(u_s - u_1\right)^2 \frac{S_i}{A_2} \end{array} \right) \qquad 3.86$$

The total pressure drop across the annulus as shown by the equation (3.86) can be obtained by dividing the annulus into sections and summing up the pressure drops in all sections. The circulating bottom-hole pressure is the sum of the total pressure drop across the annulus and the back pressure applied at the surface.

$$CBHP = \Delta P_{an} + P_b \qquad 3.87$$

3.1.9 Foam Flow across the Bit Nozzle.

The determination of the pressure drop across the bit needs modification of the momentum equation for the suspended foam. Due to the fact that high pressure foam flows through the bit nozzles, the frictional, gravitational and mass transfer terms can be neglected in comparison to the acceleration term in equation (3.82).

$$\frac{\partial\left(C_f \rho_f u_f^2\right)}{\partial s} = -C_f \frac{\partial p}{\partial s} \qquad 3.88$$

The finite difference equation for foam flow through the bit nozzle is given by equation (3.89).

$$P_{dp,N} = P_{an,1} + \left(\rho_f u_f{}^2{}_f\right)_{nozz} - \left(\rho_f u_f{}^2{}_f\right)_{dP,N} \qquad 3.89$$

3.1.9 Foam Flow in Drill Pipes

The flow of foam in a drill pipe is considered a steady state flow of single-phase compressible fluid in a pipe. The equation describing foam flow in pipe can be obtained by modifying equation (3.82). The modification made includes: the suspension is considered to be made of foam only, the concentration of foam is one, the flow is downwards, and finally, the area open to flow is the entire cross-sectional of the pipe. It should be noted that for pipe flow, the drag force and material transfer in equation (3.82) are not considered.

$$\frac{\partial\left(\rho_f u_f^2\right)}{\partial s} = -\frac{\partial p}{\partial s} + \rho_f g Cos\theta - \frac{2 f_f \rho_f u_f^2}{D_p} \qquad 3.90$$

The finite difference formulation of equation (3.90) is given as follows

$$P_{dp,i} = P_{dp,i+1} - \Delta s g Cos\theta \rho_{f,i+1} + \left(\frac{2 f_f \rho_f u_f^2}{D_p}\right)_{i+1} + \left(\rho_f u_f^2\right)_{i+1} - \left(\rho_f u_f^2\right)_i \qquad 3.91$$

D_p is the diameter of the pipe open to flow.

An iterative calculation procedure is required to solve equation (3.91)

CHAPTER 4

METHOD OF NUMERICAL SOLUTION FOR THE FOAM -CUTTINGS FLOW MODEL

The proposed model for the cuttings transport in inclined well is solved by a numerical method described in this chapter. This numerical model can also be applied to vertical and horizontal well with some changes in the momentum equations of foam and solid and that of the bed if formed.

4.1 Discretization of the Physical Model.

A staggered grid system shown in Fig 4.1 is used to discretize the flowing system and an algorithm of semi-implicit method is used to solve the discretized pressure-linked equations. With this system, pressure and velocities are calculated at different nodes with the pressure nodes at the center of the control volume, and the velocities on the faces of the control volume. This strategy as suggested by Patankar (1980) would prevent wavy velocity field and the inconsistency usually associated with the conventional grid system. It also ensures a uniform pressure field since the pressure difference between two adjacent grid nodes becomes the natural driving force for the velocity component between these grid points.

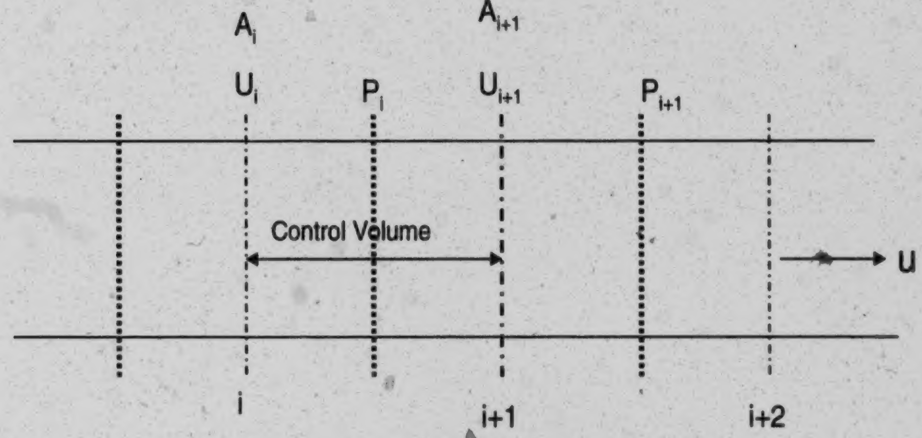

Figure 4.1: Staggered grid system

4.2 Discretization of Momentum Equations.

4.21 Discretization of the Momentum Equations of the Solid Component.

The momentum equation for the solid component in the upper layer is given by equation (4.1).

$$\begin{aligned}&\frac{\partial\left(C_s\rho_s u_s^2\right)}{\partial s}+\frac{\partial\left(C_s\rho_s u_s\right)}{\partial t}=\\&-C_s\frac{\partial p}{\partial s}-C_s\rho_s gCos\,\theta-\frac{1}{2}C_s f_s\rho_s u_s^2\frac{S_2}{A_2}-\frac{1}{2}C_s f_s\rho_s\left(u_s-u_1\right)^2\frac{S_i}{A_2}+\qquad 4.1\\&\frac{3C_s}{4d_s}\rho_f C_D\left(u_f-u_s\right)^2+u_1v_E C_{s1}\rho_s\frac{S_i}{A_2}Cos\,\theta-u_s v_D C_s\rho_s\frac{S_i}{A_2}Cos\,\theta.\end{aligned}$$

Discretizing equation (4.1) gives;

$$\begin{aligned}&\frac{\partial\left(A_2C_s\rho_s u_s\right)}{\partial t}+\frac{\partial\left(\dot m_s u_s\right)}{\partial s}=\\&-C_sA_2\frac{\partial p}{\partial s}-C_sA_2\rho_s gCos\theta-\frac{1}{2}C_s f_s\rho_s u_s^2S_2-\frac{1}{2}C_s f_s\rho_s\left(u_s-u_1\right)^2S_i+\qquad 4.2\\&A_2B_v\left(u_f-u_s\right)+u_1v_E C_{s1}\rho_s S_i Cos\theta-u_s v_D C_s\rho_s S_i Cos\theta.\end{aligned}$$

Replacing the derivatives by forward difference approximation implicitly, numerical expression for equation (4.2) at node i+1 and time step n+1 is obtained:

$$\begin{aligned}&\frac{\left(A_2C_s\rho_s u_s\right)_{i+1}^{n+1}-\left(A_2C_s\rho_s u_s\right)_{i+1}^{n}}{\Delta t}+\frac{\left(\dot m_s u_s\right)_{i+1}^{n+1}-\left(\dot m_s u_s\right)_{i}^{n+1}}{\Delta s}=\\&\left(A_2C_s\right)_{i+1}^{n+1}\left(\frac{P_i^{n+1}-P_{i+1}^{n+1}}{\Delta s}\right)-\left(A_2C_s\rho_s gCos\theta\right)_{i+1}^{n+1}+\left(A_2B_v\right)_{i+1}^{n+1}\left(\left(u_f\right)_{i+1}^{n+1}-\left(u_s\right)_{i+1}^{n+1}\right)\qquad 4.3\\&-\left(C_1u_s\right)_{i+1}^{n+1}-\left(D_1\left(u_s-u_1\right)\right)_{i+1}^{n+1}+\left(\rho_s S_i Cos\theta\right)_{i+1}^{n+1}\left(\left(u_1v_E C_{si}\right)_{i+1}^{n+1}-\left(u_s v_D C_s\right)_{i+1}^{n+1}\right)\end{aligned}$$

Where

$$C_1=\frac{C_s\rho_s}{2}f_s u_s S_2 \qquad 4.4$$

$$D_1 = \frac{C_s \rho_s}{2} f_s (u_s - u_1) S_i \qquad 4.5$$

Re-arranging equation (4.3)

$$(u_s)_{i+1}^{n+1} \left(\frac{\Delta s}{\Delta t} (A_2 C_s \rho_s)_{i+1}^{n+1} + (\dot{m}_s)_{i+1}^{n+1} + \Delta s (A_2 B_v)_{i+1}^{n+1} + C_1 + D_1 + \Delta s (v_D C_s \rho_s S_i Cos\,\theta)_{i+1}^{n+1} \right) =$$
$$\frac{\Delta s}{\Delta t} (\dot{m}_s)_{i+1}^{n} + (\dot{m}_s u_s)_i^{n+1} + (A_2 C_s)_{i+1}^{n+1} \left(P_i^{n+1} - P_{i+1}^{n+1} \right) - \Delta s (A_2 C_s \rho_s g Cos\,\theta)_{i+1}^{n+1} +$$
$$\Delta s (A_2 B_v)_{i+1}^{n+1} (u_f)_{i+1}^{n+1} + \Delta s (u_1 v_E C_{si} \rho_s S_i Cos\,\theta)_{i+1}^{n+1} + \Delta s \left((D_1 u_1)_{i+1}^{n+1} \right)$$

4.6

Setting

$$(E_s)_{i+1}^{n+1} = \frac{\Delta s}{\Delta t} (A_2 C_s \rho_s)_{i+1}^{n+1} + (\dot{m}_s)_{i+1}^{n+1} + \Delta s (A_2 B_v)_{i+1}^{n+1} + C_{1i+1}^{n+1} + D_{1i+1}^{n+1} + \Delta s (v_D C_s \rho_s S_i Cos\theta)_{i+1}^{n+1}$$

4.7

Then,

$$(u_s)_{i+1}^{n+1} = \frac{1}{(E_s)_{i+1}^{n+1}} \left(\begin{array}{l} \frac{\Delta s}{\Delta t} (\dot{m}_s)_{i+1}^{n} + (\dot{m}_s u_s)_i^{n+1} + (A_2 C_s)_{i+1}^{n+1} \left(P_i^{n+1} - P_{i+1}^{n+1} \right) - \Delta s (A_2 C_s \rho_s g Cos\theta)_{i+1}^{n+1} + \\ \Delta s (A_2 B_v)_{i+1}^{n+1} (u_f)_{i+1}^{n+1} + \Delta s (u_1 v_E C_{si} \rho_s S_i Cos\theta)_{i+1}^{n+1} + \Delta s \left((D_1 (u_1))_{i+1}^{n+1} \right) \end{array} \right)$$

4.8

$$(u_s)_{i+1}^{n+1} = (Q_s)_{i+1}^{n+1} + \frac{(A_2 C_s)_{i+1}^{n+1} \left(P_i^{n+1} - P_{i+1}^{n+1} \right)}{(E_s)_{i+1}^{n+1}} \qquad 4.9$$

With

$$(Q_s)_{i+1}^{n+1} = \frac{1}{(E_s)_{i+1}^{n+1}} \left(\begin{array}{l} \frac{\Delta s}{\Delta t} (\dot{m}_s)_{i+1}^{n} + (\dot{m}_s u_s)_i^{n+1} - \Delta s (A_2 C_s \rho_s g Cos\theta)_{i+1}^{n+1} + \Delta s (A_2 B_v)_{i+1}^{n+1} (u_f)_{i+1}^{n+1} + \\ \Delta s (u_1 v_E C_{si} \rho_s S_i Cos\theta)_{i+1}^{n+1} + \Delta s \left((D_1 (u_1))_{i+1}^{n+1} \right) \end{array} \right)$$

4.10

4.22 Discretization of the Momentum Equations of the Fluid (foam) Component.

The momentum equation for the foam component in the upper layer given by equation

$$\frac{\partial\left(C_f\rho_f u_f^2\right)}{\partial s}+\frac{\partial\left(C_f\rho_f u_f\right)}{\partial t}=$$
$$-C_f\frac{\partial p}{\partial s}-C_f\rho_f gCos\,\theta-\frac{1}{2}C_f f_f\rho_f u_f^2\frac{S_2}{A_2}-\frac{1}{2}C_f f_f\rho_f\left(u_f-u_1\right)^2\frac{S_i}{A_2}-$$
$$\frac{3C_s}{4d_s}\rho_f C_D\left(u_f-u_s\right)^2+\rho_f C_{f1}\frac{S_i}{A_2}Cos\,\theta\left(u_1 v_E-u_f v_D\frac{C_s}{C_b}\right)$$

4.11

Modify equation 4.11 as follows

$$\frac{\partial\left(A_2C_f\rho_f u_f^2\right)}{\partial t}+\frac{\partial\left(\dot{m}_f u_f\right)}{\partial s}=$$
$$-C_fA_2\frac{\partial p}{\partial s}-C_fA_2\rho_f gCos\,\theta-\frac{1}{2}C_f f_f\rho_f u_f^2S_2-\frac{1}{2}C_f f_f\rho_f\left(u_f-u_1\right)^2S_i-$$
$$A_2B_\upsilon\left(u_f-u_s\right)+\rho_f C_{f1}S_iCos\,\theta\left(u_1 v_E-u_f v_D\frac{C_s}{C_b}\right)$$

4.12

Replacing the derivatives by forward difference approximation implicitly, numerical expression for equation 4.12 at node i+1 and time step n+1 is obtained:

$$\frac{\left(A_2C_f\rho_f u_f\right)_{i+1}^{n+1}-\left(A_2C_f\rho_f u_f\right)_{i+1}^{n}}{\Delta t}+\frac{\left(\dot{m}_f u_f\right)_{i+1}^{n+1}-\left(\dot{m}_f u_f\right)_{i}^{n+1}}{\Delta s}=$$
$$\left(A_2C_f\right)_{i+1}^{n+1}\left(\frac{P_i^{n+1}-P_{i+1}^{n+1}}{\Delta s}\right)-\left(A_2C_f\rho_f gCos\,\theta\right)_{i+1}^{n+1}-\left(A_2B_\upsilon\right)_{i+1}^{n+1}\left(\left(u_f\right)_{i+1}^{n+1}-\left(u_s\right)_{i+1}^{n+1}\right)-$$
$$\left(E_1u_f\right)_{i+1}^{n+1}-\left(F_1\left(u_f-u_1\right)\right)_{i+1}^{n+1}+\left(\rho_f C_{f1}S_iCos\,\theta\right)_{i+1}^{n+1}\left(\left(u_1 v_E-u_f v_D\frac{C_s}{C_b}\right)_{i+1}^{n+1}\right)$$

4.13

Where

$$E_1 = \frac{C_f \rho_f}{2} f_f u_f S_2 \qquad 4.14$$

$$F_1 = \frac{C_f \rho_f}{2} f_f \left(u_f - u_1\right) S_i \qquad 4.15$$

Re-arranging equation 4.13

$$\left(u_f\right)_{i+1}^{n+1}\left(\frac{\Delta s}{\Delta t}\left(A_2 C_f \rho_f\right)_{i+1}^{n+1} + \left(\dot{m}_f\right)_{i+1}^{n+1} + \Delta s\left(A_2 B_\upsilon\right)_{i+1}^{n+1} + \Delta s\left(\rho_f C_{f1} S_i \frac{C_s}{C_b} v_D Cos\theta\right)_{i+1}^{n+1}\right) =$$
$$\frac{\Delta s}{\Delta t}\left(\dot{m}_f\right)_{i+1}^{n} + \left(\dot{m}_f u_f\right)_i^{n+1} + \left(A_2 C_f\right)_{i+1}^{n+1}\left(P_i^{n+1} - P_{i+1}^{n+1}\right) - \Delta s\left(A_2 C_f \rho_f g Cos\theta\right)_{i+1}^{n+1} +$$
$$\Delta s\left(A_2 B_\upsilon\right)_{i+1}^{n+1}\left(u_s\right)_{i+1}^{n+1} + \Delta s\left(\rho_f C_{f1} S_i v_E Cos\theta\right)_{i+1}^{n+1}\left(u_1\right)_{i+1}^{n+1} - \Delta s\left(\left(E_1 u_f\right)_{i+1}^{n+1} + \left(F_1\left(u_f - u_1\right)\right)_{i+1}^{n+1}\right)$$
$$4.16$$

Setting

$$\left(E_f\right)_{i+1}^{n+1} = \frac{\Delta s}{\Delta t}\left(A_2 C_f \rho_f\right)_{i+1}^{n+1} + \left(\dot{m}_f\right)_{i+1}^{n+1} + \Delta s\left(A_2 B_\upsilon\right)_{i+1}^{n+1} + E_{1_{i+1}}^{n+1} + F_{1_{i+1}}^{n+1} + \Delta s\left(\rho_f C_{f1} S_i \frac{C_s}{C_b} v_D Cos\theta\right)_{i+1}^{n+1}$$
$$4.17$$

Then,

$$\left(u_f\right)_{i+1}^{n+1} = \frac{1}{\left(E_f\right)_{i+1}^{n+1}}\left(\begin{array}{l}\frac{\Delta s}{\Delta t}\left(\dot{m}_f\right)_{i+1}^{n} + \left(\dot{m}_f u_f\right)_i^{n+1} + \left(A_2 C_f\right)_{i+1}^{n+1}\left(P_i^{n+1} - P_{i+1}^{n+1}\right) - \Delta s\left(A_2 C_f \rho_f g Cos\theta\right)_{i+1}^{n+1} + \\ \Delta s\left(A_2 B_\upsilon\right)_{i+1}^{n+1}\left(u_s\right)_{i+1}^{n+1} + \Delta s\left(\rho_f C_{f1} S_i v_E Cos\theta\right)_{i+1}^{n+1}\left(u_1\right)_{i+1}^{n+1} + \Delta s\left(\left(F_1\left(u_1\right)\right)_{i+1}^{n+1}\right)\end{array}\right)$$
$$4.18$$

$$\left(u_f\right)_{i+1}^{n+1} = \left(Q_f\right)_{i+1}^{n+1} + \frac{\left(A_2 C_f\right)_{i+1}^{n+1}\left(P_i^{n+1} - P_{i+1}^{n+1}\right)}{\left(E_f\right)_{i+1}^{n+1}} \qquad 4.19$$

With

$$\left(Q_f\right)_{i+1}^{n+1} = \frac{1}{\left(E_f\right)_{i+1}^{n+1}} \left(\begin{array}{l} \frac{\Delta s}{\Delta t}\left(\dot{m}_f\right)_{i+1}^{n} + \left(\dot{m}_f u_f\right)_{i}^{n+1} - \Delta s\left(A_2 C_f \rho_f g Cos\theta\right)_{i+1}^{n+1} + \Delta s\left(A_2 B_v\right)_{i+1}^{n+1}\left(u_s\right)_{i+1}^{n+1} + \\ \Delta s\left(\rho_f C_{f1} S_i v_E Cos\theta\right)_{i+1}^{n+1}\left(u_1\right)_{i+1}^{n+1} + \Delta s\left(\left(F_1\left(u_1\right)\right)_{i+1}^{n+1}\right) \end{array} \right)$$

4.20

4.2.3 Discretization of the Momentum Equations of the Cuttings Bed.

The momentum equation for the cuttings bed is given by equation (4.21)

$$\frac{\partial\left(\rho_1 u_1^2\right)}{\partial s} + \frac{\partial\left(\rho_1 u_1\right)}{\partial t} =$$
$$-\frac{\partial p}{\partial s} - \rho_1 g Cos\theta - \frac{1}{2} f_b \rho_1 u_1^2 \frac{S_B}{A_1} + \frac{1}{2} C_s f_s \rho_s \left(u_s - u_1\right)^2 \frac{S_i}{A_1} +$$
$$+\frac{1}{2} C_f f_f \rho_f \left(u_f - u_1\right)^2 \frac{S_i}{A_1} + u_s v_D C_s \rho_s \frac{S_i}{A_1} + u_f v_D \rho_f \frac{C_{f1}}{C_{s1}} C_s \frac{S_i}{A_1} Cos\theta - u_1 v_E \rho_1 \frac{S_i}{A_1} - \frac{F_1}{A_1 \Delta s}$$

4.21

Discretizing equation 4.21 gives;

$$\frac{\partial\left(A_1 \rho_1 u_1^2\right)}{\partial s} + \frac{\partial\left(A_1 \rho_1 u_1\right)}{\partial t} =$$
$$-A_1 \frac{\partial p}{\partial s} - \rho_1 A_1 g Cos\,\theta - \frac{1}{2} f_b \rho_1 u_1^2 S_B + \frac{1}{2} C_s f_s \rho_s \left(u_s - u_1\right)^2 S_i$$
$$+\frac{1}{2} C_f f_f \rho_f \left(u_f - u_1\right)^2 S_i + \left(u_s v_D C_s \rho_s S_i + u_f v_D \rho_f \frac{C_{f1}}{C_{s1}} C_s S_i - u_1 v_E \rho_1 S_i\right) \cos\theta - \frac{F_1}{\Delta s}$$

4.22

Replacing the derivatives by forward difference approximation implicitly, numerical expression for equation 4.22 at node i+1 and time step n+1 is obtained:

$$\frac{\left(A_1 \rho_1 u_1\right)_{i+1}^{n+1} - \left(A_1 \rho_1 u_1\right)_{i+1}^{n}}{\Delta t} + \frac{\left(\dot{m}_1 u_1\right)_{i+1}^{n+1} - \left(\dot{m}_1 u_1\right)_{i}^{n+1}}{\Delta s} =$$
$$\left(A_1\right)_{i+1}^{n+1}\left(\frac{P_i^{n+1} - P_{i+1}^{n+1}}{\Delta s}\right) - \left(A_1 \rho_1 g Cos\theta\right)_{i+1}^{n+1} - \left(G_1 u_1\right)_{i+1}^{n+1} + \left(H_1\left(u_s - u_1\right)\right)_{i+1}^{n+1} + \left(I_1\left(u_f - u_1\right)\right)_{i+1}^{n+1} +$$
$$\left(\left(u_s v_D C_s \rho_s S_i\right)_{i+1}^{n+1} + \left(u_f v_D \rho_f \frac{C_{f1}}{C_{s1}} C_s S_i\right)_{i+1}^{n+1} - \left(u_1 v_E \rho_1 S_i\right)_{i+1}^{n+1}\right)\left(Cos\theta\right)_{i+1}^{n+1} - \left(\frac{F_1}{\Delta s}\right)_{i+1}^{n+1}$$

4.23

Where

$$G_1 = \frac{\rho_1}{2} f_B u_1 S_B \qquad 4.24$$

$$H_1 = \frac{\rho_s}{2} f_s (u_s - u_1) S_i \qquad 4.24b$$

$$I_1 = \frac{\rho_f}{2} f_f (u_f - u_1) S_i \qquad 4.25$$

Re-arranging equation 4.23

$$\begin{aligned}
&(u_1)_{i+1}^{n+1}\left(\frac{\Delta s}{\Delta t}(A_1\rho_1)_{i+1}^{n+1} + (\dot{m}_1)_{i+1}^{n+1} + \Delta s(G_1)_{i+1}^{n+1} + \Delta s(H_1)_{i+1}^{n+1} + \Delta s(I_1)_{i+1}^{n+1} + \Delta s(v_E\rho_1 S_i Cos\theta)_{i+1}^{n+1}\right) = \\
&\frac{\Delta s}{\Delta t}(\dot{m}_1)_{i+1}^{n} + (\dot{m}_1 u_1)_i^{n+1} + (A_1)_{i+1}^{n+1}\left(P_i^{n+1} - P_{i+1}^{n+1}\right) - \Delta s(A_1\rho_1 g Cos\theta)_{i+1}^{n+1} + \Delta s\left((H_1 u_s)_{i+1}^{n+1} + \Delta s(I_1 u_f)_{i+1}^{n+1}\right) \\
&+\left((u_s v_D C_s \rho_s S_i)_{i+1}^{n+1} + \left(u_f v_D \rho_f \frac{C_{f1}}{C_{s1}} C_s S_i\right)_{i+1}^{n+1}\right)\Delta s(Cos\theta)_{i+1}^{n+1} - (F_1)_{i+1}^{n+1}
\end{aligned}$$

4.26

Setting

$$(E_B)_{i+1}^{n+1} = \frac{\Delta s}{\Delta t}(A_1\rho_1)_{i+1}^{n+1} + (\dot{m}_1)_{i+1}^{n+1} + \Delta s(G_1)_{i+1}^{n+1} + \Delta s(H_1)_{i+1}^{n+1} + \Delta s(I_1)_{i+1}^{n+1} + \Delta s(v_E\rho_1 S_i Cos\theta)$$

4.27

Then,

$$(u_1)_{i+1}^{n+1} = \frac{1}{(E_B)_{i+1}^{n+1}}\left(\begin{array}{l}
\frac{\Delta s}{\Delta t}(\dot{m}_1)_{i+1}^{n} + (\dot{m}_1 u_1)_i^{n+1} + (A_1)_{i+1}^{n+1}\left(P_i^{n+1} - P_{i+1}^{n+1}\right) - \Delta s(A_1\rho_1 g Cos\theta)_{i+1}^{n+1} \\
+\Delta s\left((H_1 u_s)_{i+1}^{n+1}\right) + \Delta s(I_1 u_f)_{i+1}^{n+1} + \left((u_s v_D C_s \rho_s S_i)_{i+1}^{n+1} + \left(u_f v_D \rho_f \frac{C_{f1}}{C_{s1}} C_s S_i\right)_{i+1}^{n+1}\right) \\
\Delta s(Cos\theta)_{i+1}^{n+1} - (F_1)_{i+1}^{n+1}
\end{array}\right)$$

4.28

$$(u_1)_{i+1}^{n+1} = (Q_B)_{i+1}^{n+1} + \frac{(A_1)_{i+1}^{n+1}\left(P_i^{n+1} - P_{i+1}^{n+1}\right)}{(E_B)_{i+1}^{n+1}} \tag{4.29}$$

With

$$(Q_B)_{i+1}^{n+1} = \frac{1}{(E_B)_{i+1}^{n+1}} \left(\begin{array}{l} \frac{\Delta s}{\Delta t}(\dot{m}_1)_{i+1}^{n} + (\dot{m}_1 u_1)_i^{n+1} - \Delta s(A_1 \rho_1 g Cos\theta)_{i+1}^{n+1} + \Delta s\left((H_1 u_s)_{i+1}^{n+1}\right) + \Delta s(I_1 u_f)_{i+1}^{n+1} \\ + \left((u_s v_D C_s \rho_s S_i)_{i+1}^{n+1} + \left(u_f v_D \rho_f \frac{C_{f1}}{C_{s1}} C_s S_i \right)_{i+1}^{n+1} \right) \Delta s(Cos\theta)_{i+1}^{n+1} - (F_1)_{i+1}^{n+1} \end{array} \right) \tag{4.30}$$

4.3 Formulation of Velocity –Correction Equations

In this study, the SIMPLE method developed by Patankar (1980) for single-phase fluid and modified by Crowe (1998) for two phase flow is used for the calculation of velocities in unknown pressure field. The SIMPLE method involves making a first guess for the pressure field and then solving the momentum equations to obtain the velocity field. An equation for correction of the guessed pressure field using the resulting velocity field is needed in the iteration. This pressure correction equation is obtained by introducing the velocity correction equation into the continuity equation.

Assuming the velocity is a function of the two pressures on each side of the velocity node, we obtain:

$$(u_f)_{i+1}^{n+1} = (u_f)_{i+1}^{n+1}\left(P_i^{n+1}, P_{i+1}^{n+1}\right) \tag{4.31}$$

$$(u_s)_{i+1}^{n+1} = (u_s)_{i+1}^{n+1}\left(P_i^{n+1}, P_{i+1}^{n+1}\right) \tag{4.32}$$

$$(u_1)_{i+1}^{n+1} = (u_1)_{i+1}^{n+1}\left(P_i^{n+1}, P_{i+1}^{n+1}\right) \tag{4.33}$$

Pressure changes at nodes i and i+1 would cause corresponding change in the velocities at these nodes. This change in velocity can be estimated by applying the Taylor series expansion to the velocity-pressure functions as given below:

$$(\Delta u_f)_{i+1}^{n+1} = \left(\frac{\partial u_{f\,i+1}^{\;n+1}}{\partial P_i^{n+1}}\right)\Delta P_i^{n+1} + \left(\frac{\partial u_{f\,i+1}^{\;n+1}}{\partial P_{i+1}^{n+1}}\right)\Delta P_{i+1}^{n+1} \qquad 4.34$$

$$(\Delta u_s)_{i+1}^{n+1} = \left(\frac{\partial u_{s\,i+1}^{\;n+1}}{\partial P_i^{n+1}}\right)\Delta P_i^{n+1} + \left(\frac{\partial u_{s\,i+1}^{\;n+1}}{\partial P_{i+1}^{n+1}}\right)\Delta P_{i+1}^{n+1} \qquad 4.35$$

$$(\Delta u_1)_{i+1}^{n+1} = \left(\frac{\partial u_{1\,i+1}^{\;n+1}}{\partial P_i^{n+1}}\right)\Delta P_i^{n+1} + \left(\frac{\partial u_{1\,i+1}^{\;n+1}}{\partial P_{i+1}^{n+1}}\right)\Delta P_{i+1}^{n+1} \qquad 4.36$$

The derivatives in equations 4.34, 4.35 and 4.36 can be obtained by taking the derivatives of equations 4.9, 4.19 and 4.29 respectively.

$$\frac{\partial u_{f\,i+1}^{\;n+1}}{\partial P_{i+1}^{n+1}} = -\frac{(C_f A_2)_{i+1}^{n+1}}{E_{f\,i+1}^{\;n+1}} \qquad 4.37$$

$$\frac{\partial u_{f\,i+1}^{\;n+1}}{\partial P_i^{n+1}} = \frac{(C_f A_2)_{i+1}^{n+1}}{E_{f\,i+1}^{\;n+1}} \qquad 4.38$$

and

$$\frac{\partial u_{s\,i+1}^{\;n+1}}{\partial P_{i+1}^{n+1}} = -\frac{(C_s A_2)_{i+1}^{n+1}}{E_{s\,i+1}^{\;n+1}} \qquad 4.39$$

$$\frac{\partial u_{s\,i+1}^{\;n+1}}{\partial P_i^{n+1}} = \frac{(C_s A_2)_{i+1}^{n+1}}{E_{s\,i+1}^{\;n+1}} \qquad 4.40$$

also

$$\frac{\partial u_{1\,i+1}^{\;n+1}}{\partial P_{i+1}^{n+1}} = -\frac{(A_1)_{i+1}^{n+1}}{E_{B\,i+1}^{\;n+1}} \qquad 4.41$$

$$\frac{\partial u_{1\,i+1}^{\;n+1}}{\partial P_i^{n+1}} = \frac{(A_1)_{i+1}^{n+1}}{E_{B\,i+1}^{\;n+1}} \qquad 4.42$$

Introducing equations 4.37 to 4.42 into 4.34 to 4.36, the velocity correction formulas for the fluid, solid and the moving bed at node i+1 are derived:

$$(\Delta u_f)_{i+1}^{n+1} = \frac{(A_2 C_f)_{i+1}^{n+1}\left(\Delta P_i^{n+1} - \Delta P_{i+1}^{n+1}\right)}{(E_f)_{i+1}^{n+1}} \tag{4.43}$$

$$(\Delta u_s)_{i+1}^{n+1} = \frac{(A_2 C_s)_{i+1}^{n+1}\left(\Delta P_i^{n+1} - \Delta P_{i+1}^{n+1}\right)}{(E_s)_{i+1}^{n+1}} \tag{4.44}$$

$$(\Delta u_1)_{i+1}^{n+1} = \frac{(A_1)_{i+1}^{n+1}\left(\Delta P_i^{n+1} - \Delta P_{i+1}^{n+1}\right)}{(E_B)_{i+1}^{n+1}} \tag{4.45}$$

Applying equations 4.43 to 4.45 to the velocity changes

$$(\Delta u_f)_i^{n+1} = \frac{(A_2 C_f)_i^{n+1}\left(\Delta P_{i-1}^{n+1} - \Delta P_i^{n+1}\right)}{(E_f)_i^{n+1}} \tag{4.46}$$

$$(\Delta u_s)_i^{n+1} = \frac{(A_2 C_s)_i^{n+1}\left(\Delta P_{i-1}^{n+1} - \Delta P_i^{n+1}\right)}{(E_s)_i^{n+1}} \tag{4.47}$$

$$(\Delta u_1)_i^{n+1} = \frac{(A_1)_i^{n+1}\left(\Delta P_{i-1}^{n+1} - \Delta P_i^{n+1}\right)}{(E_B)_i^{n+1}} \tag{4.48}$$

In addition, the mass inflow rate from the reservoir changes with wellbore pressure as follows:

$$\Delta s_{f\,i+1}^{\;n+1} = -K^{'}.\Delta P_{i+1}^{n+1} \tag{4.49}$$

$K^{'}$ is a constant calculated from the reservoir inflow model given by equations 3.68 to 3.70 for sudden change in pressures at node i and i+1.

4.4 Discretization of the Mass Balance Equations.

4.41 Discretization of the continuity equation for the solid component in upper layer.

The mass balance equation for the suspended solid component in the upper layer is represented by equation given as:

$$\frac{\partial(\rho_s C_s)}{\partial t}+\frac{\partial(\rho_s u_s C_s)}{\partial s}=-\rho_s v_D C_s\frac{S_i}{A_2}+\rho_s v_E C_{s1}\frac{S_i}{A_2} \qquad 4.50a$$

Discretizing equation 4.50a,

$$\frac{(A_2\rho_s C_s)_{i+1}^{n+1}-(A_2\rho_s C_s)_{i+1}^{n}}{\Delta t}+\frac{(A_2\rho_s u_s C_s)_{i+1}^{n+1}-(A_2\rho_s u_s C_s)_{i}^{n+1}}{\Delta s}=(\rho_s v_E C_b S_i)_{i+1}^{n+1}-(\rho_s v_D C_s S_i)_{i+1}^{n+1} \qquad 4.50b$$

The concentration of the suspended solids in the upper layer is given as:

$$(C_s)_{i+1}^{n+1}=\frac{\frac{\Delta s}{\Delta t}(A_2\rho_s C_s)_{i+1}^{n}+(A_2\rho_s u_s C_s)_{i}^{n+1}+(\rho_s v_E C_b S_i)_{i+1}^{n+1}\Delta s}{\frac{\Delta s}{\Delta t}(A_2\rho_s)_{i+1}^{n+1}+(A_2\rho_s u_s)_{i+1}^{n+1}+(\rho_s v_D S_i)_{i+1}^{n+1}\Delta s} \qquad 4.51$$

4.42 Discretization of the continuity equation for the foam component in upper layer.

The mass balance equation for the foam component in the upper layer is represented by equation given as:

$$\frac{\partial(\rho_f C_f)}{\partial t}+\frac{\partial(\rho_f u_f C_f)}{\partial s}=-\frac{C_{f1}}{C_b}\rho_f v_D C_s\frac{S_i}{A_2}+\rho_f v_E C_{f1}\frac{S_i}{A_2}+S_f \qquad 4.52a$$

Discretizing equation 4.52a,

$$\frac{\left(A_2\rho_f C_f\right)_{i+1}^{n+1}-\left(A_2\rho_f C_f\right)_{i+1}^{n}}{\Delta t}+\frac{\left(A_2\rho_f u_f C_f\right)_{i+1}^{n+1}-\left(A_2\rho_f u_f C_f\right)_{i}^{n+1}}{\Delta s}=-\left(\frac{C_{f1}}{C_b}\rho_f v_D C_s S_i\right)_{i+1}^{n+1}$$

$$+\left(\rho_f v_E C_{f1} S_i\right)_{i+1}^{n+1}+\left(A_2 S_f\right)_{i+1}^{n+1}$$

4.52b

The concentration of the foam in the upper layer is

$$\left(C_f\right)_{i+1}^{n+1}=\frac{\frac{\Delta s}{\Delta t}\left(A_2\rho_f C_f\right)_{i+1}^{n}+\left(A_2\rho_f u_f C_f\right)_{i}^{n+1}+\left(\rho_f v_E C_{f1} S_i\right)_{i+1}^{n+1}\Delta s-\left(\frac{C_{f1}}{C_b}\rho_f v_D S_i\right)_{i+1}^{n+1}.\Delta s+\left(A_2 S_f\right)_{i+1}^{n+1}.\Delta s}{\frac{\Delta s}{\Delta t}\left(A_2\rho_f\right)_{i+1}^{n+1}+\left(A_2\rho_f u_f\right)_{i+1}^{n+1}}$$

4.53

4.43 Discretization of the continuity equation for the moving bed.

The mass balance equation for the foam component in the upper layer is represented by equation given as:

$$\frac{\partial(A_1\rho_1)}{\partial t}+\frac{\partial(A_1\rho_1 u_1)}{\partial s}=\left(\rho_s+\frac{C_{f1}}{C_b}\rho_f\right)v_D C_s\frac{S_i}{A_1}-\rho_1 v_E\frac{S_i}{A_2} \qquad 4.54a$$

Discretizing the above equation,

$$\frac{(A_1\rho_1)_{i+1}^{n+1}-(A_1\rho_1)_{i+1}^{n}}{\Delta t}+\frac{(A_1\rho_1 u_1)_{i+1}^{n+1}-(A_1\rho_1 u_1)_{i}^{n+1}}{\Delta s}=\left(\left(\rho_s+\frac{C_{f1}}{C_b}\rho_f\right)v_D C_s S_i\right)_{i+1}^{n+1}-(\rho_1 v_E S_i)_{i+1}^{n+1}$$

4.54b

4.5 Formulation of Pressure-Correction Equation

The concentration at node i+1 is assumed to be a function of the velocities at node i and i+1 and the source term. Using the Taylor series expansion, the concentration changes for the solid and foam components are obtained:

$$\left(C_f\right)_{i+1}^{n+1}=\left(C_f^{*}\right)_{i+1}^{n+1}+\left(\frac{\partial C_{f\,i+1}^{\;n+1}}{\partial u_{f\,i}^{\;n+1}}\right)\Delta u_{f\,i}^{\;n+1}+\left(\frac{\partial C_{f\,i+1}^{\;n+1}}{\partial u_{f\,i+1}^{\;n+1}}\right)\Delta u_{f\,i+1}^{\;n+1}+\left(\frac{\partial C_{f\,i+1}^{\;n+1}}{\partial s_{f\,i+1}^{\;n+1}}\right)\Delta s_{f\,i+1}^{\;n+1} \qquad 4.55$$

$$(C_s)_{i+1}^{n+1} = (C_s^*)_{i+1}^{n+1} + \left(\frac{\partial C_{s\,i+1}^{\ n+1}}{\partial u_{s\,i}^{\ n+1}}\right)\Delta u_{s\,i}^{\ n+1} + \left(\frac{\partial C_{s\,i+1}^{\ n+1}}{\partial u_{s\,i+1}^{\ n+1}}\right)\Delta u_{s\,i+1}^{\ n+1} \qquad 4.56$$

The superscript * represents the value from previous iteration. By taking the indicated derivatives of the function of concentration and velocity the following equations are obtained:

$$\left(\frac{\partial C_{f\,i+1}^{\ n+1}}{\partial u_{f\,i}^{\ n+1}}\right) = \frac{(A_2\rho_f C_f)_i^{n+1}}{\frac{\Delta s}{\Delta t}(A_2\rho_f)_{i+1}^{n+1} + (A_2\rho_f u_f)_{i+1}^{n+1} s} \qquad 4.57$$

$$\left(\frac{\partial C_{f\,i+1}^{\ n+1}}{\partial u_{f\,i+1}^{\ n+1}}\right) = \frac{-(A_2\rho_f)_{i+1}^{n+1}\left(\frac{\Delta s}{\Delta t}(A_2\rho_f C_f)_{i+1}^{n} + (A_2\rho_f u_f C_f)_i^{n+1} + (\rho_f v_E C_{f1} S_i)_{i+1}^{n+1}\Delta s - \left(\frac{C_{f1}}{C_b}\rho_f v_D S_i\right)_{i+1}^{n+1}\Delta s + (A_2 S_f)_{i+1}^{n+1}\Delta s\right)}{\left(\frac{\Delta s}{\Delta t}(A_2\rho_f)_{i+1}^{n+1} + (A_2\rho_f u_f)_{i+1}^{n+1}\right)^2}$$

4.58

$$\left(\frac{\partial C_{f\,i+1}^{\ n+1}}{\partial s_{f\,i+1}^{\ n+1}}\right) = \frac{(A_2)_{i+1}^{n+1}.\Delta s}{\frac{\Delta s}{\Delta t}(A_2\rho_f)_{i+1}^{n+1} + (A_2\rho_f u_f)_{i+1}^{n+1}} \qquad 4.59$$

$$\left(\frac{\partial C_{s\,i+1}^{\ n+1}}{\partial u_{s\,i}^{\ n+1}}\right) = \frac{(A_2 C_s)_i^{n+1}}{\frac{\Delta s}{\Delta t}(A_2)_{i+1}^{n+1} + (A_2 u_s)_{i+1}^{n+1} + (v_D S_i)_{i+1}^{n+1}\Delta s} \qquad 4.60$$

$$\left(\frac{\partial C_{s\,i+1}^{\ n+1}}{\partial u_{s\,i+1}^{\ n+1}}\right) = \frac{-(A_2)_{i+1}^{n+1}\left(\frac{\Delta s}{\Delta t}(A_2 C_s)_{i+1}^{n} + (A_2 u_s C_s)_i^{n+1} + (v_E C_b S_i)_{i+1}^{n+1}\Delta s\right)}{\left(\frac{\Delta s}{\Delta t}(A_2)_{i+1}^{n+1} + (A_2 u_s)_{i+1}^{n+1} + (v_D S_i)_{i+1}^{n+1}\Delta s\right)^2} \qquad 4.61$$

There is a need to discretize a final equation: the sum of the concentration is equal to unity, in order to complete the set of momentum and mass equations.

$$(C_s)_{i+1}^{n+1} + (C_f)_{i+1}^{n+1} = 1 \qquad 4.62$$

Introducing equations 4.55 and 4.56 into equation 4.62 yields the equation (4.63):

$$\left(C_f^*\right)_{i+1}^{n+1}+\left(\frac{\partial C_{f\,i+1}^{\;n+1}}{\partial u_{f_i}^{\;n+1}}\right)\Delta u_{f_i}^{\;n+1}+\left(\frac{\partial C_{f\,i+1}^{\;n+1}}{\partial u_{f\,i+1}^{\;n+1}}\right)\Delta u_{f\,i+1}^{\;n+1}+\left(\frac{\partial C_{f\,i+1}^{\;n+1}}{\partial s_{f\,i+1}^{\;n+1}}\right)\Delta s_{f\,i+1}^{\;n+1}+\left(C_s^*\right)_{i+1}^{n+1}+\left(\frac{\partial C_{s\,i+1}^{\;n+1}}{\partial u_{si}^{\;n+1}}\right)\Delta u_{si}^{\;n+1}+$$

$$\left(\frac{\partial C_{s\,i+1}^{\;n+1}}{\partial u_{s\,i+1}^{\;n+1}}\right)\Delta u_{s\,i+1}^{\;n+1}\doteq 1$$

4.63

Introducing equations 4.43 to 4.49 and 4.57 to 4.61 into equation 4.63

$$\frac{\left(A_2\rho_f C_f\right)_i^{n+1}}{\frac{\Delta s}{\Delta t}\left(A_2\rho_f\right)_{i+1}^{n+1}+\left(A_2\rho_f u_f\right)_{i+1}^{n+1}}\cdot\frac{\left(A_2C_f\right)_i^{n+1}\left(\Delta P_{i-1}^{n+1}-\Delta P_i^{n+1}\right)}{\left(E_f\right)_i^{n+1}}-$$

$$\frac{\left(A_2\rho_f\right)_{i+1}^{n+1}\left(\frac{\Delta s}{\Delta t}\left(A_2\rho_f C_f\right)_{i+1}^{n}+\left(\dot{m}_f\right)_i^{n+1}+\left(\rho_f v_E C_{f1}S_i\right)_{i+1}^{n+1}\Delta s-\left(\frac{C_{f1}}{C_b}\rho_f v_D S_i\right)_{i+1}^{n+1}\Delta s+\left(A_2S_f\right)_{i+1}^{n+1}\Delta s\right)}{\left(\frac{\Delta s}{\Delta t}\left(A_2\rho_f\right)_{i+1}^{n+1}+\left(A_2\rho_f u_f\right)_{i+1}^{n+1}\right)^2}\cdot$$

$$\frac{\left(A_2C_f\right)_{i+1}^{n+1}\left(\Delta P_i^{n+1}-\Delta P_{i+1}^{n+1}\right)}{\left(E_f\right)_{i+1}^{n+1}}+\frac{\left(A_2\right)_{i+1}^{n+1}\Delta s}{\frac{\Delta s}{\Delta t}\left(A_2\rho_f\right)_{i+1}^{n+1}+\left(A_2\rho_f u_f\right)_{i+1}^{n+1}}\Delta s_{f\,i+1}^{\;n+1}+\frac{\left(A_2C_s\right)_i^{n+1}}{\frac{\Delta s}{\Delta t}\left(A_2\right)_{i+1}^{n+1}+\left(A_2u_s\right)_{i+1}^{n+1}+\left(v_D S_i\right)_{i+1}^{n+1}\Delta s}\cdot$$

$$\frac{\left(A_2C_s\right)_i^{n+1}\left(P_{i-1}^{n+1}-P_i^{n+1}\right)}{\left(E_s\right)_i^{n+1}}\;\frac{\left(A_2C_s\right)_{i+1}^{n+1}\left(\Delta P_i^{n+1}-\Delta P_{i+1}^{n+1}\right)}{\left(E_s\right)_{i+1}^{n+1}}\frac{\left(A_2\right)_{i+1}^{n+1}\left(\frac{\Delta s}{\Delta t}\left(A_2C_s\right)_{i+1}^{n}+\left(A_2u_sC_s\right)_i^{n+1}+\left(v_E C_b S_i\right)_{i+1}^{n+1}\Delta s\right)}{\left(\frac{\Delta s}{\Delta t}\left(A_2\right)_{i+1}^{n+1}+\left(A_2u_s\right)_{i+1}^{n+1}+\left(v_D S_i\right)_{i+1}^{n+1}\Delta s\right)^2}$$

$$=1-\left(C_f^*\right)_{i+1}^{n+1}-\left(C_s^*\right)_{i+1}^{n+1}$$

4.64

The above equation is the pressure correction equation. This equation can be expressed in a more compacted form:

$$L_i^{n+1}\Delta P_{i-1}^{n+1}-\left(L_i^{n+1}+U_i^{n+1}\right)\Delta P_i^{n+1}+\left(U_i^{n+1}-T_i^{n+1}\right)\Delta P_{i+1}^{n+1}=1-\left(C_f^*\right)_{i+1}^{n+1}-\left(C_s^*\right)_{i+1}^{n+1}$$

4.65

Where

$$L_i^{n+1} = \frac{\left(A_2\rho_f C_f\right)_i^{n+1}}{\frac{\Delta s}{\Delta t}\left(A_2\rho_f\right)_{i+1}^{n+1} + \left(A_2\rho_f u_f\right)_{i+1}^{n+1}} \frac{\left(A_2 C_f\right)_i^{n+1}}{\left(E_f\right)_i^{n+1}} + \frac{\left(A_2 C_s\right)_i^{n+1}}{\frac{\Delta s}{\Delta t}\left(A_2\right)_{i+1}^{n+1} + \left(A_2 u_s\right)_{i+1}^{n+1} + \left(v_D S_i\right)_{i+1}^{n+1}\Delta s} \frac{\left(A_2 C_s\right)_i^{n+1}}{\left(E_s\right)_i^{n+1}} \tag{4.66}$$

$$U_i^{n+1} = \frac{\left(A_2\rho_f\right)_{i+1}^{n+1}\begin{pmatrix}\frac{\Delta s}{\Delta t}\left(A_2\rho_f C_f\right)_{i+1}^{n} + \left(\dot{m}_f\right)_i^{n+1} + \left(\rho_f v_E C_{f1} S_i\right)_{i+1}^{n+1}\Delta s - \\ \left(\frac{C_{f1}}{C_b}\rho_f v_D S_i\right)_{i+1}^{n+1} .\Delta s + \left(A_2 S_f\right)_{i+1}^{n+1}\Delta s\end{pmatrix}_{i+1}^{n+1}}{\left(\frac{\Delta s}{\Delta t}\left(A_2\rho_f\right)_{i+1}^{n+1} + \left(A_2\rho_f u_f\right)_{i+1}^{n+1}\right)^2} .$$

$$\frac{\left(A_2 C_f\right)_{i+1}^{n+1}}{\left(E_f\right)_{i+1}^{n+1}} + \frac{\left(A_2 C_s\right)_{i+1}^{n+1}}{\left(E_s\right)_{i+1}^{n+1}} . \frac{\left(A_2\right)_{i+1}^{n+1}\left(\frac{\Delta s}{\Delta t}\left(A_2 C_s\right)_{i+1}^{n} + \left(A_2 u_s C_s\right)_i^{n+1} + \left(v_E C_b S_i\right)_{i+1}^{n+1}\Delta s\right)}{\left(\frac{\Delta s}{\Delta t}\left(A_2\right)_{i+1}^{n+1} + \left(A_2 u_s\right)_{i+1}^{n+1} + \left(v_D S_i\right)_{i+1}^{n+1}\Delta s\right)^2} \tag{4.67}$$

$$T_i^{n+1} = \frac{C'\left(A_2\right)_{i+1}^{n+1}.\Delta s}{\frac{\Delta s}{\Delta t}\left(A_2\rho_f\right)_{i+1}^{n+1} + \left(A_2\rho_f u_f\right)_{i+1}^{n+1}.\Delta s} \tag{4.68}$$

The equation above is the pressure formulation of the continuity equation. The tri-diagonal matrix developed by Thomas can be used to solve this equation. The solutions from the compacted pressure equation (4.65) are added to the old pressure values to correct the pressure field and also introduced into equations 4.46 to 4.49, 4.55 and 4.56 to correct the velocity fields, source term and concentrations. Solving the momentum equations again, new velocity fields are obtained. With this, concentrations are calculated by using equations 4.51 and 4.53. If continuity condition is met, calculation will switch to next time step until specified maximum time is reached.

4.6 Numerical Method for Transient Foam-Solids Flow Model.

This section deals with how the already derived numerical solution is applied to compressible foam flow with and without source term effect.

Case-1: No source term.

For this case, the foam density and quality should be adjusted for change in pressure and temperature.

Case-2: With source term effects.

The source term as already discussed has effect on velocity, pressure, and concentration distribution. Because the source term also affects the foam quality transiently, the foam quality needs to be adjusted for new pressure condition after stable solutions for pressure, velocity, concentration and density were obtained with the effect of source term S_f. The gas continuity or the liquid continuity equation obtained from equation 3.74 can be used as the adjusting equation. Re-writing equation 3.74 as a function of foam quality

$$\begin{aligned}&\frac{\partial}{\partial t}\left(C_f A_2\left((1-\Gamma)\rho_L+\Gamma\rho_g\right)\right)+\frac{\partial}{\partial x}\left(C_f A_2 u_f\left((1-\Gamma)\rho_L+\Gamma\rho_g\right)\right)=A_2\left(S_g+S_L\right)+\\&\left(v_E C_{f1}S_i-\frac{C_{fi}}{C_{s1}}C_s v_D S_i\right)\left((1-\Gamma)\rho_L+\Gamma\rho_g\right)\end{aligned} \qquad 4.69$$

To satisfy the continuity of both liquid and gas phases, equation 4.69 is divided into two parts.

$$\frac{\partial}{\partial t}\left(C_f A_2\left((1-\Gamma)\rho_L\right)\right)+\frac{\partial}{\partial x}\left(C_f A_2 u_f\left((1-\Gamma)\rho_L\right)\right)=A_2 S_L+\left(v_E C_{f1}S_i-\frac{C_{fi}}{C_{s1}}C_s v_D S_i\right)\left((1-\Gamma)\rho_L\right) \qquad 4.70$$

and

$$\frac{\partial}{\partial t}\left(C_f A_2\left(\Gamma\rho_g\right)\right)+\frac{\partial}{\partial x}\left(C_f A_2 u_f\left(\Gamma\rho_g\right)\right)=A_2 S_g+\left(v_E C_{f1}S_i-\frac{C_{fi}}{C_{s1}}C_s v_D S_i\right)\left(\Gamma\rho_g\right) \qquad 4.71$$

Either of equation 4.70 or 4.71 could be used for the adjustment of foam quality.

The gas equation can be discretized as follows:

$$\frac{\left(C_f A_2\left(\Gamma\rho_g\right)\right)_{i+1}^{n+1}-\left(C_f A_2\left(\Gamma\rho_g\right)\right)_{i+1}^{n}}{\Delta t}+\frac{\left(C_f A_2 u_f\left(\Gamma\rho_g\right)\right)_{i+1}^{n+1}-\left(C_f A_2 u_f\left(\Gamma\rho_g\right)\right)_{i}^{n+1}}{\Delta s}=$$

$$\left(A_2 S_g\right)_{i+1}^{n+1}+\left(v_E C_{f1} S_i-\frac{C_{fi}}{C_{s1}} C_s v_D S_i\right)_{i+1}^{n+1}\left(\Gamma\rho_g\right)_{i+1}^{n+1}$$

$$\Gamma_{i+1}^{n+1}=\frac{\left(C_f A_2 u_f\left(\Gamma\rho_g\right)\right)_{i}^{n+1}+\frac{\Delta s}{\Delta t}\left(C_f A_2\left(\Gamma\rho_g\right)\right)_{i+1}^{n}+\Delta s\left(\left(A_2 S_g\right)_{i+1}^{n+1}\right)}{\left(C_f A_2 u_f \rho_g\right)_{i+1}^{n+1}+\frac{\Delta s}{\Delta t}\left(C_f A_2 \rho_g\right)_{i+1}^{n+1}-\left(v_E C_{f1} S_i-\frac{C_{fi}}{C_{s1}} C_s v_D S_i\right)_{i+1}^{n+1}\left(\rho_g\right)_{i+1}^{n+1}} \tag{4.72}$$

When using equation (4.72) for the first control cell, the injection gas rate at the boundary should be used.

$$\left(C_f A_2 u_f\left(\Gamma\rho_g\right)\right)_{0}^{n+1}=\dot{m}_{gin} \tag{4.73}$$

CHAPTER 5
RESULTS AND DISCUSSIONS

Results from sensitivity analyses of the factors controlling cuttings transport with foam were presented in this chapter. Verification of the model predictions were also provided by comparing model results with experimental data.

5.1 Verification of Model Predictions

The model predictions were compared with the experimental data collected from the LPAT flow loop facility at the University of Tulsa (Capo, 2003). The input data used for the comparison study are given in Table 5.1.

Table 5.1: Input Data Used for Model Verification Study

Length of inclined wells(ft)	90
Diameter of hole(in)	8.0
Outer diameter of pipe(in)	4.5
Cutting size (cm)	2.311
Density of cuttings(g/cm^3)	2.613
Back pressure(psi)	14.7-20.0
Nozzle diameter (in)	28/32
Inclination of well(degree)	45

Table 5.2: Comparison of Model Predictions with Experimental Results

Test	Qair (scfm)	Qliquid (gpm)	ROP (ft/hr)	ΔP(Experiment) (psia)	ΔP(Model) (psia)	% Error
1	60	108	59.9	26.85	25.6	4.655
2	80	120	32.5	30.99	26.1	15.78
3	35	96	27.7	22.44	27.3	21.65
4	135	64	86.6	32.70	28.0	14.37

The results of the comparison of model predictions with experimental data are shown in Table 5.2. It was seen that the numerical method under predicted pressure drop observed during cuttings transport experiment conducted in 45^0 inclined well. The difference between measured and calculated pressure value varied between 4.6 to 21.6% .

5.2 Sensitivity Analyses of the Factors Affecting Cuttings Transport

The base data used for the simulation study are shown in Table 5.3. The sensitivity analyses were conducted to show effects of gas and liquid injection rates, drilling rate, back pressure, reservoir influx and inclination on the bottomhole pressure and cuttings concentration profile along the inclined well.

5.2.1 Effect of Gas Injection Rate on Bottomhole Pressure and Cuttings Concentration

Figures 5.1 and 5.2 illustrate the effect of gas injection rate on the cuttings concentration and bottomhole pressure respectively. The gas injection rate has significant effect on the cuttings transport process. Increasing the gas injection rate yields better cuttings transport reflected by reduction in the average cuttings concentration in the annulus (figure 5.1). Increased gas flow rate increases foam quality which in turn increases the effective viscosity of the foam and, hence, the cuttings lifting capacity of the foam is increased. The effect of gas injection rate is more pronounced at lower gas injection rates.

The bottomhole pressure decreases as gas injection rate increases. This is because increasing the gas rate reduces the density of foam which in turn decreases the hydrostatic pressure hence reducing the bottomhole pressure. The reduction of bottomhole pressure can also be attributed to the reduction of average cuttings concentration in the annulus with increasing gas injection rate. The hydrostatic pressure has more impact on the bottomhole pressure when the foam flow rate is not too high (i.e. frictional pressure losses are low).

Table 5.3: Base Data Used for Simulation of Foam Drilling in Inclined Wells

Back Pressure	40 psia
Reservoir Pressure	500 psia
Time Increment	60 sec
Number of Control volume	30
Length of inclined well	400ft
Hole Diameter	8.5in
Drill Pipe OD	4.5 in
Drill Pipe ID	3.826 in
Eccentricity	1.0
Cutting Size	0.5in
Cutting specific gravity	2.7
Bit nozzle size (3 nozzles)	28/32 in
Surface temperature	60 ^{0}F
Geothermal gradient	1.5 ^{0}F/100 ft
Foam	Air + water
Drilling rate	60 ft/hr
Gas injection rate	40scfm
Liquid Injection rate	40gpm
Gas specific PI	0 scfm/ft/psia
Water specific PI	0 gpm/ft/psia
Oil specific PI	0 gpm/ft/psia
Inclination	60 deg
Thickness of reservoir	100 ft

5.2.2 Effect of Liquid Injection Rate on Bottomhole Pressure and Cuttings Concentration

The effect of liquid injection rate on the average cuttings concentration and bottomhole pressure is also illustrated by figures 5.1 and 5.2. Liquid injection rate has little influence on the cuttings concentration compared to the effect of gas injection rate. Results also indicate that at very low or very high gas injection rate, the effect of increasing liquid rate has negligible effect on the cuttings concentration. Increasing liquid injection rates increases the bottomhole pressure but reduces the foam quality, which in turns, reduces the effective viscosity and, therefore, so does the lifting and transport ability of foam.

Figure 5.2 shows that the bottomhole pressure increases with increasing liquid injection rate. Increasing the liquid injection rates reduces the foam quality (increase in foam density) which as a result, increases the hydrostatic pressure. This increase in bottomhole pressure can also be explained in terms of increase in cuttings accumulation associated with increase in the liquid injection rate with resulting increase in the foam-cuttings density in the annulus.

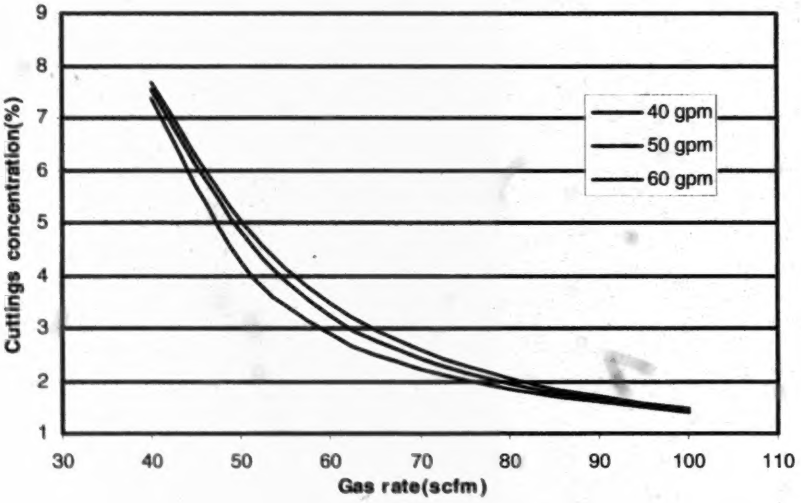

Fig. 5.1 Average cuttings concentration variation gas and liquid injection rate

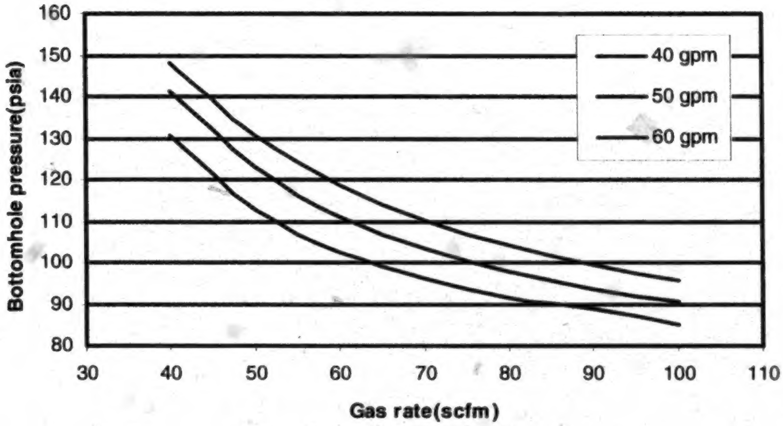

Fig. 5.2 Bottomhole pressure variation with gas and liquid injection rate

5.2.3 Effect of Drilling Rate on Bottomhole Pressure and Cuttings Concentration

Figures 5.3 and 5.4 illustrate the effect of drilling rate on the cuttings concentration and bottomhole pressure respectively. For fixed gas and liquid injection rates, cuttings concentration increases with increasing drilling rate (fig. 5.3).

The bottomhole pressure increases as the drilling rate increases (fig. 5.4). This effect is attributed to increase in the average cuttings concentration in the annulus with increasing drilling rate. The effect of drilling rate on the bottomhole pressure is more pronounced at lower gas rates.

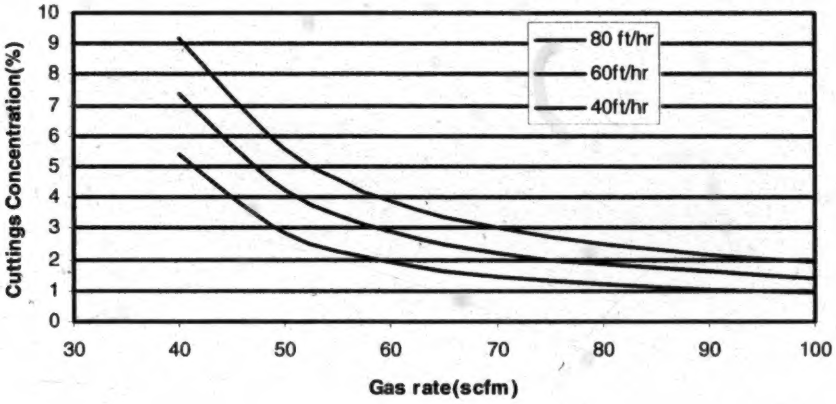

Fig. 5.3 Average cuttings concentration variation drilling rate.

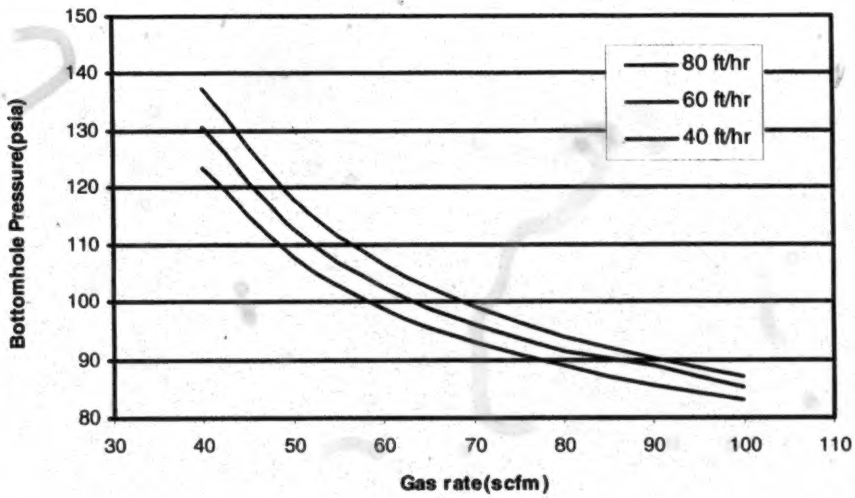

Fig. 5.4 Bottomhole pressure variation with drilling rate.

5.2.4 Effect of Inclination on Bottomhole Pressure and Cuttings Concentration

Figures 5.5 to 5.7 illustrate the effect of well inclination on the cuttings concentration and the bottomhole pressure in the annulus. Generally, cuttings concentration increases as inclination angle of the well from the vertical increases (fig. 5.5).

Similarly, Figure 5.6 depicts that an increase in the bottomhole pressure with increase in well inclination.

As shown in fig. 5.7 to keep the cuttings concentration in the annulus constant (say at 2%) more gas needs to be injected as the inclination of the well from the vertical increases while keeping the liquid rate constant.

Figure 5.8 shows that the distribution of cuttings along the well under steady state flow condition for different angle of inclinations of the well. For all angles of inclination, the cuttings distribution along the well was similar with the highest cuttings concentration at the bottom and the lowest at the top. Also shown by figure 5.8 is that cuttings concentration at any particular cross section of the wellbore increases with increasing inclination angle.

Results also indicate that effect of inclination on both bottomhole pressure and average cutting concentration in the annulus is more pronounced at lower gas injection rate.

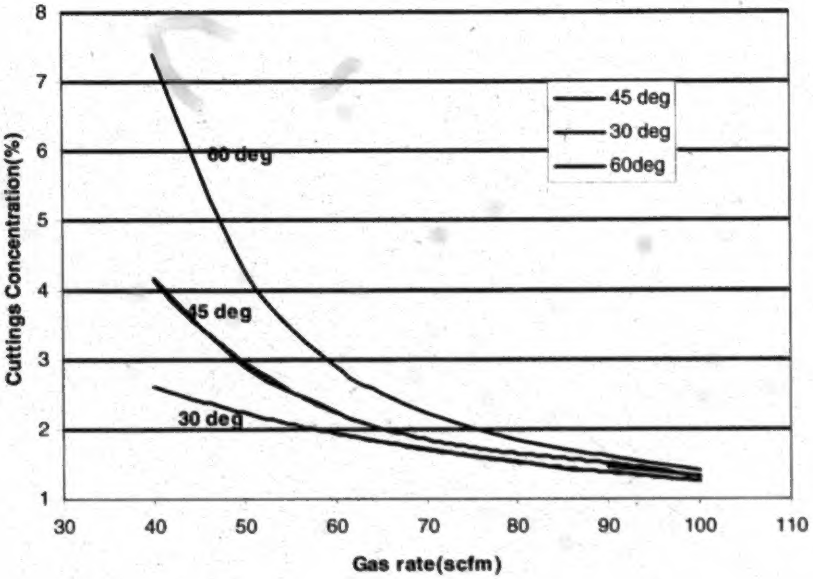

Fig. 5.5 Average cuttings concentration variation with inclination

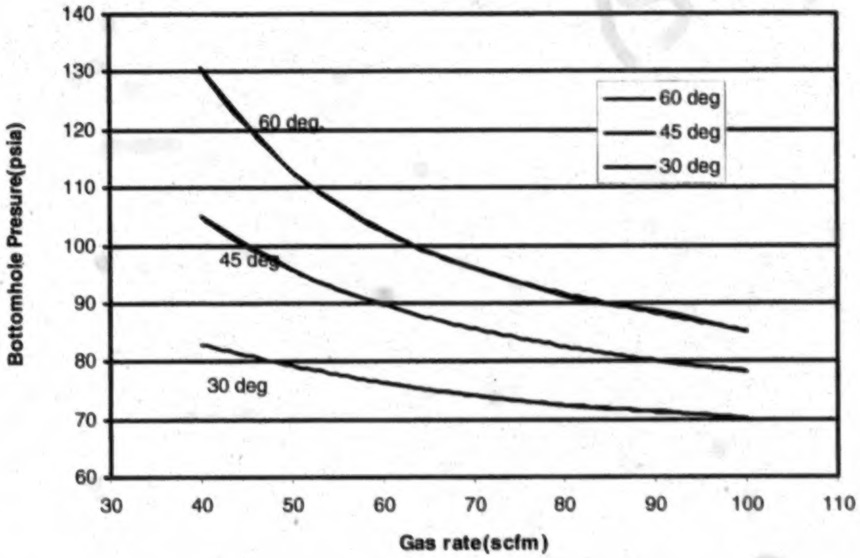

Fig. 5.6 Bottomhole pressure variation with inclination

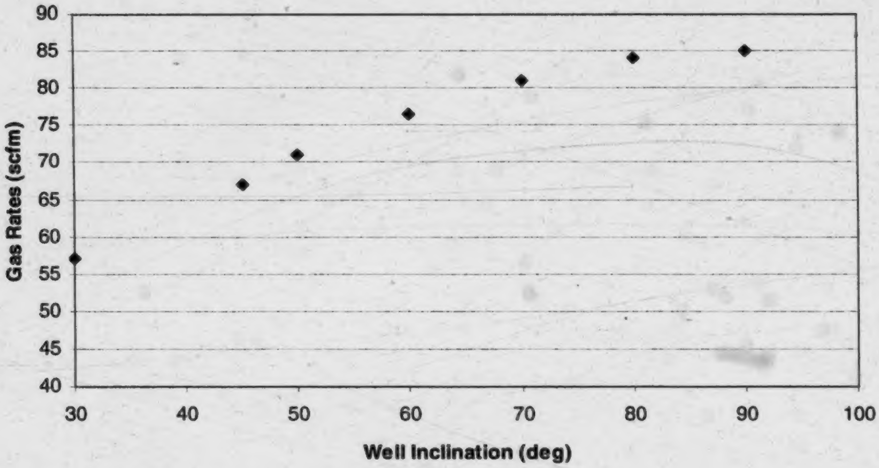

Fig. 5.7 Gas injection rate variation with well inclination

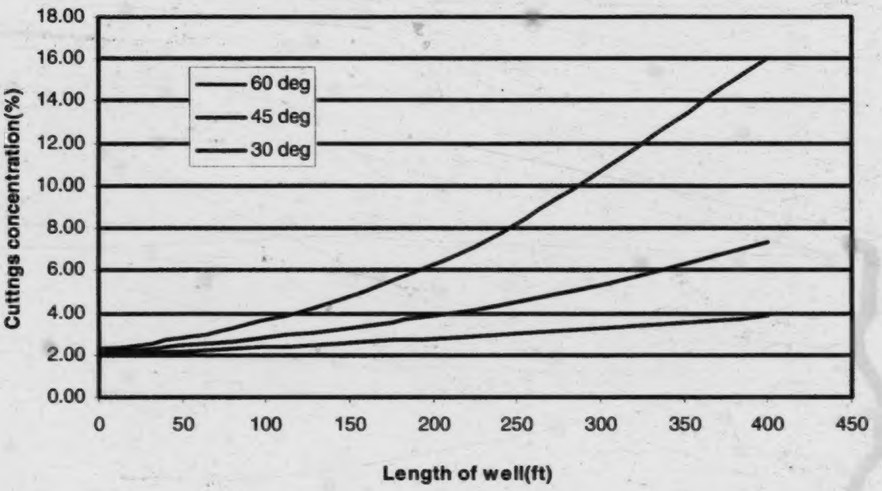

Fig. 5.8 Cuttings concentration profile variation with inclination

5.2.5 Effect of Back Pressure on Cuttings Concentration and Bottomhole Pressure

Increasing back pressure increases the cuttings concentration along the wellbore for a fixed gas and liquid injection rate (fig. 5.9). This effect is due to decrease in foam quality as back pressure increases.

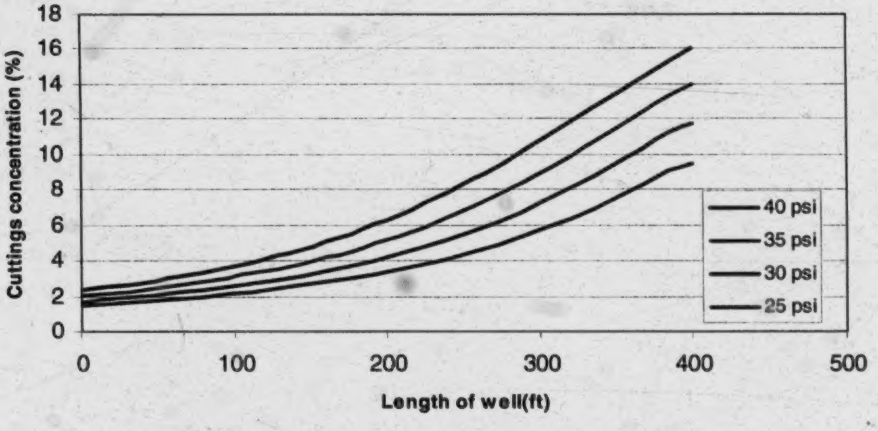

Figure 5.9: Cuttings concentration variation with back pressure

Increasing back pressure increases the average pressure along the wellbore, hence, an increase in the bottomhole pressure (fig. 5.10). This can also be attributed to increasing cuttings concentration resulting from increasing the back pressure.

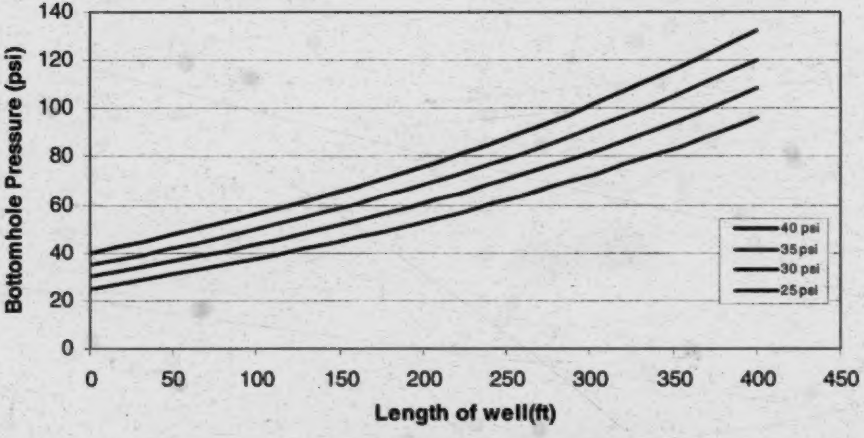

Figure 5.10: Variation of bottomhole pressure with back pressure

5.2.6 Effect of Water Influx on Bottomhole Pressure and Cuttings Concentration

Increase in water influx increases the cuttings concentration along the wellbore for a fixed gas and liquid injection rate (fig. 5.11). This effect is due to the fact that foam quality is reduced as water influx increases. Increasing volume of water reduces the effective viscosity of foam and, therefore, dwindles the lifting capacity of the foam.

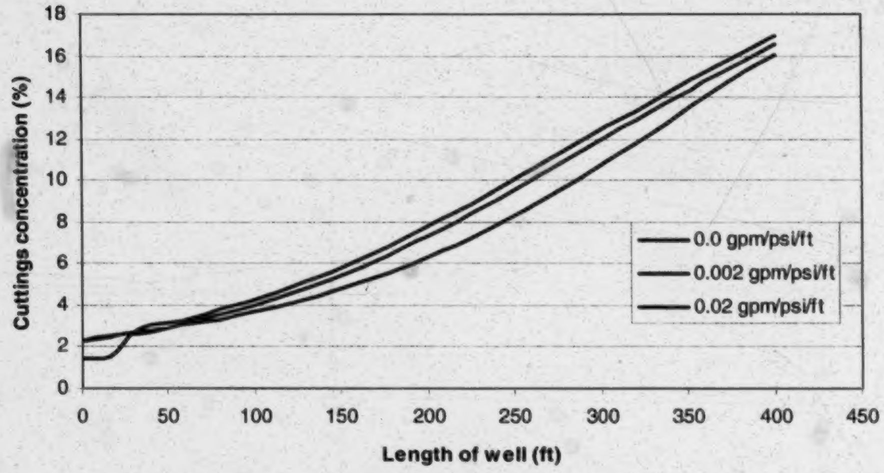

Fig. 5.11 Cuttings concentration profile variation with water influx from reservoir

Figure 5.12 shows the effect water influx on the pressure across the length of the wellbore under steady state flow condition. Increasing water influx from the reservoir also increases the pressure along the wellbore. This increase in pressure along the well is caused by higher foam density due to water influx from the reservoir and the increasing cuttings concentration associated with the water influx.

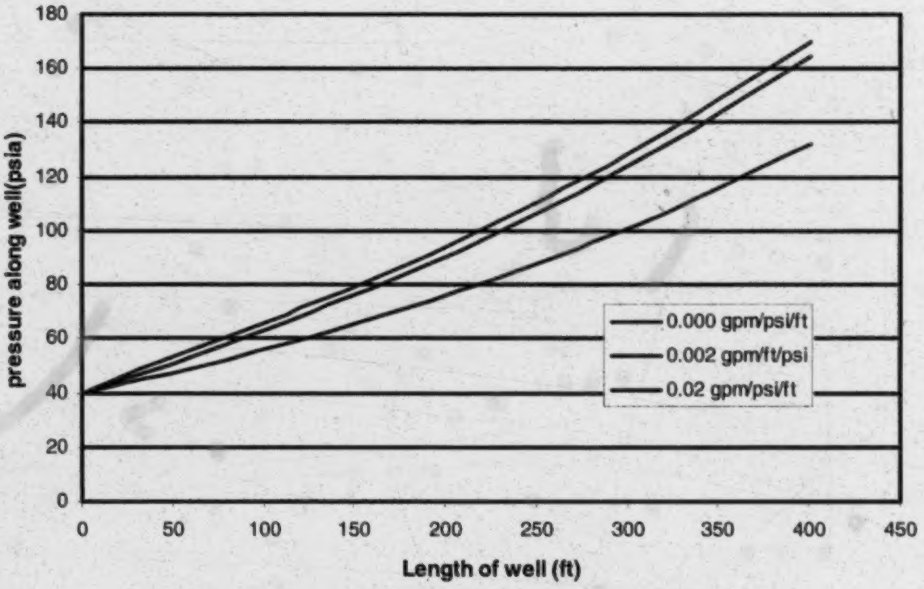

Fig. 5.12 Pressure profile variation with water influx from reservoir.

5.2.7 Effect of Gas Influx on Bottomhole Pressures and Cuttings Concentrations

Figure 5.13 and 5.14 illustrate the effect of reservoir gas influx on the cuttings concentration and pressure profile along the length of the well respectively. The influx of gas into the wellbore has a positive effect on the cuttings transport process reducing cuttings concentration as shown in figure 5.13. The influx of gas increases the effective viscosity of foam and, therefore, increases the cuttings lifting and transport ability of foam

Increasing gas influx rate reduces bottomhole pressure (fig. 5.14). This is because of the fact that influx of gas into the wellbore increases the foam quality, which in turns reduces the density of foam. The decrease in the cuttings concentration resulting from increase in the gas influx also contribute to the reduction of the bottomhole pressure.

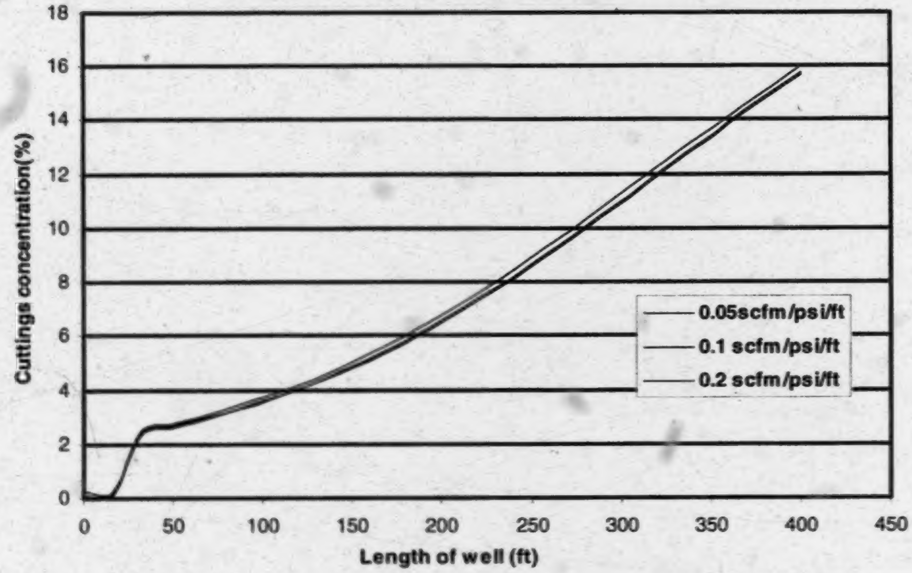

Fig. 5.13: Cuttings concentration variation with gas influx from the reservoir

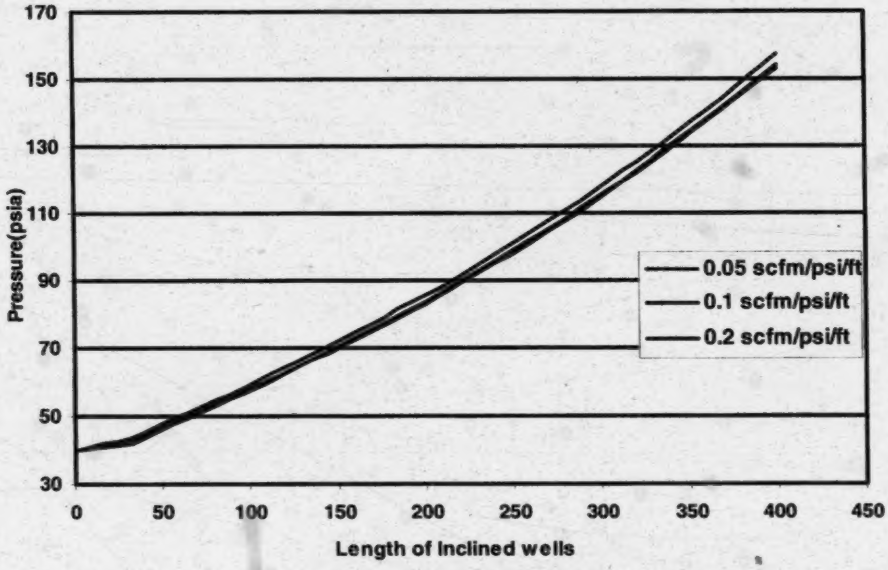

Fig. 5.14: Pressure profile variation with gas influx from reservoir

5.2.8 Transient Bottomhole Pressure and Cuttings Concentration

Figure 5.15 illustrates the changes in the average cuttings concentration in the annulus as a function of time. The trend in figure 5.15 is very similar to that in figure 5.16. This similarity in trend indicates that change in the bottomhole pressure as a function of time is directly proportional to change in the average cuttings concentration as a function of time, irrespective of the inclination angle.

Figure 5.16 shows changes in bottomhole pressure with time as drilling progresses for different drilling rate at 60 degree inclination. It takes longer for the bottomhole pressure to stabilize as the drilling rate increases.

Figure 5.17 and 5.18 further illustrate variation of cuttings concentration and bottomhole pressures with time at different inclination angles. From figure 5.18, it is seen that for a fixed drilling rate that the time it takes for the bottomhole pressure to stabilize increases with increasing inclination angle. It is also seen that the bottomhole pressures at all times increases with increase in inclination. Figure 5.17 shows a similar trend to figure 5.18. The change in bottomhole pressure is directly related to the in cuttings concentration irrespective of the inclination of the well.

Fig. 5.19 illustrates the distribution of cuttings along the well at different times for a fixed drilling rate. Results indicate that cuttings are not uniformly distributed even after stabilization. Here, steady state flow was achieved after about 50 minutes and that maximum cuttings concentration still occurs at the bottom of the hole.

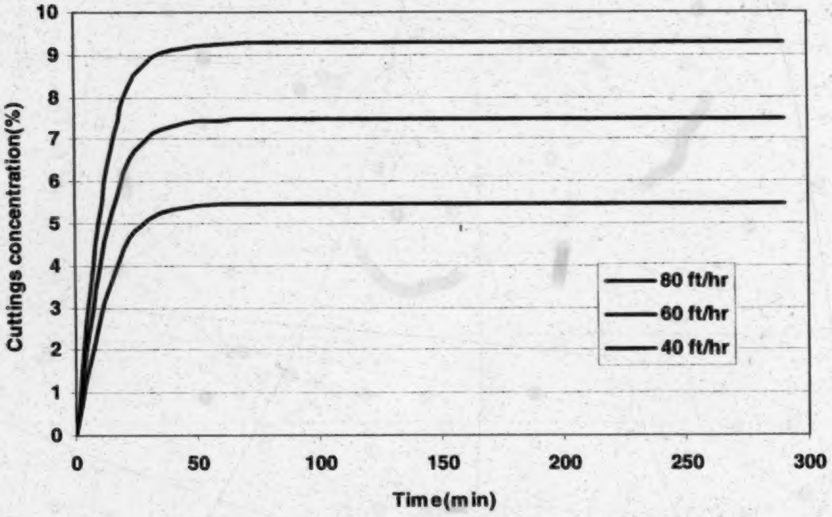

Fig. 5.15 Transient average cuttings concentration at different drilling rate

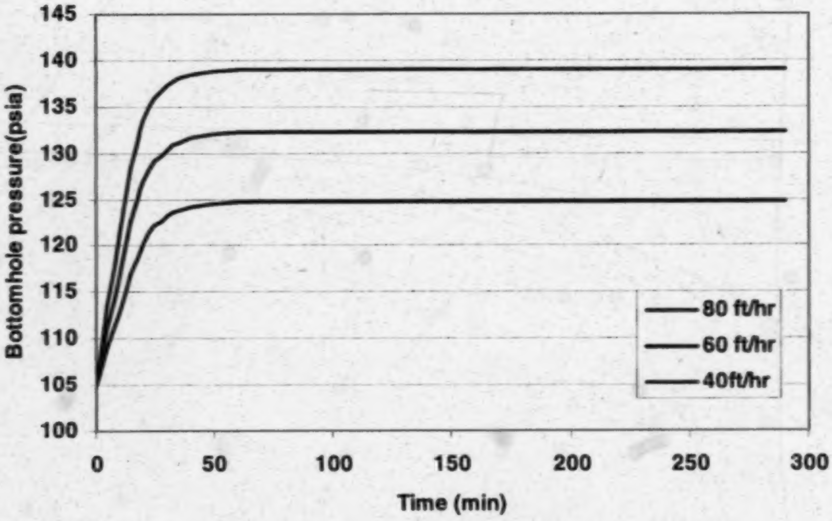

Fig. 5.16 Transient bottomhole pressure

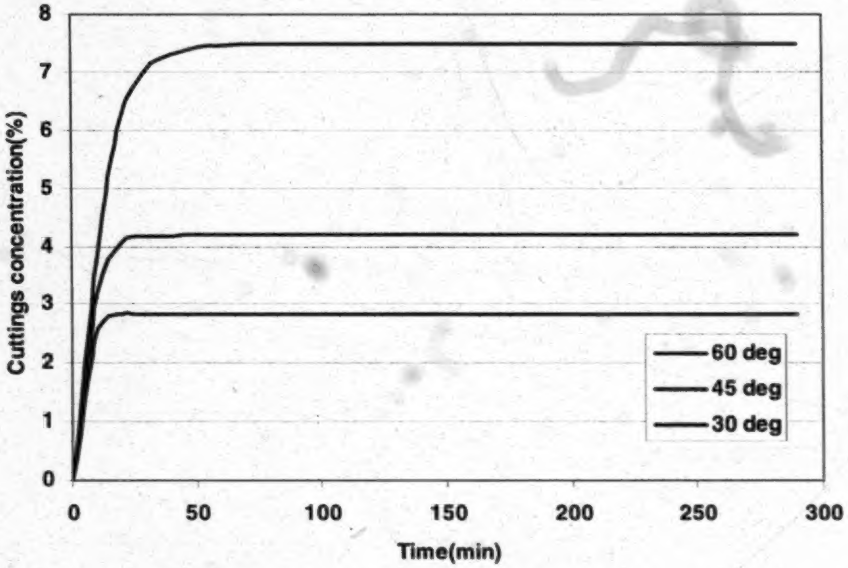

Fig. 5.17 Transient average cuttings concentration at different inclination

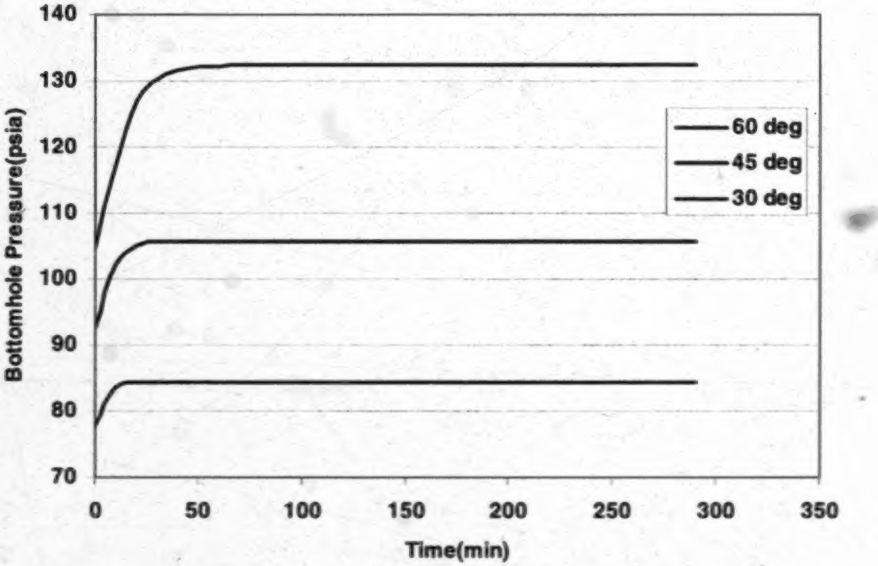

Fig. 5.18 Transient bottomhole pressure at different inclination

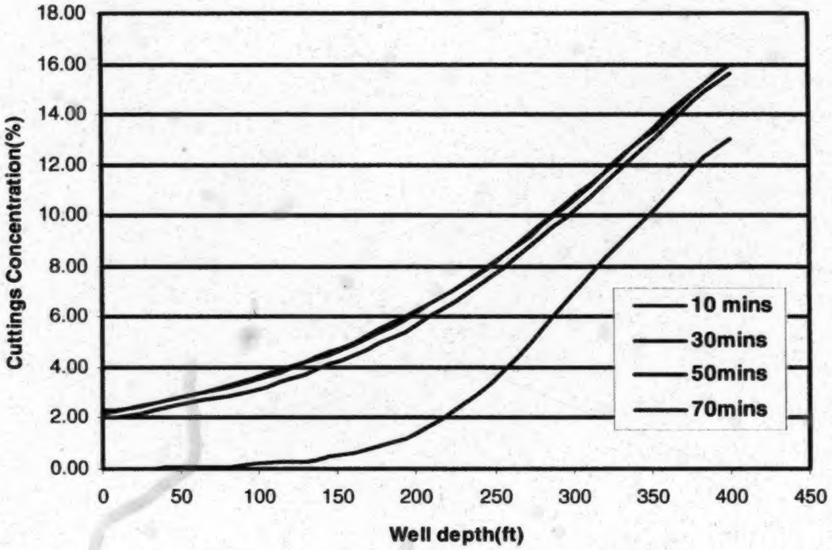

Fig. 5.19 Cuttings concentration profile along wellbore

CHAPTER 6

CONCLUSIONS AND RECOMMENDATIONS

6.1 Conclusions

A numerical simulation study of cuttings transport with foam in inclined wells has been conducted. A transient mechanistic model has been developed and numerically solved to predict cuttings transport efficiency with foam in inclined wells. This chapter summarizes the findings of this study.

- A 1-D unsteady state mechanistic model of cuttings transport with foam in inclined wells has been developed. The model is numerically solved to predict the optimum foam flow rate (liquid and gas rate) and rheological properties that would maximize cuttings transport efficiency in inclined wells.
- The model developed in this study was verified using experimental results obtained by Capo (2003). The model predictions of pressure drop values were found to be lower than the measured pressure drop values by about 4 to 21%.
- Increasing gas injection rate significantly increases the cuttings transport efficiency.
- The liquid injection rate has little effect on the cuttings transport efficiency when compared to the effect of gas injection rate. Increasing the liquid injection rate while keeping the gas injection rate constant reduces the cuttings transport efficiency.
- The well inclination is a major factor controlling cuttings transport efficiency in inclined wells. The cuttings transport efficiency decreases with increase in well inclination from the vertical under the same flow condition. More gas needs to be injected to keep the cuttings concentration constant as the inclination increases.
- Increasing back pressure increases bottomhole pressure and cuttings concentration.
- The influx of gas into the wellbore has a positive effect on the cuttings transport efficiency. The effect of gas influx is more pronounced in the low gas injection rate region.

- The influx of water into the wellbore has a negative effect on the cuttings transport efficiency. The effect of water influx is more significant at high gas injection rate region.
- The concentration of cuttings in the wellbore increases with increasing drilling rate.
- The average concentration of cuttings in the annulus and the bottomhole pressure do not stabilize immediately after drilling resumes. The time it takes for cuttings concentration and bottomhole pressure to stabilize increases with increasing drilling rate and inclination of the well.
- Even when steady state flow is achieved, the distribution of cuttings along the annulus is not uniform. The highest concentration of cuttings occurs at the bottom of the hole and the lowest occur at the top.

6.2 Recommendations for future investigations.

For further study of cuttings transport with foam in inclined wells, the following areas can be considered:

- Development of cuttings transport model with foam treated as a yield power law fluid.
- The effect of reservoir water influx salinity on foam stability and the cuttings transport efficiency

REFERENCES

1 Acharya, R.A. Mashelkar and J. Ulbrecht, Rheol. Acta, 15 (1979) 454.

2 Anderson, G.W.: "Use of Preformed Foam in Low Pressure Reservoir Wells," paper SPE 12425, 5th Off-shore South east Asia, Singapore, February 21-24, 1984.

3 Aarestad, T.V. and Blikra, H., Torque and Drag: Key Factors in Extended Reach drilling; IADC/SPE 27491, SPE/IADC Drilling Conference, Dallas, February 15-18, 1994.

4 Alfsen, T.E., Heggen, S., and Tjotta, H., Pushing the Limits of Extend Reach drilling: New World Record in Extended –Reach Drilling from Platform Stat fjord 'C'. Well C2; New. World Record in Extended –Reach Drilling from Platform Stat fjord 'C' SPEDC, 2, 71, Trans., AIME, P. 299, June 1995.

5 Bagnold, R. A. 1954 Experiments on gravity-free dispersion of large solid spheres in a Newtonian fluid under shear. Proc. R. Soc. A225, 49-63

6 Bagnold, R. A. 1957 the flow of cohesionless grains in fluids. Phil. Trans. R. Soc. A249, 235-297

7 Bassal, A.A., A Study of the Effect of Drill Pipe Rotation on Cuttings Transport in Inclined Wellbores; Ms thesis, U. of Tulsa, Tulsa, OK, 1995.

8 Bennion, D.B., Thomas, F.B., Bietz, R.F. and Bennion, D.W.: "Underbalanced Drilling: Praises and Perils," SPEDC (Dec. 1998), p. 214-221

9 Bensten, N.W. and Veny, J.N., Preformed stable foam in drilling and evaluating shallow gas wells in Alberta; JPT, p.1237-1240, October 1976.

10 Beyer, A.H., Millhone, R. S., and Foote, R.W.: "Flow Behavior of Foam as a Well Circulating Fluid," paper SPE 3986, the 47th Annual Fall Meeting of the Society of petroleum Engineers of AIME, San Antonio, Tex., Oct.8-11, 1972.

11 Foams, J.J. Bikerman, Springer-Verlag, New York (1973).

12 Blauer, R.E., Mitchell, B.J., and Kohlhaas, C.A.: "Determination of Laminar,

Turbulent, and Transitional Foam Flow Losses in Pipes," paper SPE 4885, the 1974 SPE Annual California Regional Meeting, San Francisco, California, 4-5 April 1974.

13 Becker, T.E., Azar. J.J., and Okrajni, S.S., Correlations of Mud rheological Properties with Cuttings Transport Performance in Directional Drilling; SPE 29025, EUROPEC 90, The Hague, Netherlands, October 22-24, 1990.

14 Bird, R. B. Stewart, W. E. and Lightfoot, E. N.: Transport Phenomena, John Wiley & Sons Inc., New York City (1960) 56-60 and 190-94.

15 Bonilla, L.F. and Shah, S.N.: "Experimental Investigation on the Rheology of Foams," paper SPE 59752, the 2000 SPE/CERI Gas Technology Symposium, Calgary, Alberta, Canada, 3-5 April 2000.

16 Bonilla, L.F. and Shah, S.N.: "Experimental Investigation on the Rheology of Foams," paper SPE 59752, the 2000 SPE/CERI Gas Technology Symposium, Calgary, Alberta, Canada, 3-5 April 2000.

17 Bourgoyne, A.T. Jr. and Young, F.S. Jr.: "A Multiple Regression Approach to Optimal Drilling and Abnormal Pressure Detection," SPE J., August 1974, pp.371-384.

18 Bourgoyne A.T. Jr., Young F.S. Jr., Martin E.C., Millheim K.K.,: "Applied Drilling Engineering," SPE Textbook series, Vol.2 , Second Edition, 1992, p. 128-130, 156-160

19 Brown, N.P. and Bern, P.A., Cleaning Deviated Holes; New Experimental and Theoretical Studies; SPE/IADC 18636, SPE/IADC Drilling Conference, New Orleans, 28 Feb.-3 March, 1989.

20 Buscall, R., Donaldson, R.B., Ottewill, R.H., Segal D., "Equilibrium Properties of Foam Films Formed from Non-Ionic Surface Agents", Number 6, pp.73-89.

21 Buslov, R., Towler, B.F., and Amian, A.V.: "Calculation of Pressure for Foams in Well Completion Process," paper SPE 36490, the 1996 SPE Annual Technical Conference and Exhibition, Denver, Colorado, 6-9 October 1996

22 Cade, R., Kirvelis, R., Nafta, M., and Jennings, J.: "Does Underbalanced Drilling Really Add Reserves?" Paper SPE 81626, the IADC/SPE Underbalanced Technology Conference, Houston, March 26-28 2003.

23 Campos, W., A Mechanistic Modeling of Cuttings Transport in Highly Inclined Wells; Ph.D. Thesis Dissertation, the University of Tulsa, U.S.A., 1995.

24 Capes, C.A. and Nakamura, K., Vertical Pneumatic Conveying: An Experimental Study with Particles in the Intermediate and Turbulent Flow Regimes; The Canadian Journal of Chemical Engineering, Vol.51, p.31-38 February 1973.

25 Capo, J., "Cuttings Transport with Foam at Intermediate Inclined wells", M.Sc Thesis, University of Tulsa (2003).

26 Ceylan, K., Hardem, S., and Abbasov, T.: Power Technol., 102 (1999) 286.

27 Chhabra, R.P.: "Motion of Spheres in Power Law (Visco-inelastic) Fluid at Intermediate Reynolds Numbers: A Unified Approach", Chem. Process. (1990) 28, 89-94.

28 Chhabra, R. P. " Sedimentation of particles in non-Newtonian media"; Department of Chemical Engineering, Indian Institute of Technology, India (2002)

29 Chien, S.F.: "Settling Velocity of Irregularly Shaped Particles," SPEDC (December 1994).

30 Chung, C.: "Drag on Object Moving through Foam," PhD Dissertation, Lowa State University, Ames, Iowa (1991).

31 Clark, R.K. and Bickham, K.L.: "A Mechanistic Model for Cuttings Transport," paper SPE 28306. The SPE 69th Annual Technical Conference and Exhibition, New Orleans, LA, 25-28 September 1994.

32 Bubbles, Drops, and Particles, CLIFT, R., Academic press, New York (1978)

33 Crowe, C.T, "Multiphase Flow with Droplets and Particles, CRC press (1998).

34 Culen, M.S., Harthi, S., and Hashimi, H.: "A Direct Comparison Between Convention and Underbalanced Drilling Techniques in the Saih Rawl Field, Oman," paper SPE 81629, the IADC/SPE Underbalanced Technology Conference

and Exhibition, Houston, Texas, 25-26 March 2003.

35 Darby, R., Chemical Engineering, 103 (December 1996) 109.

36 David, A. and Marsden, S.: "The Rheology of Foam," paper SPE 2544, the 1969 SPE Annual Fall Meeting, Denver, Colorado, 28 September-1 October, 1969.

37 Dedegil, M.Y.: "Drag Coefficient and Setting Velocity of Particles in Non-Newtonian Suspensions," Journal of Fluid Engineering (September 1987) 109.

38 Doan, Q.T., Oguztoreli, M., Masuda, Y., Yonezawa, T., Kobayashi, A. and Kamp, A.: "Modeling of Transient Cuttings Transport in Underbalanced Drilling," SPEJ (June 2003).

39 Doane, R.D., Bennion, D.B. Eilers, D.M. and New, E.R., Successful Drilling of an Underbalanced Horizontal well in the Rigel Halfway Pool- Laboratory Screening and field Results; SPE 37065, SPE international Conference on Horizontal Well Technology, Calgary, Canada, 18-20 November 1996.

40 Doron, P., Granica, D. and Barnea, D.: "Slurry Flow in Horizontal Pipes-Experimental and Modelling," International Journal of Multiphase Flow (1987) 13.

41 Eck-Olsen, J., Sletten, H., Reynolds J.T. and Samuell, J.G. North Sea Advances in Extended-Reach Drilling; SPE/IADC Drilling Conference, Amsterdam. 23-25 February 1993.

42 Enzendorfer, C., Harris, R., Valko, P., Economides, M.: "Pipe Viscometry Foams", Journal of Rheology, 39, March/April 1995, 345-358.

43 Essary, R.L., and Rogers, E.E., Technique and results of foam Redrilling Operations-san Joaquin valley, California; SPE 5715, symposium o formation damage control, Houston, TX., Jan 29-30, 1976

44 Fang, G.: "Experimental Study of Free Settling of Cuttings in Newtonian and Non-Newtonian Drillings Fluids: Drag Coefficient and Settling Velocity," SPE 26125; 1992.

45 Flak, K., and McDonald, C., An overview of Underbalanced Drilling Application

in Canada; SPE 30129, SPE European Formation Damage Conference, The Hague, The Netherlands, 15-16 May 1995.

46 Ford, J.T., Peden, J.M., Oyeneyin, M.B., Gao, E. and Zarrough, R.: "Experimental Investigation of Drilled Cuttings Transport in Inclined Boreholes," Paper SPE 20421, the 65th Annual Technical Conference and Exhibition, New Orleans, LA, September 23-26, 1990.

47 Ford, J.T., Gao, E., Oyeneyin, M.B., Peden, J.M., Larrucia, M.B. and Parker, D.: "A New MTV Computer Package for Hole-Cleaning Design and Analysis," SPECDC (September 1996), p. 168-172.

48 Ford, J. et al., Development of Mathematical Models Describing drilled cuttings transport in Deviated Wells; paper 93-1102 presented at the 1993 CADE/CAODC Spring Drilling Conference, Calgary, 14-16 April.

49 Fraser I.M and Moore R. H., Guidelines for Stable Foam Drilling through Permafrost; SPE/IADC 16055, SPE/IADC Drilling Conference, New-Orleans, LA, March 15-18, 1987.

50 Fredrickson, A.G. and Bird, R.B. “Non-Newtonian Flow in Annuli,” Ind. and Eng. Chemistry, (1958), Vol.50, No.3, pp.347-52.

51 Fredrickson, A.G. and Bird, R.B. “Friction Factor for Axial Non-Newtonian Annular Flow,” Ind. and Eng. Chemistry, (1958), Vol.50, No.10, pp.1599-1600.

52 Friberg, S., and Satio, H., “Foam Stability and Association of Surfactants”, Number 2, pp.33-38

53 Fullerton H.B.,: “Constant Energy System for Well Programming” Smith Tool, Irvine, CA, August 1973.

54 Frik, H., Horizontal Drilling in Low Pressure Reservoirs with a Foam Mud System; DGMK spring Conference, Celle, Germany, p.177-185, April 27-28, 1995.

55 Gadala-Maria, F.A., 1979 The rheology of concentrated suspensions. Ph.D. Thesis, Stanford University, CA.

56 Gardiner, B.S., Dlugogorski, B.Z., Jameson, G.J.: “Rheology of Fire- Fighting Foams", Fire Safety Journal 31, (1998) 61-75.

57 Gardiner, B.S., Dlugogorski, B.Z., Jameson, G.J.: "Prediction of Pressure Losses in Pipe Flow of Aqueous Foams,” Ind. Eng. Chem.Res. 1999.

58 Gavignet, A.A. and Sobey, I.J.: "Model Aids Cuttings Transport Prediction," JPT (Sept. 1989), Trans., AIME, 287, p.917-920.

59 Gavignet, A.A. and Wick, C.J. : “ Computer Processing Improves Hydraulic Optimization with New Methods,” SPE Drilling Engineering, December 1987, pp. 309-315

60 Guo, B., Miska, S., Hareland, G.: "A Simple Approach to Determination of Bottom Hole Pressure in Directional Foam Drilling," ASME Drilling Technology Symposium (1995), p.61-66.

61 Hall, D.L. and Roberts, R.D.: "Offshore Drilling with Preformed Stable Foam," paper SPE 12794, the 1984 California Regional Meeting, Long Beech, CA, 11-13 April 1984.

62 Hannegan, D.M. and Divine, R.: "Underbalanced Drilling -- Perceptions and Realities of Today's Technology in Offshore Applications," paper SPE 74448, the IADC/SPE Drilling Conference, Dallas, Texas, 26-28 Feb. 2002.

63 Harris, P.C. and Reidenbach, V.G.: "High-Temperature Rheological Study of Foam Fracturing Fluids," JPT (May 1987), p.613-619.

64 Harris, P.C., Klebenow, D.E. and Kundert, D.P.: "Constant-Internal-Phase Design Improves Stimulation Results," SPEPE (February 1991), 15-22.

65 Hemphill, T. and Larsen, T.I., Hole-Cleaning Capabilities of Oil-Based and Water-Based Drilling Fluids: A Comparative Experimental Study; SPE 26328, SPE Annual Technical Conference and Exhibition, Houston, 3-6 October, 1993.

66 Herzhaft, B., Toure, A., Bruni, F. and Saintpere, S.: "Aqueous Foams for Underbalanced Drilling: The Question of Solids," paper SPE 62898, the 2000 SPE Annual Technical Conference and Exhibition, Dallas, Texas, 1-4 October.

67 Iyoho, A.W.: "Drilled-Cuttings Transport by Non-Newtonian Drilling Fluids through Inclined, Eccentric Annuli," Ph.D. dissertation (1980), The University of Tulsa.

68 Jalukar, L.S., Study of Hole Size Effect on Critical and Subcritical Drilling Fluid Velocities in Cuttings Transport for Inclined Wellbores; MS thesis, U. of Tulsa, Tulsa, OK, 1993.

69 Jaramillo, M.: "Bitterweed S. (Caballos) Field: A Case History in Changing Economics Using Underbalanced Drilling and Open Hole Completions," paper SPE 81647, the IADC/SPE Underbalanced Technology Conference and Exhibition, Houston, Texas, 25-26 March 2003.

70 James H. A., "How to Relate Bit Weight and Rotary Speed to Bit Hydraulic Horsepower," Reprinted from Drilling-DCW, May 1975

71 Kamp, A.M. and Rivero, M.: "Layer Modeling for Cuttings Transport in Highly Inclined Wellbores, "paper SPE 53942, the 1999 Latin American and Caribbean Petroleum Conference, Caracas, Venezuela, 21-23 April 1999.

72 Kelessidis, V. C. and Mpanelis, G.E.,; Flow Pattern and Minimum Suspension Velocity For Efficient Cuttings Transport in Horizontal and Deviated Well in Coiled-Tubing Drilling, SPE 81746 Presented at the SPE/ICoTA Coiled Tubing Drilling Conference Held in Houston, TX, U.S.A., 8-9 April 2003.

73 Kendall, W.A., and Goins, W.C.: "Design and Operation of a Jet Bit Programs for Maximum Hydraulic Horse, Impact Force or Jet Velocity," Pet. Tech. (Oct. 1960) Trans., AIME (1960) 219, 238-248.

74 Kenny, P., Sunde, E., and Hemphill, T., Hole Cleaning Modeling: What's 'n' Got to Do with It?; IADC/SPE 35099, IADC/SPE Drilling Conference, New Orleans, 12-15 March, 1996.

75 Khan, S.A., Schnepper, C.A.,and Robert, C.: "Foam Rheology: III. Measurement of Shear Flow Properties," Journal of Rheology (1988) 32, 1, 69-92.

76 Kitsios, E., Kamphuis, H., Quaresma, V., Rovig, J.W. and Reynolds, E.: "Underbalanced Drilling Trough Oil Production Zones with Stable Foam in

Omen," paper SPE 27525, the 1994 IADC/SPE Drilling Conference, Dallas, Texas, 15-18 February 1994.

77 Konno, H. and Saito, S., Pneumatic Conveying of Solids Through Straight Pipes; Journal of Chemical Engineering of Japan, Vol.2, No,2, p.211-217, 1969

78 Krug, J.A and Mitchell, B.J.: "Charts Help Find Volume, Pressure Needed for Foam Drilling," Oil & Gas J. (7 February 1972).

79 Lage, A.C.V.M., Fjelde, K.K and Time, R.W.: "Underbalanced Drilling Dynamics: Two-Phase Flow Modeling and Experiments," SPEJ (March2003), p.61-70.

80 Lage, A.C.V.M., Nakagawa, E.Y., de Souza, A.A., and Santos, M.M.: "Recent Case Histories of Foam Drilling in Brazil," paper SPE 36098, the Fourth Latin American and Caribbean Petroleum Engineering Conference, Port-of-Spain, Trinidad & Tobago, 23-26 April 1996.

81 Larsen, T.I.: "A Study of the Critical Fluid Velocity in Cuttings Transport for Inclined Wellbores," M.S. thesis (1990), The University of Tulsa.

82 Larsen, T.I., Pilehvari, A.A and Azar, J.J.: Development of a New Cuttings Transport Model for High-Angle Wellbores Including Horizontal Wells," SPEDC (June 1997), p.129-135.

83 Leighton, D. and Acrivos, A. 1986 Viscous Re-suspension. Chem. Engng Sci. 41, 1377-1384.

84 Li, Y. and Kuru, E.,: " Numerical Modeling of Cutting Transport with Foam in Vertical Wells," Paper Presented at the Canadian International Petroleum Conference, Calgary, Alberta, 10-12 June 2003.

85 Li, Y.: Numerical Modeling of Cuttings Transport with Foam In Vertical and Horizontal Wells, "Ph.D. Thesis, University of Alberta, August 2004.

86 Liu, G. and Medley, G.H.: "Foam Computer Model Helps in Analysis of Underbalanced Drilling," Oil & Gas J. (1 July 1996).

87 Lord, D.L.: "Analysis of Dynamic and Static Foam Behavior," JPT (January

1981).

88 Lourenco, A.M., "Study of Foam Flow under Simulated Downhole Conditions".

89 Lourenco, A.M.F., Martins, A.L., Sa, C.H.M, Brandao, E.M. and Shayegi, S.: "Drilling with Foam: Stability and Rheology Aspects," Proceedings of ETCE/OMAE 2000 joint Conference on Energy for the New Millennium, New Orleans, LA, February 14-17, 2000.

90 Luo, Y., Bern, P.A and Chambers, B.D.: "Flow-Rate Prediction for Cleaning Deviated Wells," paper SPE 23884, the 1992 IADC/SPE Drilling Conference, New Orleans, Louisiana, February 18-21, 1992.

91 Luo, S., Hong, R., Meng, Y., Zhang, L., Li, Y., and Qin, C.: "Underbalanced Drilling in High-Loss Formation Achieved Great Success- A Field Case Study," paper SPE 59260, the 2000 IADC/SPE Drilling Conference, New Orleans, Louisiana, 23-25 Feb.2000.

92 Luo, Y., Bern, P.A., Chambers, B.D., Kellingray, D. : "Simple Charts to Determine Hole Cleaning Requirements in Deviated Wells," IADC/SPE 27486, IADC/SPE Conference, Dallas, TX, U.S.A., 1994

93 Matijasic, G. and Glasnovic, A., Chem. Biochem. Eng. Quart., 15 (2001) 21.

94 Martins, A.L., Lourenco, A.M.F., Sa, C.H.M. and Petrobras, S.A.: "Foam Property Requirements for Proper Hole Cleaning While Drilling Horizontal Wells in Underbalanced Conditions," SPEDC (December 2001), p. 195-200.

95 Martins, A.L and Santana, C.C.: "Evaluation of Cuttings Transport in Horizontal and Near Horizontal Wells - A Dimensionless Approach," paper SPE 23643, the Second Latin American Petroleum Engineering, Caracas, Venezuela, 8-11 March 1992.

96 Martins, A.L, SA, C.H.M., Lourenco, A.M.F., Freire, and Campos, W., Optimizing Cuttings Circulation in Horizontal Well Drilling; SPE 35341, International Petroleum Conf., Villahermosa, Mexico, 5-7 March, 1996.

97 Martins, A.L, SA, C.H.M., Lourenco, A.M.F., Freire, L.G.M., Campos, W.,

Experimental Determination of Interfacial Friction Factor in Horizontal Drilling with a Bed of Cuttings; SPE 36075, 4th Latin American and Caribbean Petroleum Engineering Conference, Port of Spain, Trinidad and Tobago, 23-26 April, 1996.

98 Underbalanced Drilling Manual, McLennan, J., Carden, R.S., Curry, D., Stone, C. R., and Wyman, R.E., Gas Research Institute, Chicago, Illinois (1997).

99 Meng, Y.F., Lou, P.Y., Jiao, D., Lao, R.K., and Lao, H., "Horizontal Well Technology with Cycling Using of Inert Foam,"; SPE International Conf. on Horizontal Well Technology, Calgary, Canada, 18-20 November, 1996.

100 Meyer, B.R., "Generalized drag Coefficient Application for All flow Regimes," Oil & Gas J. (26 May 1986).

101 Miska, S. and Skalle, P. : " Theoretical Description of a New Method of Optimal Program Design," SPE J. August 1981, pp. 425-434

102 Mitchell, B.J.: "Viscosity of Foams," PhD dissertation, University of Oklahoma (1969).

103 Naganawa, S., Oikawa, A., Masuda, Y., Yonezawa, T., Hoshino, M. and Acuna, P.: "Cuttings Transport in Directional and Horizontal Wells While Aerated Mud Drilling," paper SPE 77195, the IADC/SPE Asia Pacific Drilling Technology, Jakarta, Indonesia, 9-11 September 2002.

104 Negrao, A.F., Lage, A.C.V.M., and Cunha, J.C.: "An Overview of Air/Gas/Foam Drilling in Brazil," SPEDC (June 1999) 14(2), p. 109-114.

105 Nguyen, D. and Rahman, S.S.: "A Three-Layer Hydraulic Program for Effective Cuttings Transport and Hole Cleaning in Highly Deviated and Horizontal Wells," SPEDC (September 1998).

106 Okpobiri, G.A. and Ikoku, C.U.: "Volumetric Requirements for Foam and Mist Drilling Operations," SPEDE (February 1986).

107 Okrajni, S.S. and Azar, J.J.: "The Effects of Mud Rheology on Annular Hole Cleaning in Directional Wells," SPEDE (August1986), p.297-308.

108 Oroskar, A.R. and Turian, R.M.: "The Critical Velocity in Pipeline Flow of

Slurries," AIChE Journal (1980), 26, p.550-558.

109 Owayed, J.F.: "Simulation of Water Influx during Underbalanced Foam Drilling," MS thesis, University of Tulsa, Tulsa, OK (1997).

110 Ozbayoglu, M.E., Kuru, E., Miska, S., and Takach, N.: "A Comparative Study of Hydraulic Models for Foam Drilling," JCPT (2002),p.52-56.

111 Ozbayoglu, E.M., Miska, S.Z., Reed, T. and Takach, N.: "Cuttings Transport with Foam in Horizontal & Highly-Inclined Wellbore," paper SPE 79856, the SPE/IADC Drilling Conference, Amsterdam, The Netherlands, 19-21 February 2003.

112 Patankar S.V.: "Numerical Heat Transfer and Fluid Flow", Hemisphere Publishing Corporation, New York (1980).

113 Peden, J.M. and Luo, Y.: "Settling Velocity of Variously shaped Particles in Drilling and Fracturing Fluids," SPEDE (Dec. 1987).

114 Peden, J.M., Ford, J.T., Oyeneyin, M.B., "Comprehensive Experimental Investigation of Drilled Cuttings Transport in Inclined Wells Including the Effects of Rotation and Eccentricity". SPE 20295. The Hague, Netherlands, 22-24, October 1990.

115 Princen, H.M.: "Rheology of Foams and Highly Concentrated Emulsions. II. Experimental Study of the Yield Stress and Wall Effects for Concentrated Oil-in-Water Emulsions", Journal of Colloid and Interface Science, Vol. 105, N 1, May 1985.

116 Randall, B.V.: "Optimum Hydraulics in the Oil Patch," Pet Eng. Int.., September 1975, p. 36.

117 Raza, S.H. and Marsden, S.S.: "The Streaming Potential and the Rheology of Foam" SPEJ, December 1967, Vol.7, pp.359-368.

118 Reidenbach, V.G., Harris, P.C., Lee, Y.N., and Lord, D.L.: "Rheological Study of Foam Fracturing Fluids Using Nitrogen and Carbon Dioxide," SPEPE (January 1986), p.31-41.

119 Rojas, Y., and Vieira, P., Borrell, M., Blanco, J., Ford, M., Nieto, L., Lopez, G. and Atencio, B.: "Field Application of Near-Balanced Drilling Using Aqueous Foams in Western Venezuela," paper SPE 74449, the IADC/SPE Drilling Conference, Dallas, Texas, 26-28 February 2002.

120 Ross, S., “Bubbles and Foams”, Industrial and Engineering Chemistry, Vol. 61, No 10, pp.48-55 (October, 1969)

121 Saintpere, S., Herzhaft, B. and Toure, A.: "Rheological Properties of Aqueous Foams for Underbalanced Drilling," paper SPE 56633, the 1999 Annual Technical Conference and Exhibition, Houston, Texas, 3-6 October.

122 Sample, K.J. and Bourgoyne, A.T.: “An Experimental Evaluation of Correlations Used for Predicting Cutting Slip Velocity,” SPE 6645, presented at the SPE ATCE, Denver, CO, U.S.A., October 9-12, 1977.

123 Sample, K.J. and Bourgoyne, A.T. : “ Development of Improved Laboratory and Field Procedures for Determining Carrying Capacity of Drilling Fluids,” SPE 7497, presented at the SPE ATCE, Houston, TX, U.S.A., October 1-4, 1977

124 Sanghani, V. and Ikoku, C.U.: "Rheology of Foam and its Implications in drilling and Cleanout Operations," Journal of Energy Resources Technology (September 1983) 105, p.362-371.

125 Seeberger, M.H., Matlock, R.W., and Hanson, P.M., Oil Muds in Large-Diameter, Highly Deviated Wells: Solving the Cuttings Removal Problem; SPE/IADC 18635 SPE/IADC Drilling Conf., New Orleans, 28 February-3 March, 1989.

126 Shah, S.N.: "Proppant setting Correlations for Non-Newtonian Fluid under Static and Dynamic Conditions, "SPE Journal (April 1982).

127 Shah, S.N and Lord, D.L.: "Hydraulic Fracturing Slurry Transport in Horizontal Pipes," SPEDE (Sept. 1990), p.225-232.

128 Shook, C.A., Gillies, R.G., Kristoff, B.J., and Small, M.H.: "Sand Transport Mechanism in Horizontal Wells," 4th petroleum Conf. of South Saskatchewan Section, petroleum society of CIM hold with CANMED, Regina, Saskatchewan, Canada, Oct.7-9. 1991.

129 Sifferman, T.R. and Becker, T.E., Hole Cleaning in Full-Scale Inclined Wellbores; SPEDE, 115; Trans., AIME, P.293, June 1992.

130 Skelland, A.H.P., Non-Newtonian Flow and Heat Transfer; John Wiley and Sons, Inc., New York, 1967.

131 Stevenic, B.C., Design and Construction of a Large-Scale Wellbore Simulator and Investigation of Hole Size Effects on Critical Cuttings Transport Velocity in Highly Inclined Wells; MS thesis, U. of Tulsa, Tulsa, OK, 1991.

132 Swanson, B.W., Thorogood, J.R., and Gardner, A.: " The Design and Field Implementation of Drilling Hydraulics Application for Drilling Optimization," SPE 27548 presented at the European Petroleum Computer Conference , Aberdeen, U.K., 15-17 March, 1994

133 Tian, S., Medley, G.H and Stone, C.R.: "Optimizing Circulation while Drilling Underbalanced," World Oil (June 2000), p.48-55.

134 Thondavadi, N.N. and Lemlich, R.: "Flow Properties of Foam with and without Solid Particles," Ind. Eng. Chem. Process Des. (1985), p.748-753.

135 Tomren, P.H., Iyoho, A.W. and Azar, J.J.: "Experimental Study of Cuttings Transport in Directional Wells," SPEDE (February1986), p.43-56.

136 Tulay, A. and Ozbelge, Solids Friction Factor Correlation for Vertical Upward Pneumatic Conveyings; International Journal of Multiphase Flow, Vol.10, No.4, p.459-465, 1984.

137 Valko, P. and Economides, M.J.: "Volume Equalized Constitutive Equations for Foamed Polymer Solutions," Journal of Rheology (August 1992), 36(6), p.1033-1055.

138 Valko, P. and Economides, M.J., "Foam-Proppant Transport," SPEPF (November 1997).

139 Wang, Z., Rommetveit, R., Bijleveld, A., Maglione, R. and Gazaniol, D.; "Underbalanced Drilling Requires Downhole Pressure Management," Oil and Gas Journal (June 16, 1997), p. 54-60.

140 Wilson, K. C., 1970 Slip point of bed in Solid-Liquid pipeline flow. Proc. ASCE, J. Hydraul. Div. 96(HY1), 1-12.

141 Wilson, K.C., A Unified Physically Based Analysis of Solid-Liquid Pipeline Flow; Proc. 4th Int. Conf. On Hydraulic Transport of Solids in Pipes, Banff, Alberta, Canada, Paper A1, pp.1-6, 1976.

142 Wiright, K., Chukwu, A.A. Khataniar, S., Patil, S. : " An Economic Appraisal of Hole Cleaning Using Hydraulic Horsepower and Jet Impact Force," SPE83496, presented at the SPE Western regional Meeting, Long Beach , CA, U.S.A., 19-24 May 2003

143 Yang, W.C, A Correlation for Solid Friction Factor in Vertical Pneumatic conveying Lines; AICHE Journal, Vol.24, No. 3, p.548-552, May 1978

144 Yarborough, L. and Hall, K. R.: How to Solve Equation of State for Z-factors," Oil and Gas Journal (February 18, 1974), p.86-88.

APPENDIX A

CONTINUITY EQUATIONS FOR THE TWO LAYER MODEL

In this study, the Eulerian approach is used to derive the governing equation of foam-cuttings flow. Foam rheological behavior is represented by the power law type fluid.

Basic Definitions.

For a good understanding of the mathematical derivation of the mass and momentum equations for this model in both layers, a sound knowledge of some basic concepts is needed.

The bulk density of the suspended solid in the drilling fluid in region two is defined as the ratio of the mass of the suspended solid to the total volume of the suspension given by;

$$\overline{\rho}_s = \lim_{\Delta V \to \Delta V_0} \frac{\Delta M_s}{\Delta V} \qquad \text{A-1}$$

The bulk density of the suspended solid is related to the actual density of this phase by the formula given below.

$$\overline{\rho}_s = C_s \rho_s \qquad \text{A-2}$$

The volume fraction of the suspended solid is

$$C_s = \lim_{\Delta V \to \Delta V_0} \frac{\Delta V_s}{\Delta V} \qquad \text{A-3}$$

Where Δv_o is the limiting volume which remains unchanged even with a slight increase in volume.

Similarly, the volume fraction for the foam in the upper layer is given as

$$C_f = \lim_{\Delta V \to \Delta V_0} \frac{\Delta V_f}{\Delta V} \qquad \text{A-4}$$

The sum of the above volume fractions: for the dispersed and continuous phase in the suspension would yield unity.

$$C_s + C_f = 1 \qquad \text{A-5}$$

The local velocity of solids suspended in the foam in layer 2 can be represented by either the volume average velocity of the particle or mass average velocity of the particle.

The volume average velocity of particles is represented by

$$u_s = \frac{\sum_k u_{sk}}{N} \qquad \text{A-6}$$

N is the number of particle in an average volume.

The mass average velocity of particles is represented by

$$\bar{u}_s = \frac{\sum_k m_{sk} u_{sk}}{\sum_k m_{sk}} = \frac{\sum_k m_{sk} u_{sk}}{V_2 C_s \rho_s} \qquad \text{A-7}$$

From Eqn. A-7

$$V_2 C_s \rho_s \bar{u}_s = \sum_k V_2 (C_s \rho_s u_s)_k \qquad \text{A-8}$$

This gives

$$C_s \rho_s \bar{u}_s = \sum_k (C_s \rho_s u_s)_k$$

When the particles are of uniform size,

$$\overline{u}_s = u_s \quad \text{A-9}$$

With the above, the mass flow rate and the foam flow rate for the second region can be expressed as

$$\dot{m}_s = A_2 \sum_k (C_s \rho_s u_s)_k = A_2 C_s \rho_s u_s \quad \text{A-10}$$

And

$$\dot{m}_f = A_2 C_f \rho_f u_f \quad \text{A-11}$$

Continuity Equations

The continuity equations are derived based on the law of conservation of mass, which states that the mass rate generated within a control volume is equal to the sum of the rate of accumulation and the rate of mass efflux through the control volume.

Continuity Equations for the Cutting Bed

The moving bed of density ρ_1 assumed to slide up the inclined wells in the control volume is shown in figure **A-2**. The total mass of moving bed flowing out of the control volume through surface 2 during the time interval of Δt is:

$$(M_B)_2 = (\dot{m}_B.\Delta t)_2 = (A_1 \rho_1 u_1)_2.\Delta t \quad \text{A-12}$$

The total mass of moving bed flowing into the control volume through surface 1 during the time interval of Δt is:

$$(M_B)_1 = (\dot{m}_B.\Delta t)_1 = (A_1 \rho_1 u_1)_1.\Delta t \quad \text{A-13}$$

Mass accumulation in the control volume at Δt is:

$$(M_B)_{acc} = \frac{\partial (M_B.\Delta t)}{\partial t} = A_1 \Delta s \frac{\partial (\rho_1)}{\partial t}.\Delta t \quad \text{A-14}$$

Mass of solid and fluid deposited from suspension to bed in Δt is:

$$M_{Dep}=\left(\rho_s C_s v_D S_i \Delta s+\frac{C_{f1}}{C_{s1}}\rho_f C_s v_D S_i \Delta s\right).\Delta t \qquad \text{A-15}$$

Mass of solid and fluid re-suspended from bed to the suspension in Δt is:

$$M_{ent}=\rho_1 C_{s1} v_e S_i \Delta s \Delta t \qquad \text{A-16}$$

By law of conservation of mass

$$M_{B2}-M_{B1}+M_{acc}=M_{Dep}-M_{Ent} \qquad \text{A-17}$$

By dividing result obtained in the above equation **A-17** by $A_1 \Delta t \Delta s$ and taking limit with respect to Δs, the equation becomes

$$\frac{\partial \rho_1}{\partial t}+\frac{\partial(\rho_1 u_1)}{\partial s}=\left(\rho_s+\frac{C_{f1}}{C_{s1}}\rho_f\right)C_s v_D \frac{S_i}{A_1}-\rho_1 v_E \frac{S_i}{A_1} \qquad \text{A-18}$$

Continuity Equations for the Solid Component of the Suspension

For the drilling case, solids particle in the upper layer with density of ρ_s flowing upwards with the fluid in the control volume are shown in figure A-2. The total mass of solid particles flowing out of the control volume through surface 2 during the time interval of Δt is:

$$(M_s)_2=(\dot{m}_s.\Delta t)_2=(A_2 C_s \rho_s u_s)_2.\Delta t \qquad \text{A-19}$$

The total mass of solid particles flowing into the control volume through surface 1 during the time interval of Δt is:

$$(M_s)_1=(\dot{m}_s.\Delta t)_1=(A_2 C_s \rho_s u_s)_1.\Delta t \qquad \text{A-20}$$

Mass accumulation in the control volume at Δt is:

$$(M_s)_{acc} = \frac{\partial(M_s.\Delta t)}{\partial t} = A_2\Delta s\frac{\partial(C_s\rho_s)}{\partial t}\Delta t \qquad \text{A-21}$$

Applying the law of conservation of mass,

$$(M_s)_2 - (M_s)_1 + (M_s)_{acc} = M_{ent,s} - M_{Dep,s} \qquad \text{A-22}$$

By dividing result obtained in the above equation A-22 by $A_2\Delta t\Delta s$ and taking limit with respect to Δs, the equation becomes

$$\frac{\partial(\rho_s C_s)}{\partial t} + \frac{\partial(\rho_s u_s C_s)}{\partial s} = -\rho_s v_D C_s \frac{S_i}{A_2} + \rho_s v_E C_{s1}\frac{S_i}{A_2} \qquad \text{A-23}$$

Continuity Equations for the Fluid Component of the Suspension

The principle of the derivation of the continuity equation for the foam phase is similar to that for the suspended solids except that the mass of fluid influx from the reservoir has to be incorporated into the source term of the mass conservation equation.

Mass of fluid entering the control volume

$$(M_f)_2 = (\dot{m}_f.\Delta t)_2 = (A_2 C_f \rho_f u_f)_2.\Delta t \qquad \text{A-24}$$

Mass of fluid leaving the control volume

$$(M_f)_1 = (\dot{m}_f.\Delta t)_1 = (A_2 C_f \rho_f u_f)_1.\Delta t \qquad \text{A-25}$$

The accumulated mass of fluid within control volume

$$(M_f)_{acc} = \frac{\partial(M_f.\Delta t)}{\partial t} = A_2\Delta s\frac{\partial(C_f\rho_f)}{\partial t}.\Delta t \qquad \text{A-26}$$

By conservation of mass,

$$(M_f)_2 - (M_f)_1 + (M_f)_{acc} = M_{ent,f} - M_{Dep,f} + M_{res-\inf lux} \qquad \text{A-27}$$

By dividing result obtained in the above equation A-27 by $A_2\Delta t\Delta s$ and taking limit with respect to Δs, the equation becomes

$$\frac{\partial(\rho_f C_f)}{\partial t} + \frac{\partial(\rho_f u_f C_f)}{\partial s} = -\frac{C_{f1}}{C_{s1}}\rho_f C_s v_D \frac{S_i}{A_2} + \rho_f v_E C_{f1}\frac{S_i}{A_2} + s_f \qquad \text{A-28}$$

Where

$$s_f = \frac{\rho_o q_{re,o} + \rho_w q_{re,w} + \rho_g q_{re,g}}{A_2\Delta s} \qquad \text{A-29}$$

APPENDIX B

MOMENTUM BALANCE EQUATIONS FOR THE TWO LAYER MODEL

The momentum balance for the suspended solids

During the time Δt, the total momentum due to solids entering or leaving the control surfaces of the control volume of arbitrary length Δs and constant cross-sectional area A_2 for layer 2 are;

The total momentum due to solids entering the control volume through surface 1 in Δt is:

$$(M_s u_s)_1 = (\dot{m}_s u_s)_1 .\Delta t = \left(A_2 \sum_k \left(C_s \rho_s u_s^2\right)_k \right)_1 .\Delta t \qquad \text{B-1}$$

The total momentum due to solids leaving the control volume through surface 2 in Δt is:

$$(M_s u_s)_2 = (\dot{m}_s u_s)_2 .\Delta t = \left(A_2 \sum_k \left(C_s \rho_s u_s^2\right)_k \right)_2 .\Delta t \qquad \text{B-2}$$

Where

M_s is the mass of the solid cuttings and $\dot{m}_s$ is the mass flow rate of the solid cuttings.

Accumulation of momentum in the control volume is represented as

$$(M_s u_s)_{acc.} = \frac{\partial\left(\sum (M_{sk} u_{sk})_{acc}\right)}{\partial t} .\Delta t$$

$$(M_s u_s)_{acc.} = \frac{\partial\left(A_2 \Delta s \sum \left(C_s \rho_s u_s\right)_k\right)}{\partial t} .\Delta t \qquad \text{B-3}$$

Considering the concept of average mass velocity of the particles, the above equation becomes

$$(M_s u_s)_{acc.} = A_2 \Delta s \frac{\partial(C_s \rho_s u_s)}{\partial t} . \Delta t \qquad \text{B-4}$$

The total momentum change in the control volume

$$(M_s u_s)_{total} = (M_s u_s)_2 - (M_s u_s)_1 + (M_s u_s)_{acc.} \qquad \text{B-5}$$

$$(M_s u_s)_{total} = A_2 \left[\left(\sum C_s \rho_s u_s^2\right)_2 - \left(\sum C_s \rho_s u_s^2\right)_1 + \Delta s \frac{\partial(C_s \rho_s u_s)}{\partial t} \right] . \Delta t \qquad \text{B-6}$$

The forces responsible for this change in momentum are;

Pressure Force

$$F_{prs} = C_s A_2 (P_1 - P_2) = -C_s A_2 \Delta P \qquad \text{B-7}$$

Gravity Force

$$F_{gs} = -C_s A_2 \rho_s g \Delta s Cos\theta \qquad \text{B-8}$$

Drag Forces

The total drag force in the control volume is obtained by summing up the drag forces acting on individual particle in the suspension. The drag force over a particle is given by

$$F_{Dsk} = \frac{1}{2} \rho_f C_D A_{sk} (u_f - u_{sk})^2$$

The total drag on all the particles is given by

$$F_{Ds} = \frac{1}{2}\rho_f C_D \sum_k \left(A_{sk}\left(u_f - u_{sk}\right)^2\right) \qquad \text{B-9}$$

Where,

$$A_{sk} = \pi d_{sk}^2 / 4$$

$$F_{Ds} = \frac{N_s}{2}\rho_f C_D A_s \left(u_f - u_s\right)^2 \qquad \text{B-9b}$$

N_s = Volume occupied by suspended solid in layer 2/Volume of solid.

$$= \frac{6C_s V_s}{\pi d^3} \qquad \text{B-9c}$$

Shear Forces

The shear force which result due to contact between the wall of the hole and the solid in the suspension is obtained using

$$F_{s-w} = -\tau_{s-w} S_{s-w} \Delta s \qquad \text{B-10}$$

Where

$$\tau_{s-w} = \frac{1}{2} C_s f_S \rho_S u_S^2 \qquad \text{B-10b}$$

Therefore,

$$F_{s-w} = -\frac{1}{2} C_s f_S \rho_S u_S^2 S_{s-w} \Delta s \qquad \text{B-11}$$

The shear force due to contact between the suspended solids and the moving bed is given by

$$F_{s-B} = -\tau_{s-i}.S_i.\Delta s \qquad \text{B-12}$$

Where

$$\tau_{s-i} = \frac{1}{2} C_s f_s \rho_2 (u_2 - u_1)^2 \qquad \text{B-12b}$$

Therefore,

$$F_{s-B} = -\frac{1}{2} C_s f_s \rho_s (u_2 - u_1)^2 S_i \Delta s \qquad \text{B-13}$$

By equating the total force acting on the particles in the control volume to the total momentum change per unit time, the equation B-14 is obtained.

$$A_2 \Delta t \left[\left(\sum_k (C_s \rho_s u_s^2)_k \right)_2 - \left(\sum_k (C_s \rho_s u_s^2)_k \right)_1 + \Delta s \frac{\partial (C_s \rho_s \bar{u}_s)}{\partial t} \right] = (-C_s A_2 \Delta P - C_s A_2 \rho_s g \Delta s Cos\theta -$$
$$\frac{1}{2} C_s f_S \rho_S u_S^2 .S_2 .\Delta s - \frac{1}{2} C_s f_i \rho_S (u_S - u_1)^2 .S_i .\Delta s + \frac{1}{2} \rho_f C_D \sum_k \left(A_{sk} (u_f - u_{sk})^2 \right) +$$
$$u_1 v_E C_{s1} \rho_s S_i \Delta s Cos\theta - u_s v_D C_s \rho_s S_i \Delta s Cos\theta). \Delta t \qquad \text{B-14}$$

Divide both sides of Eqn. B-14 by $A_2 \Delta t \Delta s$ and taking limit to obtain,

$$\frac{\partial \left(\sum (C_s \rho_s u_s^2)_k \right)}{\partial s} + \frac{\partial (C_s \rho_s \bar{u}_s)}{\partial t} = -C_s \frac{\partial p}{\partial s} - C_s \rho_s g Cos\theta - \frac{1}{2} C_s f_S \rho_S u_S^2 \frac{S_2}{A_2} - \frac{1}{2} C_s f_s \rho_S (u_S - u_1)^2 \frac{S_i}{A_2} +$$
$$\frac{N_s}{2V_2} \rho_f C_D A_s (u_f - u_s)^2 + u_1 v_E C_{s1} \rho_s \frac{S_i}{A_2} Cos\theta - u_s v_D C_s \frac{S_i}{A_2} Cos\theta.$$

B-15

Simplifying the above equation, the momentum equation for the suspended solids in the upper region is given written

$$\frac{\partial\left(C_s\rho_s u_s^2\right)}{\partial s}+\frac{\partial\left(C_s\rho_s u_s\right)}{\partial t}=-C_s\frac{\partial p}{\partial s}-C_s\rho_s gCos\theta-\frac{1}{2}C_s f_S\rho_S u_S^2\frac{S_2}{A_2}-\frac{1}{2}C_s f_s\rho_S\left(u_S-u_1\right)^2\frac{S_i}{A_2}+$$
$$\frac{3C_s}{4d_s}\rho_f C_D\left(u_f-u_s\right)^2+u_1 v_{ent}C_{s1}\rho_s\frac{S_i}{A_2}Cos\theta-u_s v_D C_s\frac{S_i}{A_2}Cos\theta.$$

B-16

Momentum Equation for the Fluid in Layer 2.

During the time Δt, the total momentum entering or leaving the control surfaces are;

$$\left(M_f u_f\right)_1=\left(\dot{m}_f u_f\right)_1.\Delta t=A_2\left(C_f\rho_f u_f^2\right)_1.\Delta t \qquad \text{B-17}$$

$$\left(M_f u_f\right)_2=\left(\dot{m}_f u_f\right)_2.\Delta t=A_2\left(C_f\rho_f u_f^2\right)_2.\Delta t \qquad \text{B-18}$$

$$\left(M_f u_f\right)_{acc}=\frac{\partial\left(A_2\Delta sC_f\rho_f u_f\right)}{\partial t}.\Delta t \qquad \text{B-19}$$

The total momentum change per unit time associated with the fluid in the suspension must equal the force causing the change. The forces considered here is the same as that considered for solids in suspension.

Total change in momentum

$$A_2\left(C_f\rho_f u_f^2\right)_2.\Delta t - A_2\left(C_f\rho_f u_f^2\right)_1.\Delta t+\frac{\partial\left(A_2\Delta sC_f\rho_f u_f\right)}{\partial t}.\Delta t=$$
$$\left(F_{prf}+F_{Grf}+F_{f-w}+F_{f-B}+F_{Df}+F_{Dep}+F_{Ent}\right)\Delta t \qquad \text{B-20}$$

Where

$$F_{prf}=C_f A_2\left(p_1-p_2\right)=-C_f A_2\Delta p \qquad \text{B-21}$$

$$F_{Grf}=-C_f A_2\rho_f g\Delta sCos\theta \qquad \text{B-22}$$

$$F_{f-w}=-\tau_{f-w}S_{f-w}\Delta s=-\frac{1}{2}C_f f_f\rho_f u_f^2 S_{f-w}\Delta s \qquad \text{B-23}$$

$$F_{f-B} = -\tau_{f-i} S_i \Delta s = -\frac{1}{2} C_f f_f \rho_f \left(u_f - u_1\right)^2 S_i \Delta s \qquad \text{B-24}$$

$$F_{Df} = \frac{N_s}{2} \rho_f C_D A_s \left(u_f - u_s\right)^2 \qquad \text{B-25}$$

$$F_{Entf} = u_1 v_e C_{f1} \rho_f S_i \Delta s \qquad \text{B-26}$$

$$F_{Depf} = -u_{fs} v_D \frac{C_{f1}}{C_{s1}} C_s \rho_f S_i \Delta s \qquad \text{B-27}$$

$$A_2 \Delta t \left[\left(C_f \rho_f u_f^2\right)_2 - \left(C_f \rho_f u_f^2\right)_1\right] + \frac{\partial\left(A_2 \Delta s C_f \rho_f u_f\right)}{\partial t} \Delta t = (-C_f A_2 \Delta p - C_f A_2 \rho_f g \Delta s Cos\theta -$$
$$\frac{1}{2} C_f f_f \rho_f u_f S_{f-w} \Delta s - \frac{1}{2} C_f f_f \rho_f \left(u_f - u_1\right)^2 S_i \Delta s - \frac{N_s}{2} \rho_f C_D A_s \left(u_f - u_s\right)^2 + u_1 v_E C_{f1} \rho_f S_i \Delta s Cos\theta$$
$$-u_{fs} v_D \frac{C_{f1}}{C_{s1}} C_s \rho_f S_i \Delta s Cos\theta) \Delta t$$

B-28

Divide both sides of Eqn. B-28 by $A_2 \Delta s \Delta t$ and taking limit with respect to Δs to obtain the final momentum equation for the fluid flowing in region 2.

$$\frac{\partial\left(C_f \rho_f u_f^2\right)}{\partial s} + \frac{\partial\left(C_f \rho_f u_f\right)}{\partial t} = -C_f \frac{\partial p}{\partial s} - C_f \rho_f g Cos\theta - \frac{1}{2} C_f f_f \rho_f u_f^2 \frac{S_{f-w}}{A_2} - \frac{1}{2} C_f f_f \rho_f \left(u_f - u_1\right)^2 \frac{S_i}{A_2}$$
$$-\frac{3C_s}{4d_s} \rho_f C_D \left(u_f - u_s\right)^2 + u_1 v_e C_{f1} \rho_f \frac{S_i}{A_2} Cos\theta - u_f v_D \frac{C_{f1}}{C_{s1}} C_s \rho_f \frac{S_i}{A_2} Cos\theta$$

B-29

Momentum Balance for the Moving Bed.

For the moving bed, the following momentum expressions are obtained.

$$\left(M_B u_B\right)_1 = \left(A_1 \rho_1 u_1^2 . \Delta t\right)_1 \qquad \text{B-30}$$

$$\left(M_B u_B\right)_2 = \left(A_1 \rho_1 u_1^2 . \Delta t\right)_2 \qquad \text{B-31}$$

$$(M_B u_B)_{acc} = \frac{\partial(A_1 \rho_1 u_1 .\Delta s)}{\partial t} .\Delta t \qquad \text{B-32}$$

Force due to pressure drop across the bed is given by

$$F_{prB} = -A_1 \Delta P \qquad \text{B-33}$$

Force due to the weight of the bed tending to pull the bed back into the lower side of the hole.

$$F_{GrB} = -A_1 \rho_1 g \Delta s Cos\, \theta \qquad \text{B-34}$$

Where

$$\rho_1 = \rho_s C_{s1} + \rho_f (1 - C_{s1}) \qquad \text{B-35}$$

Shear forces due to contact between the moving bed and the layer of fluid containing solid particles and also due to contact between it and the wellbore are given as

$$F_{B-s} = \tau_{B-i} S_{B-i} \Delta s = \frac{1}{2} C_s f_s \rho_S (u_S - u_1)^2 S_i \Delta s + \frac{1}{2} C_f f_f \rho_f (u_f - u_1)^2 S_i \Delta s \qquad \text{B-36}$$

$$F_{B-2} = \tau_{B-w} S_{B-w} \Delta s = \frac{1}{2} f_{B-w} \rho_1 (u_1)^2 S_{B-w} \Delta s \qquad \text{B-37}$$

With

$$f_{B-i} = f_i \qquad \text{B-38}$$

The forces associated with the deposition and entrainment of cuttings from and to the moving bed are obtained by using;

$$F_{B-Dep} = \left(u_s v_D C_s \rho_s S_i \Delta s + u_{fs} v_D C_s \frac{C_{f1}}{C_{s1}} \rho_f S_i \Delta s \right) Cos\theta \qquad \text{B-39}$$

$$F_{B-Ent} = u_1 v_e \rho_1 S_i \Delta s Cos\theta \qquad \text{B-40}$$

By equating the total momentum change to the total force acting on the bed per unit time, and dividing both sides of the equation by $A_1 \Delta s \Delta t$,

The momentum balance equation for the moving bed is obtained as

$$\frac{\partial(\rho_1 u_1^2)}{\partial s} + \frac{\partial(\rho_1 u_1)}{\partial t} = -\frac{\partial p}{\partial s} - \rho_1 g Cos\theta + \frac{1}{2}\frac{S_i}{A_1}\left(C_s f_s \rho_s (u_s - u_1)^2 + C_f f_f \rho_f (u_f - u_1)^2\right) -$$
$$\frac{1}{2} f_{B-w} \rho_1 u_1^2 \frac{S_{B-w}}{A_1} + \left(u_s V_D C_s \rho_s \frac{S_i}{A_1} + u_f V_D \frac{C_{f1}}{C_{s1}} C_s \rho_f \frac{S_i}{A_1} - u_1 V_{ent} \rho_1 \frac{S_i}{A_1} \right) Cos\theta - \frac{F_1}{A_1 \Delta s} -$$

B-41

F_l is the frictional force which opposes the motion of the moving bed over the surface of the wellbore.

APPENDIX C

Deposition and Re-suspension During Cuttings Transport in Inclined Wells.

Below is the derivation of the an expression for the mass of cuttings and fluid deposited and entrained, and also the forces associated with the re-suspension and deposition process during cutting transport in inclined wells.

Let the mass flux of solids deposited per unit interface $=\Phi_{s,Dep} = \rho_s C_s v_{Dep}$

Mass flux of fluid deposited per unit interface $= \Phi_{f,Dep} = \frac{C_s}{C_{s1}} C_{f1}\rho_f v_{Dep}$

Mass flux of solid re-suspended per unit interface$= \Phi_{s,Sus} = \rho_s v_E C_{s1}$

Mass flux of fluid suspended per unit interface$=\Phi_{f,Sus} = C_{f1}\rho_f v_E$

Considering

Mass of solids deposited from the layer 2 into the layer 1.

$$M_{Dep,S} = \Phi_{S,Dep} S_i .\Delta t.\Delta s \qquad \text{C-1}$$

$$M_{Dep,S} = \rho_s C_s v_D S_i \Delta s \Delta t \qquad \text{C-2}$$

Mass of solids re-suspended from layer 1 to layer 2

$$M_{Sus,S} = \Phi_{s,sus} .S_i \Delta s.\Delta t \qquad \text{C-3}$$

$$M_{sus,S} = \rho_s v_E C_{s1} S_i .\Delta t.\Delta s \qquad \text{C-4}$$

Mass of fluid deposited from layer 2 to layer 1.

It should be noted that the concentration of cuttings in the bed is always constant. For a bed concentration of C_{s1}, the lower layer contains a fluid concentration of C_{f1}.

The deposition of Cs concentration of cuttings from layer 2 to layer 1 is associated with the deposition of $\frac{C_s}{C_{s1}}.C_{f1}$ of fluid to keep the cutting concentration of the bed constant. The mass of fluid associated with this deposition is obtained by using;

$$M_{Dep,f} = \Phi_{f,Dep} S_i \Delta t \Delta s \qquad \text{C-5}$$

$$M_{Dep,f} = \frac{C_s}{C_{s1}} C_{f1} \rho_f v_D S_i \Delta t \Delta s \qquad \text{C-6}$$

Mass of fluid re-suspended from layer 1 to layer 2

$$M_{sus,f} = \Phi_{f,sus} S_i \Delta t \Delta s \qquad \text{C-7}$$

$$M_{sus,f} = C_{f1} \rho_f v_E S_i \Delta t \Delta s \qquad \text{C-8}$$

Mass associated with solid transfer for upper layer.

$$M_{sus,s} - M_{Dep,s} = \rho_s S_i \Delta s \Delta t \left(v_E C_{s1} - v_D C_S \right) \qquad \text{C-9}$$

Mass associated with transfer of fluid for upper layer

$$M_{sus,f} - M_{Dep,f} = \rho_f C_{f1} S_i \Delta s \Delta t \left(v_{ent} - \frac{C_s}{C_{s1}} v_D \right) \qquad \text{C-10}$$

Mass change associated with transfer of materials to and from the moving bed

Total mass of substance re-suspended from the moving bed=Mass of solids re-suspended + Mass of fluid re-suspended.

$$M_{sus,B} = v_E S_i \Delta s \Delta t \left(\rho_s C_{s1} + \rho_f C_{f1}\right)$$
$$M_{sus,B} = v_E S_i \Delta s \Delta t \rho_1 \qquad \text{C-11}$$

Total mass of substance deposited into the moving bed= Mass of solid deposited + Mass of fluid deposited to keep its concentration constant.

$$M_{Dep,B} = C_s v_D S_i \Delta s \Delta t \left(\rho_s + \frac{C_{f1}}{C_{s1}} \rho_f \right) \qquad \text{C-12}$$

Forces associated with deposition and re-suspension

The force associated with deposition of solids from the upper to lower zone.

$$F_{Dep,s} = \rho_s C_s v_D u_s \Delta s S_i Cos\theta \qquad \text{C-13}$$

The force associated with re-suspension of solids from layer 1 to layer 2

$$F_{sus,s} = \rho_s C_{s1} v_E u_1 \Delta s S_i Cos\theta \qquad \text{C-14}$$

The force associated with the deposition of fluids from layer 2 to layer 1

$$F_{Dep,f} = \rho_f \frac{C_{f1}}{C_{s1}} C_s v_D S_i \Delta s \Delta t u_f Cos\theta \qquad \text{C-15}$$

The force associated with the re-suspension of fluid from layer 1 to layer 2

$$F_{sus,s} = \rho_f C_{f1} v_E u_1 \Delta s S_i Cos\theta \qquad \text{C-16}$$

Force change associated with the solid component in the upper zone due to deposition and re-suspension.

$$F_{sus,s} - F_{Dep,s} = \rho_s \Delta s S_i \left(C_{s1} v_E u_1 - C_s v_D u_s\right) Cos\theta \qquad \text{C-17}$$

Force change associated with the fluid component in the upper zone due to deposition and re-suspension.

$$F_{sus,f} - F_{Dep,f} = \rho_f C_{f1} \Delta s S_i \left(v_E u_1 - \frac{C_s}{C_{s1}} v_D u_s \right) Cos\theta \qquad \text{C-18}$$

Force change associated with the moving bed due deposition and re-suspension.

$$F_{Dep,B} - F_{sus,B} = \left(\Delta s S_i C_s v_D \left(\rho_s u_s + \rho_f \frac{C_{f1}}{C_{s1}} u_f \right) - v_E u_1 \Delta s S_i \rho_1 \right) Cos\theta \qquad \text{C-19}$$

APPENDIX D

WELL GEOMETRY

- Case 1- the case in which the pipe is completely above the cuttings bed i.e. $h_b \le y$

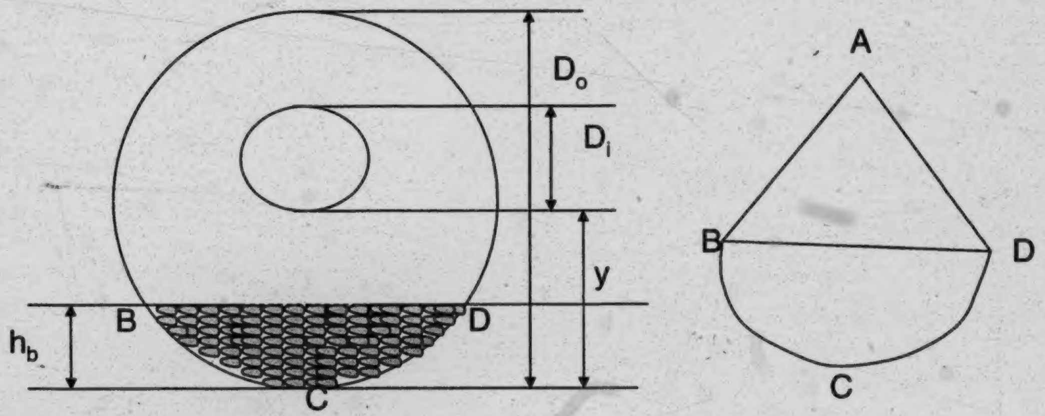

A is the centre of the wellbore.

Figure D-1: Geometry for the case in which the pipe is completely above the cuttings bed

Considering the figure for this case, the area of the bed can be obtained as follows.

A_B = Area of sector ABCD- Area of triangle ABD

Area of sector ABCD= $\frac{1}{2}r_o^2 B\hat{A}D = \frac{D_o^2}{4}\left(Cos^{-1}\left(1-\frac{2h_b}{D_o}\right)\right)$ D-1

Area of triangle ABD= $\frac{D_o^2}{4}Sin\theta Cos\theta$ D-2

From the diagram for this case,

$$Sin\,\theta = 2\sqrt{\frac{h_b}{D_o}\left(1-\frac{h_b}{D_o}\right)} \qquad \text{D-3}$$

$$Cos\theta = 1-\frac{2h_b}{D_o} \qquad \text{D-4}$$

$$A_B = \frac{D_o^2}{4}\left(Cos^{-1}\left(1-\frac{2h_b}{D_o}\right)-2\left(1-\frac{2h_b}{D_o}\right)\sqrt{\frac{h_b}{D_o}\left(1-\frac{h_b}{D_o}\right)}\right) \qquad \text{D-5}$$

$$A_s = A - A_B \qquad \text{D-6}$$

Determination of the wetted perimeters

From the diagram,

$$S_i = 2x$$

$$x^2 = \left(\frac{D_o}{2}\right)^2 - \left(\frac{D_o}{2}-h_b\right)^2 \qquad \text{D-7}$$

$$x = \sqrt{h_b\left(D_o - h_b\right)}$$

$$S_i = 2\sqrt{h_b\left(D_o - h_b\right)}$$

$S_2 =$ Length of outer circle- S_b

$$S_2 = D_o\left(\pi - Cos^{-1}\left(1-\frac{2h_b}{D_o}\right)\right) \qquad \text{D-8}$$

$$S_s = S_2 + S_1 = D_o\left(\pi - Cos^{-1}\left(1 - \frac{2h_b}{D_o}\right)\right) + \pi D_i \qquad \text{D-9}$$

$$D_2 = \frac{4A_2}{S_s + S_i} \qquad \text{D-10}$$

- Case 2- the case in which the pipe is partially covered by the cutting bed i.e. $y \le h_b \le y + D_i$

Considering the figure for this case

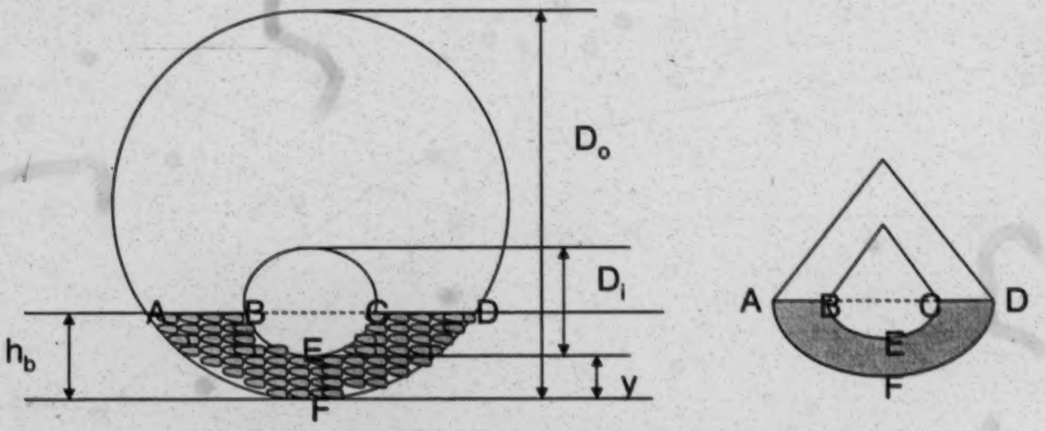

Figure D-2: Geometry for the case in which the pipe is partially covered by the cutting bed

Area of bed= Area of segment ADF – Area of segment BCE

To obtain an expression for the bed in this case, an auxiliary function which represent the area of the bed in case one is defined, represented as

$$F(D_o, h_b) = \frac{D_o^2}{4}\left(Cos^{-1}\left(1 - \frac{2h_b}{D_o}\right) - 2\left(1 - \frac{2h_b}{D_o}\right)\sqrt{\frac{h_b}{D_o}\left(1 - \frac{h_b}{D_o}\right)}\right) \qquad \text{D-11}$$

Considering this auxiliary function, the area of the bed for case two can be represented as

$$A_B = F(D_o, h_b) - F(D_i, h_b - y) \qquad \text{D-12}$$

Where

$$F(D_i, h_b - y) = \frac{D_i^2}{4}\left(Cos^{-1}\left(1 - \frac{2(h_b - y)}{D_i}\right) - 2\left(1 - \frac{2(h_b - y)}{D_i}\right)\sqrt{\frac{h_b - y}{D_i}\left(1 - \frac{h_b - y}{D_i}\right)}\right)$$

D-13

Determination of the wetted perimeters

From the diagram,

S_i = length of AD – length of BC

$$S_i = 2\sqrt{h_b(D_o - h_b)} - 2\sqrt{(h_b - y)(D_i - (h_b - y))} \qquad \text{D-14}$$

S_2 = Length of outer circle- S_3

$$S_2 = D_o\left(\pi - Cos^{-1}\left(1 - \frac{2h_b}{D_o}\right)\right)$$

S_1 = Length of outer circle- S_4

$$S_1 = D_i\left(\pi - Cos^{-1}\left(1 - \frac{2(h_b - y)}{D_i}\right)\right) \qquad \text{D-15}$$

$$S_s = S_2 + S_1 = D_o\left(\pi - Cos^{-1}\left(1-\frac{2h_b}{D_o}\right)\right) + D_i\left(\pi - Cos^{-1}\left(1-\frac{2(h_b - y)}{D_i}\right)\right)_i \quad \text{D-16}$$

$$D_2 = \frac{4A_2}{S_s + S_i}$$

- Case 3- the case in which the pipe is completely covered by the cutting bed i.e. $y + D_i \leq h_b \leq D_o$.

Considering the figure for this case, the area of the bed

Area of bed= Area of segment ABD – cross area of pipe completely buried by the bed

$$A_B = F(D_o, h_b) - \frac{\pi D_i^2}{4} \quad \text{D-17}$$

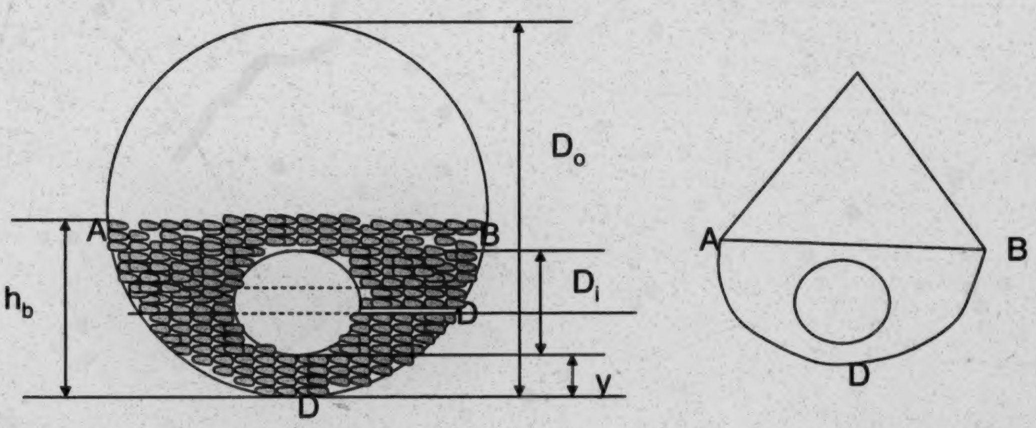

Figure D-3: Geometry for the case in which the pipe is completely covered by the cutting bed

Determination of the wetted perimeters

From the diagram,

S_i = Length of AD

$$S_i = 2\sqrt{h_b(D_o - h_b)} \qquad \text{D-18}$$

$$S_B = \pi D_i + D_o Cos^{-1}\left(1 - \frac{2h_b}{D_o}\right)$$

S_2 = Length of outer circle

$$S_2 = D_o\left(\pi - Cos^{-1}\left(1 - \frac{2h_b}{D_o}\right)\right)$$

$$S_s = S_2$$

$$D_2 = \frac{4A_2}{S_s + S_i}$$